

Flow estimation for stream restoration and wetland projects in ungaged  
watersheds using continuous simulation modeling

Janell Christine Henry

Thesis submitted to the faculty of the Virginia Polytechnic Institute and State  
University in partial fulfillment of the requirements for the degree of

Master of Science

In

Biological Systems Engineering

Theresa Wynn Thompson

W. Cully Hession

Glenn E. Moglen

April 8, 2013

Blacksburg, VA

*Keywords: rainfall-runoff, ungaged stream, stream restoration, design discharge*

Design flow estimation for stream restoration projects in ungaged watersheds  
using continuous simulation modeling

Janell Christine Henry

ABSTRACT

More than a billion dollars are spent annually on stream restoration in the United States (Bernhardt et al., 2005), but the science remains immature. A promising technique for estimating a single or range of design discharges is the generalization of a parsimonious conceptual continuous simulation model. In this study the Probability Distributed Model (PDM), was generalized for the Maryland and Virginia Piedmont. Two hundred and sixty years of daily average flow data from fifteen watersheds were used to calibrate PDM. Because the application of the study is to stream restoration, the model was calibrated to discharges greater than two times baseflow and less than flows with a return period of ten years. The hydrologic calibration parameters were related to watershed characteristics through regression analysis, and these equations were used to calculate regional model parameters based on watershed characteristics for a single “ungaged” independent evaluation watershed in the region. Simulated flow was compared to observed flow; the model simulated discharges of lower return periods moderately well (e.g., within 13% of observed for a flow with a five year return period). These results indicate this technique may be useful for stream restoration and wetland design.

## **Acknowledgements**

This thesis would not have been possible if not for my truly amazing adviser and the ever-supportive “Team Tess.” Additionally, I would like to recognize Dr. Cully Hession, Nathan Jones, and Dr. Javier Osorio, who led me through a crash course in GIS learning and Lory Willard, who helped me through the most tedious aspect of my research. Also, I owe a great deal of thanks to Dr. Glenn Moglen for helping me wrap my head around flood frequency analyses. Chris Weiss, thank you for the encouragement to pursue graduate school and for cheering me on along the way. Last, but not least, thank you, fellow biological systems *engineers* for humoring me by keeping craft night in your schedules.

## Table of Contents

Acknowledgements.....	iii
Table of Figures .....	vi
Table of Tables .....	viii
Chapter 1 Introduction .....	1
1.1 Goals and Objectives.....	2
Chapter 2 Literature Review.....	3
2.1 Dominant Discharge.....	3
2.2 Bankfull Discharge and Regional Curves .....	4
2.3 Effective Discharge .....	6
2.4 Discharge of a Specified Recurrence Interval.....	7
2.5 Flood Frequency Analysis.....	8
2.6 Index Flood Method.....	10
2.7 Regression Equations .....	10
2.8 Rainfall-Runoff Modeling.....	12
2.9 Event Models.....	13
2.10 Continuous Simulation .....	13
2.11 Conceptual Models.....	15
2.12 Regionalization of Continuous Simulation Models.....	16
2.13 Summary.....	18
Chapter 3 Methods .....	19
3.1 Watershed Selection.....	19
3.2 Watershed Area and Basin Slope .....	20
3.3 Land Use Coverage .....	21
3.4 Hydrologic Soil Group Classification .....	25
3.5 Soil Water Capacity .....	26
3.6 Model Description.....	29
3.7 Data Inputs .....	32
3.7.1 Measured Stream Discharge.....	34
3.7.2 Precipitation .....	34
3.7.3 Potential Evapotranspiration .....	35
3.8 Sensitivity Analysis.....	39
3.9 Calibration.....	41
3.9.1 Objective Function .....	42

3.9.2	Calibration to Baseflow.....	43
3.9.3	Calibration to Peak Flow.....	43
3.9.4	Specifying a Range of Flows .....	45
3.10	Regionalization of Model Parameters by Regression.....	46
3.11	Model Evaluation .....	48
3.12	Goodness-of-Fit Measures.....	48
Chapter 4	Results and Discussion.....	49
4.1	Calibration.....	49
4.2	Sensitivity Analysis.....	55
4.3	Correlation of Model Variables.....	59
4.4	Regionalization of Model Parameters .....	61
4.5	Model Evaluation .....	65
4.6	Goodness-of-Fit.....	65
Chapter 5	Conclusions .....	73
Chapter 6	References .....	75
Appendix	.....	81

## Table of Figures

Figure 2-1. Derivation of total sediment load-discharge histogram (III) from flow frequency (I) and sediment load rating curves (II). .....	6
Figure 2-2: Physiographic provinces of Virginia.....	12
Figure 3-1. A flow chart of study methods .....	20
Figure 3-2. A map showing areas of land use change in the Slade Run watershed between 1959 and 1984.....	24
Figure 3-3. A map of hydrologic soil groups for the South Fork Quantico watershed. ...	26
Figure 3-4. The PDM structure and parameters.....	29
Figure 3-5. A map of Maryland study watershed with rain gages and weather stations used in this study.....	37
Figure 3-6. A map of Virginia study watersheds with rain gages and weather stations used in this study.....	38
Figure 4-1. A hydrograph of observed and PDM calibrated simulated flow in Accotink Creek near Annandale, VA from February through June of 1984.....	50
Figure 4-2. A hydrograph of observed and PDM model evaluation flow in Northeast River watershed from April through September of 1959. ....	66
Figure 4-3. A evaluation hydrograph of observed and PDM model evaluation flow in Northeast River watershed from November 1967 through August of 1968.....	66
Figure 4-4. Peak discharge values of standard return intervals for observed and simulated daily average flows in Northeast River watershed from 1957-1966. ....	68
Figure 4-5. Peak discharge values of standard return intervals for observed and simulated daily average flows in Northeast River watershed from 1967-1976. ....	68
Figure 4-6. Peak discharges of standard return intervals of daily average flows simulated during model evaluation and plotted against discharges of standard return intervals of observed daily average streamflow. This plot is specific for the seven smallest watersheds (5.3 – 11.4 km <sup>2</sup> ) in the study.....	70
Figure 4-7. Peak discharges of standard return intervals of daily average flows simulated during model evaluation and plotted against discharges of standard return intervals of observed daily average streamflow. This plot is specific for four watersheds of intermediate size (22.9 – 67.7 km <sup>2</sup> ) in the study. ....	71

Figure 4-8. Peak discharges of standard return intervals of daily average flows simulated during model evaluation and plotted against discharges of standard return intervals of observed daily average streamflow. This plot is specific for the five largest watersheds (89.8 –149.7 km<sup>2</sup>) in the study..... 72

## Table of Tables

Table 3-1. Drainage area and basin slope of each of the study watersheds.....	21
Table 3-2. Land use categories present in the Chesapeake Bay Watershed Land Cover Data Series and the corresponding numeric code. ....	22
Table 3-3. Hydrologic soil group composition as a percent of watershed area for each of the study watersheds. ....	27
Table 3-4. Maximum soil moisture content at field capacity and saturation as a depth by watershed. ....	28
Table 3-5. Standard PDM model parameters, their function, and suggested values.. ....	32
Table 3-6. Modeled stream gages and corresponding rain gages, their distance from the watershed centroid, and time periods modeled.....	36
Table 3-7. A summary of information used to calculate evapotranspiration.....	40
Table 3-8. Discharge values of twice that of baseflow ( $Q_{2x\text{BF}}$ ) and of an average annual exceedance probability of ten percent ( $Q_{10}$ ) for each of the study gages. ....	46
Table 4-1. Goodness-of-fit measure for the calibrated time series.....	54
Table 4-2. Results from a sensitivity analysis on baseflow (at 860 days) for Accotink Creek watershed.....	56
Table 4-3. Results from a sensitivity analysis on baseflow (at 3505 days) for South Fork Quantico Creek watershed. ....	56
Table 4-4. Results from a sensitivity analysis on a small peak (at 2511 days) for Accotink Creek watershed.....	57
Table 4-5. Results from a sensitivity analysis on a small peak (at 1480 days) for South Fork Quantico Creek watershed.....	58
Table 4-6. Results from a sensitivity analysis on a large peak for Accotink Creek (gage no. 01654000) watershed.....	59
Table 4-7. Results from a sensitivity analysis on a large peak (at 2494 days) South Fork Quantico Creek watershed. ....	59
Table 4-8. Spearman's $\rho$ and Kendall's $\tau$ correlation coefficients for the calibrated model parameters. ....	60
Table 4-9. Spearman's $\rho$ and Kendall's $\tau$ correlation coefficients for the studied watershed characteristics.. ....	62

Table 4-10. Regression equations relating predicted model parameters  $b$ ,  $c_{max}$ ,  $k_1$ , and  $k_g$  (i.e.,  $b$ ,  $c_{max}$ ,  $k_1$ , and  $k_g$ ) to watershed characteristics ..... 63

## Chapter 1 Introduction

More than a billion dollars are spent annually on stream restoration in the United States (Bernhardt et al., 2005), but the science remains immature. Stream restoration projects are typically conducted in small, ungaged watersheds using a single design discharge, the bankfull discharge, or a discharge of a specified return period (i.e., 1.5 yrs or 2 yrs). Because ungaged watersheds lack observed flow data, the bankfull discharge or 2-yr discharge is estimated from regional curves or regional regression equations, respectively; however, these estimates can vary over an order of magnitude.

Stream restoration design success could be improved if flood frequency data could be accurately estimated for ungaged watersheds. A variety of methods have been developed, but these techniques are limited in application or vary in accuracy. Regional regression methods are often limited to watersheds where the hydrologic factors affecting runoff (i.e., flow regulation, urban development, or climate change effects) have not been impacted. Single event rainfall-runoff models require assumptions about pre-storm watershed conditions, which may significantly affect model predictions. Meanwhile continuous simulation models require long time series to calibrate the many model parameters. However, a promising technique for flood frequency estimation of ungaged watersheds is the regionalization of parsimonious conceptual rainfall-runoff models. Parameters of conceptual-based models are related to watersheds characteristics. Conceptual models hold the greatest promise in the modeling of ungaged watersheds due to their physical basis. The regionalization of parsimonious conceptual continuous simulation models has been the focus of many recent studies (e.g., McIntyre et al., 2005; Parajka et al., 2005; Kay et al. 2006; Young, 2006; Bárdossy, 2007; Oudin et al., 2008; Viviroli et al., 2009; Randrianasolo et al., 2011) during the past decade due to the International

Association of Hydrological Sciences' designation of 2003-2012 as the decade of the Predictions in Ungauged Basins (PUB) initiative. Nearly all of these studies have focused on European watersheds, and few, if any, have been applied to watersheds in the U.S.

Parsimonious conceptual continuous simulation models not only allow model parameters to be related to measurable watershed characteristic, they provide a continuous hydrograph. The hydrograph can be evaluated for the entire distribution of flows and studied for seasonal trends, which could allow stream restoration designs to be based on a range of flows rather than a single discharge. Additionally, the application of the information in a continuous hydrograph can be extended to wetland design, where seasonal variations in flow are important.

### *1.1 Goals and Objectives*

This study has one main research goal:

1. To develop a regionally applicable technique with minimal data requirements for estimating flows of ungauged watersheds for use in stream and wetland design.

The objectives of this research include:

1. Identify an applicable modeling technique;
2. Apply technique to the Virginia Piedmont; and
3. Assess model performance.

## Chapter 2 Literature Review

The following sections review concepts pertinent to stream restoration design discharge. The theoretical concept of dominant discharge is explained, and its three surrogates most frequently used (i.e., bankfull discharge, effective discharge, and discharge of a specified recurrence interval) are explained and their determination and usage discussed.

### *2.1 Dominant Discharge*

The parameters responsible for alluvial channel formation are the magnitude, duration, and sequencing of flows that transport sediment (Soar and Thorne, 2011). Because these parameters vary seasonally, annually, and interannually, the “dominant discharge” concept is often used. The dominant discharge is a theoretical flow that, if held constant indefinitely, would produce the same channel geometry as that formed by the actual distribution of discharges experienced by the river. The dominant discharge concept is most applicable to humid, temperate climates where most channel geomorphic formation is the result of discharges that do not significantly over-top banks and have low to moderate return intervals of one to three years (Soar and Thorne, 2011). Although the concept of a dominant discharge is not universally accepted, it is widely used for estimating design flows (Biedenharn et al., 2001). Dominant or channel-forming discharge is not a flow that can be measured but there are several candidate flows often used to represent this concept: (1) bankfull discharge; (2) effective discharge; and, (3) a discharge with a specific recurrence interval.

## *2.2 Bankfull Discharge and Regional Curves*

Bankfull discharge is the flow at which water begins to overtop the floodplain of a stable alluvial channel; it typically has a return interval of between one and two years (Wolman and Leopold, 1957). Once bankfull discharge is exceeded, bed shear stress in the channel does not appreciably increase with increasing flow, which implies that bankfull discharge is the most frequently occurring flow at this peak shear stress; thus bankfull flow is the most “effective” in transporting sediment and in channel formation. It has been shown that concentrations of bed load sediment transport actually decrease with increases of river discharges in excess of bankfull (Soar and Thorne, 2011).

To determine the bankfull discharge, a bankfull elevation must be identified and measured in the field. Williams (1978) provides a list of bankfull indicators and discussion of their usage. Once the bankfull elevation has been measured, this measurement must be related to a bankfull discharge. If there is a nearby stream gage, the bankfull stage can be extrapolated to the gage and related to a discharge using the gage stage-discharge rating curve. If a gage is not present, a synthetic stage-discharge curve can be derived using a hydrologic model (e.g., HEC-RAS) or Manning’s equation (Williams, 1978; Soar and Thorne, 2011). There are uncertainties in the application of both methods of discharge estimation, and the bankfull method is limited in application to stable alluvial channels.

Generalized regional regression curves are a common alternative approach to estimating bankfull discharge. The bankfull channel geometry characteristics of cross-sectional area, width, and average depth are highly correlated with both discharge and drainage area. In the Piedmont Physiographic Province in Virginia survey data and flow data were collected at 17 streamflow-gaging stations with drainage areas ranging from 0.75 to 287 km<sup>2</sup> (0.29 to 111 mi.<sup>2</sup>) in rural areas

with less than 20% urban land cover within the basin area. Several regression equations were developed relating bankfull geometry and bankfull discharge to drainage area. The equation (Equation 1) relating bankfull discharge to watershed area for rural streams in the Virginia Piedmont Physiographic Province follows (Lotspeich et al., 2009):

$$Q_{bkfl} = 43.895 * A^{0.9472} \quad (1)$$

where,  $Q_{bkfl}$  = estimated bankfull discharge (ft<sup>3</sup>/s); and,

$A$  = drainage area (mi<sup>2</sup>).

However, bankfull discharge estimates must be used with caution. The practice of identifying bankfull features is not an easy task. Wolman and Leopold (1957) define the bankfull discharge as “the discharge conveyed at the elevation of the active floodplain;” however, some channels have no active floodplain. Other bankfull features such as the highest depositional surface on meander bars or grain size changes in the channel boundary are difficult to identify. One bankfull indicator, the lower limit of perennial vegetation, is not applicable in the eastern U.S. (Williams, 1978). Determining the location of bankfull elevation is not a precise analytical science; it is a subjective and often inconsistent estimate (Soar and Thorne, 2011). Additionally, bankfull features can only be correctly measured in stable alluvial channels. This may be problematic because channel instability often makes a stream a candidate for restoration (Williams, 1978; Soar and Thorne, 2011). For these reasons, bankfull discharge is often difficult to determine with reasonable confidence, and the comparison of bankfull discharge to other design discharge estimates is encouraged.

### 2.3 Effective Discharge

The second dominant discharge proxy to be discussed is effective discharge. Effective discharge is defined as the flow that transports the largest fraction of the bed material load, and as such it may be a good surrogate for the channel-forming discharge of alluvial streams (Soar and Thorne, 2011). Wolman and Miller (1960) found that the effective discharge corresponds to an intermediate flood flow since frequent small floods transport too little sediment to affect channel morphology. Meanwhile, very large flood events, which have the capacity to transport a large amount of sediment, occur too infrequently to be responsible for channel formation (Biedenharn et al., 2001).

The necessary inputs for effective discharge determination are: a flow frequency distribution (line I in Figure 2-1) and a sediment transport rating curve (line II in Figure 2-1).

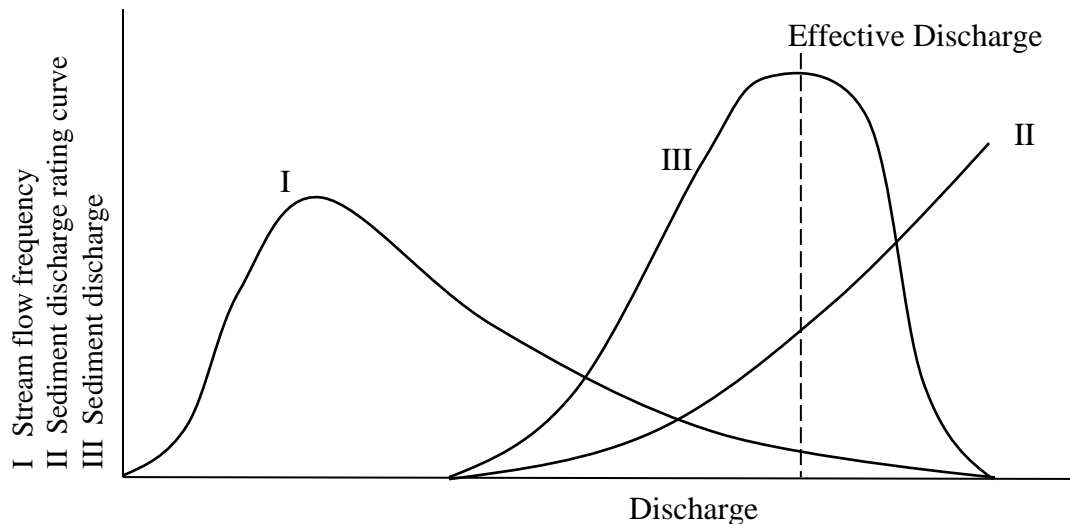


Figure 2-1. Derivation of total sediment load-discharge histogram (III) from flow frequency (I) and sediment load rating curves (II). Adapted from Biedenharn et al., 2001.

The calculation steps follow:

1. The streamflow frequency histogram is divided into flow classes.
2. The total amount of sediment transported by each class is calculated by multiplying the frequency of occurrence of each flow class by the median sediment load for that flow class.
3. The maximum of the collective sediment discharge plot is considered the effective discharge (Biedenharn et al., 2001).

However, like all of the methods available for alluvial channel design flow estimation, effective discharge has several limitations. It may not be a good representation of channel forming flow in arid climates and is not applicable after very large storm events when a stream system is in recovery (Soar and Thorne, 2011). The selection of the number of flow classes considered in calculations has a large effect on the determination of effective discharge (Biedenharn et al., 2001). Additionally, of the available approaches to specifying a design discharge for alluvial channels, effective discharge, requires the most data and effort (Soar and Thorne, 2011).

#### *2.4 Discharge of a Specified Recurrence Interval*

The third and final dominant discharge surrogate is discharge of a specified recurrence interval. As previously noted, the dominant discharge concept has been linked to flood events that occur on average every one to two years (Wolman and Leopold, 1957). Leopold et al. (1964) linked bankfull discharge to an average recurrence interval of 1.5 yrs. This value was supported by Dury (1973), Hey (1975), Castro and Jackson (2001). The 1.5-yr discharge is not always an appropriate surrogate for the channel-forming discharge. The U.S. Army Corps of Engineers

(Biedenharn et al., 2001) manual on channel rehabilitation states that for expediency the 1.5-yr discharge is often used, but acknowledges that the dominant discharge frequency may vary from one to ten years. Despite the uncertainty of selecting the specified return period of the design discharge, this method can be applied in cases where bankfull discharge measurements are inappropriate due to channel modification or instability (Hey, 1997).

For a stream that is gaged, the method for determining the discharge of a specified recurrence interval (e.g., 1.5-yr) is straightforward. Statistical analysis of observed flood events at gaging stations are used to evaluate the probability of future flood events (Arnaud and Lavabre, 2002). However, because only a small fraction of streams is gaged, streamflow data are not always available. Where observed streamflow data are not available, streamflow may be estimated using regression models, water balance approaches, or conceptual models (Mohamoud and Parmar, 2006).

### *2.5 Flood Frequency Analysis*

Discharge records are often insufficient to determine the risk of extreme events, so statistical treatment of the available flow data is used (Stedinger et al., 1993). A flood frequency analysis (FFA) may be performed to calculate the discharge that corresponds to a specific return interval. FFA is a statistical analysis of a time series of peak flood flows. A very commonly used time series for analysis is the annual maxima series, which is a record of the largest magnitude flood for each hydrologic year. The partial duration series, which is a record of all flood peaks over a specific threshold discharge, may also be used for analysis. The mean value, variance, and skew of observed annual peak discharges are calculated and used to fit a frequency distribution to the observed data (Bedient and Huber, 1992).

In an effort to standardize the various statistical approaches to FFA, the Interagency Advisory Committee on Water Data (1982) published detailed guidelines for FFA.. The recommendation in this guidance document is to fit the observed data to a log Pearson Type III distribution. The resulting frequency distribution is then used to determine the likelihood of various discharges, expressed as an annual exceedance probability. For example, a flow magnitude with a 1% exceedance probability can be described as a value with a one in 100 chance of being exceeded each year. The exceedance probability may also be expressed in terms of a return period or recurrence interval. The recurrence interval is merely the reciprocal of the exceedance probability. For example, a flood flow with a 1% exceedance probability is called the 100-year flood, meaning that such flood flow is likely to occur on average once every 100 years (Stedinger et al., 1993).

Several data assumptions must be met for flood frequency analysis to be applied, and each are detailed in IACWD (1982). First, there must be an adequate length of record of at least 10 to 20 years of streamflow data. Second, the peak flows must exhibit stationarity. This may be an issue in watersheds where hydrologic conditions have been altered by urbanization, channelization, or construction of reservoirs, etc. Thirdly, the flow sampling must have adequate temporal resolutions, where at least one sample every 15 min is considered optimum. Lastly, the flow peaks considered must be independent of each other. This assumption is met when annual maxima series are considered, but caution must be exercised when a partial duration series is used for analysis (IACWD, 1982).

In the U.S., the Geological Survey (USGS) maintains an extensive network of streams gages, where annual peak flow records are available for 28,100 sites (USGS, 2012a). This figure, however, represents a small percentage of streams in the U.S. Because only a small fraction of a

stream network is usually gaged, streamflow data are not always available at project sites targeted for stream restoration. Where insufficient or no observed streamflow data are available, discharge is usually estimated using regionalization techniques or rainfall-runoff models. Rainfall-runoff models predict flood flows from observed precipitation events (Thomas et al., 2001). Regionalization is the extension of results from flood frequency analyses at a set of gaged locations in a region to all ungaged locations within the same region (Oudin et al., 2008). Common regionalization approaches include the index flood method and regional regression equations.

### *2.6 Index Flood Method*

The index flood method is a simple regionalization technique used to construct a flood frequency curve for ungaged watersheds (Stedinger et al., 1993). The index flood method was developed by the USGS and is based on the assumption that flood flows in a hydrologically similar region, when standardized by an appropriate index flood parameter, are identically distributed (Grover et al., 2002). Available stream gage data for a region are used to develop a dimensionless flood frequency curve. An index-flood parameter that reflects watershed characteristics is used to scale the flood frequency curve to yield a flood frequency distribution specific to the study watershed (Stedinger et al., 1993).

### *2.7 Regression Equations*

Regression equations are a common statistical tool used to estimate flood discharges at ungaged stream sites. The equations are developed by regressing flood discharges to watershed characteristics (i.e., drainage area, percent forest cover, main channel length, etc.) for a group of

gaging stations within a hydrologically homogeneous region. These equations may be applied to regions with undisturbed or natural streamflow. Through regional regression equations flood characteristics at gaged sites are transferred to ungaged sites when they share physical and climatic characteristics.

The USGS maintains 161 continuous-record streamflow-gaging stations in Virginia (Bisese, 1995). Bisese (1995) used these gages to derive regional regression equations for estimating peak discharges in rural, unregulated streams in each of the Physiographic Provinces of Virginia (Figure 2-2). Flood frequency analysis was performed for each gage of the study to calculate the discharges for standard return intervals. Additionally, a range of watershed characteristics was measured including drainage area, main channel length, main channel slope, mean basin elevation, and forested area. Multivariate regression was used to develop a relationship between station peak discharge and watershed characteristics for each of the physiographic provinces. Drainage area was the most significant explanatory variable in all eight regions and the only significant explanatory variable for four of the regions (Bisese, 1995). Regional regression equations derived by Bisese (1995) for the northern Virginia Piedmont follow:

$$Q_2 = 179A^{0.655} \quad (2)$$

$$Q_5 = 317A^{0.644} \quad (3)$$

$$Q_{10} = 438A^{0.641} \quad (4)$$

$$Q_{25} = 626A^{0.640} \quad (5)$$

$$Q_{50} = 793A^{0.640} \quad (6)$$

$$Q_{100} = 984A^{0.641} \quad (7)$$

where  $Q_t$  is the estimated discharge in  $\text{ft}^3/\text{s}$  for a return period of  $t$  yrs and  $A$  is drainage area of the watershed in  $\text{mi}^2$ .

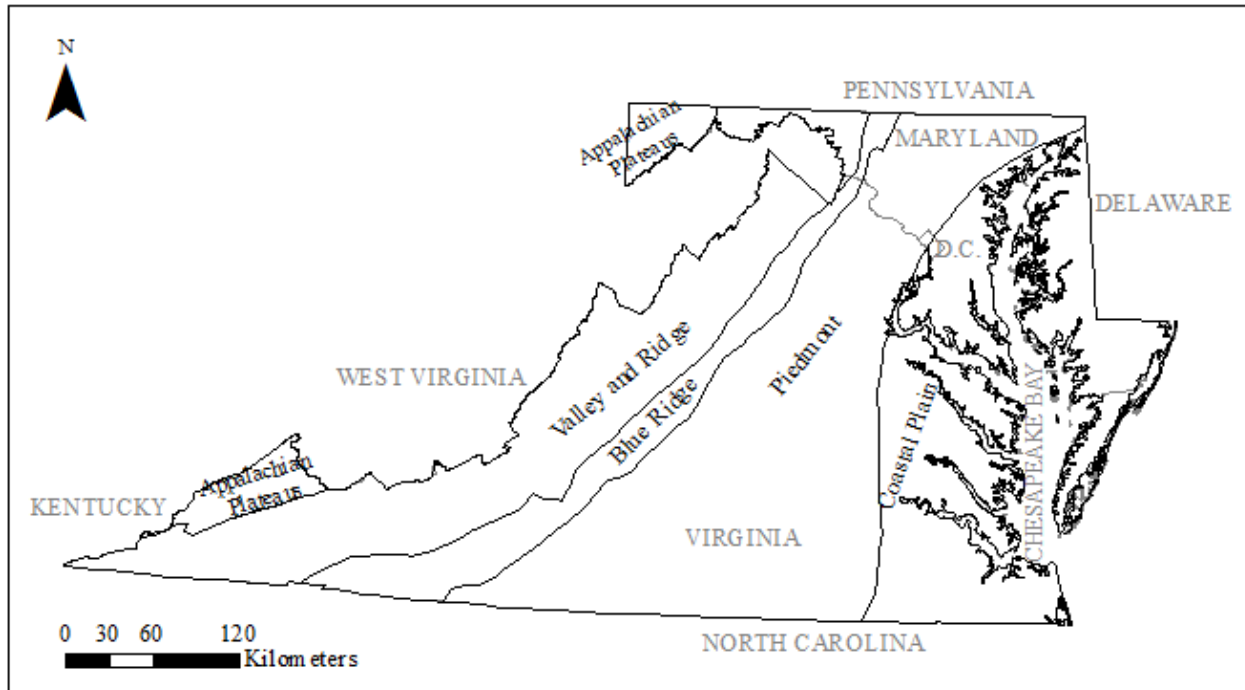


Figure 2-2: Physiographic provinces of Virginia (Fenneman and Johnson, 1946).

### 2.8 Rainfall-Runoff Modeling

If no flow data are available or the watershed under investigation is subject to flow regulation, rapid development, or effects of climate change, statistical methods may not be applicable. In such a case a rainfall-runoff model is a favorable alternative (Thomas et al., 2001; Haberlandt et al., 2008). Rainfall-runoff models transform known precipitation to synthetic discharge values (Aronica and Candela, 2007). A time series of runoff volumes (i.e., rainfall excess) or stream discharges may be analyzed using flood frequency analysis. Two types of

rainfall-runoff models are used, single event models and continuous simulation models (Thomas et al., 2001).

### *2.9 Event Models*

Single event rainfall-runoff models are used with the assumption that the frequency of a design storm equals that of the resulting flood event (Thomas et al., 2001). The U.S. Army Corps of Engineer's HEC-HMS and the USDA Natural Resources Conservation Service's TR-55 are examples of this type of model. Event modeling is easier to implement than continuous simulation due to fewer data requirements; however, it greatly simplifies the pre-storm watershed conditions (Cameron et al., 1999). This approach assumes antecedent moisture and baseflow conditions (Thomas et al., 2001). However, various initial soil moisture conditions or baseflow estimates in a watershed may lead to different flood discharges for the same rainfall event (Haberlandt et al., 2008). Additionally, event-based models are typically not calibrated to observed flood data (Thomas et al., 2001). Due to the number of assumptions required for the single event rainfall-runoff model approach, uncertainty exists in the frequency of flood discharges predicted by these models (Thomas et al., 2001).

### *2.10 Continuous Simulation*

Continuous simulation modeling does not require assumptions regarding initial watershed conditions and may be considered a favorable alternative to the single event approach (Lamb, 1999; Kay et al., 2006). Continuous simulation modeling mainly involves two parts. The first is a loss model to determine the rainfall excess from a storm event. The second part is a flood hydrograph model used to determine the runoff time series at the outlet of the watershed

(Boughton and Droop, 2003; Aronica and Candela, 2007). The loss model accounts for the interception and infiltration by simulating the wetting and drying of the watershed, while the flood hydrograph model accounts for the time delay of runoff reaching the watershed outlet. These model components operate at daily, hourly and occasionally sub-hourly time steps (Boughton and Droop, 2003). The generic conceptual continuous simulation model described avoids the assumptions required for event-based modeling. It simulates the changing antecedent moisture conditions that determine the storm runoff response for a given rainfall event. Likewise, a baseflow estimate is not required. Continuous simulation of flows also avoids the necessity of associating design flood estimates with a design storm of a specific return period. Flood estimates may instead be derived from the model flow time series (Lamb, 1999).

Continuous simulation models are often assumed to more accurately estimate flood flows than single event models because they are calibrated to observed discharges and estimate antecedent moisture conditions through water balancing (Thomas et al., 2001). Studies have supported this assumption by showing that design flows may be accurately estimated by applying flood frequency analysis to the long period of synthetic flood data generated by continuous simulation (Calver and Lamb, 1996; Lamb, 1999; Boughton and Droop, 2003). Additionally, continuous simulation has been used in a broader application of flood frequency forecasting (Young and Reynard, 2004). It provides a natural way of assessing the possible effect of climate change, by incorporating changes in climatic inputs, such as increased precipitation or potential evaporation forecasts (e.g., Kay et al., 2006). Continuous rainfall-runoff simulation, however, requires the availability of long, continuous time series of rainfall and discharge to calibrate model parameters (Aronica and Candela, 2007).

Two common continuous rainfall-runoff models are the Hydrological Simulation Program—Fortran (HSPF) and the Soil and Water Assessment Tool (SWAT). HSPF is a continuous hydrologic and water quality model developed by the USEPA (Bicknell et al., 1997). However, calibration of the many HSPF parameters is complicated enough to warrant an EPA guidance document on the subject (USEPA, 2000). Developed by the USDA Agricultural Research Service, SWAT was developed to model to impacts of land management practices. This complex model uses dozens of parameters to simulate watershed hydrology (Neitsch et al., 2002). The numerous parameters in these models and long flow time series required for calibration make model usage cumbersome and model application to ungaged systems exceedingly difficult.

### *2.11 Conceptual Models*

For rainfall-runoff modeling, models have been developed that use conceptual representations of the physical processes. Conceptual models that account for spatial variability within the watershed are “distributed models.” Watershed characteristics are treated as local values by dividing the watershed into a large number of elements or grid squares in a distributed model whereas models that assume uniform (or uniformly average) characteristics across an entire watershed or sub-watersheds are termed “lumped-parameter models” (Beven, 2012). Conceptual models hold the greatest promise in the modeling of ungaged watersheds due to the often-simplistic representations of physical processes.

Various parsimonious conceptual continuous simulation rainfall-runoff models have been developed and used to model ungaged watersheds. These models include the Probability Distributed Model (PDM), TOPMODEL, and GR4J, among others. PDM is a lumped-parameter

model where soil moisture storage is governed by a probability distribution (Moore, 2007). TOPMODEL is a semi-distributed model with only five calibration parameters (Beven and Freer, 2001). GR4J is a very simplistic lumped model with only four calibration parameters and a daily time-step developed to model rural watersheds (Perrin et al., 2003). Discussion of the application of these models to ungauged watersheds follows in the next section.

### *2.12 Regionalization of Continuous Simulation Models*

Using continuous simulation for the flood frequency estimation of ungauged watersheds is an important and ongoing area of research, especially during the last decade. The International Association of Hydrological Sciences launched the decade of the Predictions in Ungauged Basins (PUB) initiative in 2003 with the primary aim of reducing uncertainty in hydrological predictions. During this decade of the PUB, a number of researchers have studied how to transfer information from gaged sites to ungauged sites by examining the relationship of basin characteristics and model parameters. If strong correlations can be made between watershed characteristics and model parameters, then continuous rainfall-runoff simulation can be applied to ungauged sites (Calver and Lamb, 1996).

In the frequent case that the catchment of interest is ungauged or poorly gauged, conceptual model parameter values may be identified through a process of regionalization (McIntyre et al., 2005). Similar to the concept of regionalization used in the development of regional regression equations, the physically-based parameters in a conceptual model may be regionalized. For the regionalization of continuous simulation model parameters, parameter values are estimated from gaged catchments and applied to ungauged watersheds in a definable

region of consistent hydrological response (Oudin et al., 2008). A discussion of three kinds of regionalization approaches follows.

One of the most frequently used regionalization methods is based on regression (Kay et al., 2006; Young, 2006; Oudin et al., 2008; Viviroli et al., 2009). In this method, regression is used to develop a relationship between the model parameter values calibrated on gaged sites and physiographic catchment attributes (Oudin et al., 2008; Randrianasolo et al., 2011). Once these relationships have been established, one determines the parameters of an ungaged basin using the developed equations and the basin's physical and climatic attributes. The second regionalization technique is based on spatial proximity. Model parameters are calibrated from geographic neighbors and ungaged model parameters are typically estimated using a kriging approach (e.g., Parajka et al., 2005; Young, 2006; Oudin et al., 2008; Viviroli et al., 2009; Randrianasolo et al., 2011). The basis for the spatial proximity is that the physical and climatic characteristics are relatively homogeneous within a region, so that neighboring watersheds should behave similarly (Oudin et al., 2008; Randrianasolo et al., 2011). The third approach is the site-similarity method, where parameter information is transferred from a donor group of sites that are physiographically similar but not geographic neighbors. The physical watershed characteristics used are the same as those used for the regression-based approach (e.g., McIntyre et al., 2005; Parajka et al., 2005; Kay et al., 2006; Oudin et al., 2008).

Regression-based regionalization was used by Young (2006) on 260 watersheds across the U.K. using a five-parameter version of the PDM. The study showed that regression-based regionalization was more successful than the nearest neighbor approach and also that the errors in streamflow were small enough that the method could have application to water resources management in the U.K. However, a comparison study of all three regionalization approaches on

119 watersheds distributed across Wales, England, and Scotland using PDM showed that the site-similarity technique performed the best but not greatly better than the other two methods. Similarly, in a study of 320 watersheds in Australia using the IHACRES model Parajka et al. (2005) found that spatial proximity outperformed the site-similarity method. The site-similarity approach was also used successfully by Bárdossy (2007) on 16 German Rhine watersheds. In France, however, spatial proximity was the best regionalization method in a study of 913 catchments using both a six parameter version of TOPMODEL and the four parameter GR4J (Oudin et al., 2008).

Each of these techniques has produced mixed success in making predictions of flow in ungaged catchments (McIntyre et al., 2005; Kay et al. 2006; Oudin et al., 2008; Randrianasolo et al., 2011). Success, however, may be dependent upon the model selected, reliability of data, delineation of homogenous physiographic regions, and regional characteristics.

### 2.13 *Summary*

For a sufficiently gaged stream, determination of a flood frequency distribution is as simple as a statistical analysis. However, for ungaged streams, a number of techniques have been derived for flood frequency estimation. They range from statistical approaches to the use of rainfall-runoff models. Regional regression methods are limited to watersheds where the hydrologic factors affecting runoff (i.e., flow regulation, urban development, or climate change effects) have not been impacted. Single event rainfall-runoff models require assumptions about pre-storm watershed conditions, which may significantly affect model predictions. Meanwhile continuous simulation models require long time series to calibrate the many model parameters.

However, a promising technique for flood frequency estimation of ungaged watersheds is the regionalization of parsimonious conceptual rainfall-runoff models.

### **Chapter 3 Methods**

This study began with the selection of 16 watersheds from a single physiographic region and the gathering of watershed characteristics data corresponding to each watershed. One to two decades of streamflow per study gage for a total of 280 years of streamflow were modeled and calibrated to observed flows in PDM. Relationships between calibration parameters and watershed characteristics were found using regression analysis, and a single set of regression equations relating model parameter values to physical watershed characteristics for the physiographic region was sought. All possible regression relationships were evaluated using cross-validation to determine a set of regression models with the best predictive capability for the model parameters. This set of regression relationships was used to calculate model parameters for model evaluation. The watersheds were modeled using the calculated (not calibrated) model parameters, and simulated flow was compared to observed flow to evaluate the regionalized model. These major steps are represented in a flow chart in Figure 3-1.

#### *3.1 Watershed Selection*

Study watersheds were selected based on the following criteria:

1. Are located Piedmont Physiographic Province of Maryland or northern Virginia;
2. Have a drainage area of about 129.5 km<sup>2</sup> (50 mi<sup>2</sup>) or less;
3. Have at least 20 years of recorded stream discharge;

4. Less than 10% of watershed surface area is impounded; and,
5. Represent a variety of land uses were selected.

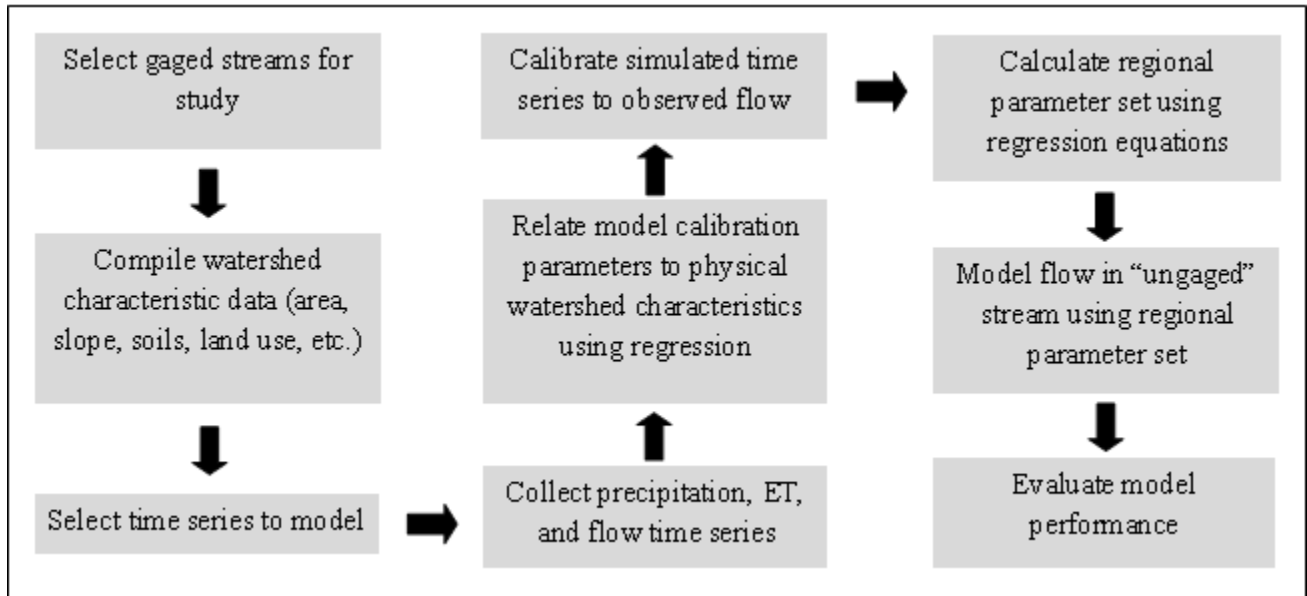


Figure 3-1. A flow chart of study methods

Sixteen watersheds were selected for this study. Five are located in the northern Virginia Piedmont while 11 are in the Maryland Piedmont. Once watersheds were selected for this study, additional characteristics were investigated. These characteristics include: basin slope, land use, hydrologic soil group, and soil water capacities. Some of these characteristics were gathered from published reports while others were calculated with spatial analysis software.

### 3.2 Watershed Area and Basin Slope

The USGS reports drainage area for their gages in many of their published studies. The drainage area of the Virginia study gages were extracted from a USGS regional regression study (Bisese, 1995). Likewise, the watershed area and basin slope data were tabulated in the Maryland

Hydrologic Report (Maryland Hydrology Panel, 2010). The basin slopes for the Virginia study gages were acquired through Jen Krstolic of the USGS (personal communication via e-mail, 13 July 2012). The basin slope reported in Table 3-1 is the average slope of the basin from upland to outlet. The drainage area for the study watersheds is provided in Table 3-1.

Table 3-1. Drainage area, basin slope, and years of record of each of the study watersheds.

Stream Gage No.	Stream Gage Name	Drainage Area (km <sup>2</sup> )	Basin Slope (km/km)	Years of Record
01496000	Northeast River at Leslie, MD	64.4	0.05	1948-1984
01496200	Principio Creek near Principio Furnace, MD	23.3	0.06	1967-1992
01581700	Winters Run near Benson, MD	89.8	0.08	1967-2013
01583000	Slade Run near Glyndon, MD	5.3	0.10	1947-2011
01584050	Long Green Creek at Glen Arm, MD	24.1	0.07	1975-2013
01584500	Little Gunpowder Falls at Laurel Brook, MD	93.3	0.08	1926-2013
01585500	Cranberry Branch near Westminster, MD	8.9	0.09	1949-2013
01588000	Piney Run near Sykesville, MD	29.5	0.08	1931-1958
01591000	Patuxent River near Unity, MD	90.3	0.11	1944-2013
01591400	Cattail Creek near Glenwood, MD	59.4	0.09	1978-2013
01591700	Hawlings River near Sandy Spring, MD	67.7	0.06	1978-2013
01646000	Difficult Run near Great Falls, VA	149.7	0.03	1935-2013
01654000	Accotink Creek near Annandale, VA	61.9	0.02	1947-2013
01658500	SF Quantico Creek near Independent Hill, VA	19.7	0.02	1951-2013
01660400	Aquia Creek near Garrisonville, VA	90.7	0.02	1972-2013
01671500	Bunch Creek near Boswells Tavern, VA	11.2	0.02	1948-1979

### 3.3 Land Use Coverage

Land use analysis was a multi-step process. First, each of the basins was delineated to facilitate the calculation of land use coverage. For the Virginia watersheds, Jen Krstolic of the USGS supplied a shapefile of the delineated watersheds (personal communication via e-mail, 13 July 2012). For the Maryland basins, each was delineated in and exported as a shapefile from

the Maryland StreamStats map interface (USGS, 2012b). The drainage areas of each of these delineations were checked against the values reported by the USGS. All were within a half percent of the reported values and accepted as sufficiently accurate.

Recent land cover data were acquired through the Chesapeake Bay Watershed Land Cover Data Series (USGS, 2013). In this data format the land use is presented as a raster (“landuse”) with 30 x 30 m cells, each coded with a number (Table 3-2) that corresponds to a specific land cover category (USGS, 2013). This data set is available for the Chesapeake Bay watershed for the years 1984, 1992, 2001, and 2006.

Table 3-2. Land cover categories present in the Chesapeake Bay Watershed Land Cover Data Series and the corresponding numeric (USGS, 2013).

Code	Land Use Description
11	Open Water
21	Developed, Open Space
22	Developed, Low Intensity
23	Developed, Medium Intensity
24	Developed, High Intensity
31	Barren Land (Rock/Sand/Clay)
41	Deciduous Forest
42	Evergreen Forest
43	Mixed Forest
52	Shrub/Scrub
71	Grassland/Herbaceous
81	Pasture/Hay
82	Cultivated Crops
90	Woody Wetlands
95	Emergent Herbaceous Wetlands

To decrease the number of land use categories considered in this study to four (e.g., urban, agricultural, forest, and open water), several of the categories were combined. All

developed areas were classified as urban. Land classified as barren was considered on a case-by-case basis. These areas were compared against aerial images acquired through the USGS EarthExplorer or Bing maps and were determined to be quarries or areas cleared for development (Microsoft Corporation, 2011; USGS, 2012c). In the latter case, these lands were classified as urban. Quarries accounted for less than 1% of any of the study watersheds. Because the majority of quarries were filled with water they were combined into the open water classification. All types of forested lands and scrub/shrub were classified as forest. Additionally, wetlands, which were less than 2% of any given watershed area and nearly all of which were woody wetlands, were classified as forested. Lastly, grasslands, pastures, and cultivated croplands were classified as agricultural lands.

Historic land use data were obtained by analyzing historic aerial photographs. The majority of these images were obtained through the USGS EarthExplorer and had, on average, a spatial scale of 1: 60,000 (USGS, 2012c). Additional images were acquired through personal correspondence with staff at Wetland Studies and Solutions, Inc. (WSSI, 2012). Tables A-1 and A-2 in the Appendix list the images and associated descriptive information (i.e., date and scale) used in the historic land use analysis of each watershed. All images were imported into ArcMap™ and geo-referenced using Bing maps as a base layer (Microsoft Corporation, 2011). Generally several images were required to cover the full extent of the watershed, and these images were joined as a mosaic.

Land use classification of the aerial images involved creating polygon feature classes, tracing areas of a particular land use, and assigning each polygon a land use code corresponding to the four main classifications described in the preceding paragraph. Anderson et al. (1976) was used to guide land use classification, and the NLCD numbering scheme was used (USGS, 2013).

Whenever possible, only areas of land use change were delineated by comparing the historic aerial photographs to the earliest available Chesapeake Bay Watershed Land Cover Data Series raster. An example of land use change analysis using polygon delineations is in Figure 3-2. In some tedious cases, where land use changes affected the majority of a watershed, the entire watershed was traced polygon-by-polygon into land use classes. The sum of the areas of polygons corresponding to each land use class was calculated and used to find percent land use coverage of the study watersheds for various time points. In the case of Piney Creek watershed (USGS gage no. 1588000), historic aerial photographs from the early 1950's were not found.

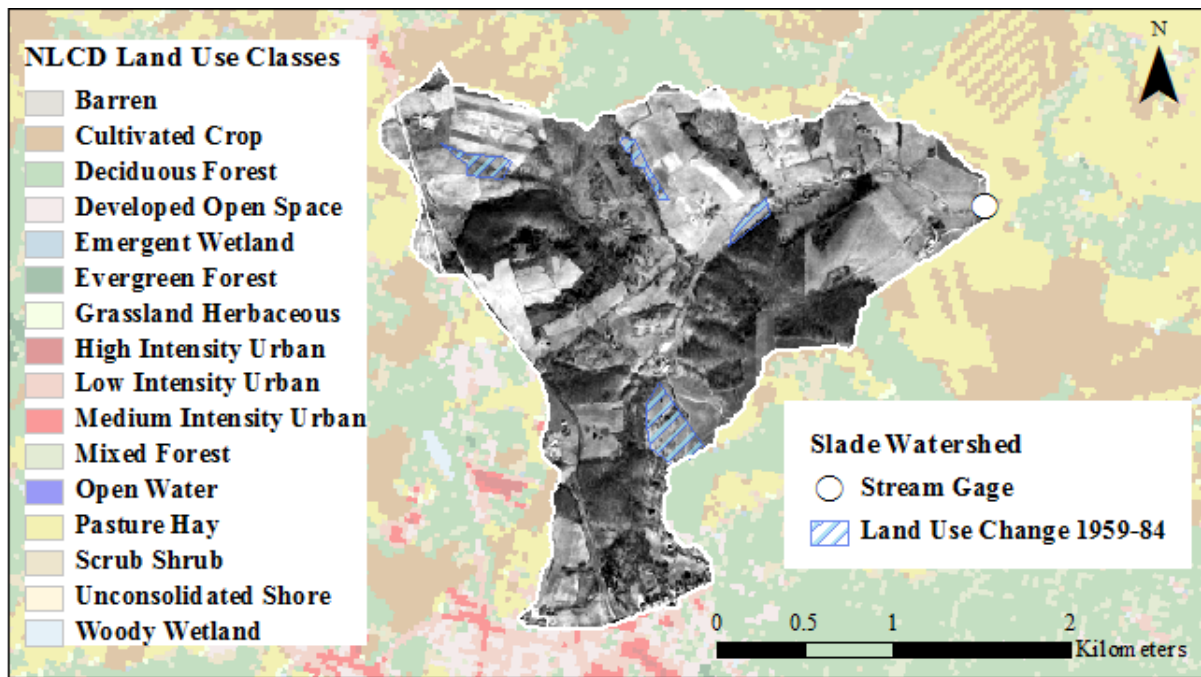


Figure 3-2. A map showing areas of land use change in the Slade Run watershed (USGS gage no. 01583000) between 1959 and 1984. A black-and-white aerial photograph shows the watershed in 1959 and the underlying layer shows a 1984 color-coded land use classification (USGS, 2013). A comparison of the two images revealed land use changes that are represented by diagonal blue hatching.

However, USGS topographic quadrant maps of the watershed from 1950 and 1953 were available and used to detect land use changes (USGS, 2012d). A summary of land use coverage for the study watersheds is available in the Appendix in Table A-3.

### *3.4 Hydrologic Soil Group Classification*

The hydrologic soil group (HSG) classification was the soil characteristic considered in this study. This classification is based on runoff potential and takes into account soil texture, depth to limiting layer, and soil transmission rate (Maidment, 1993). The data required for this analysis were downloaded from the USDA Soil Survey Geographic (SSURGO) database (NRCS, 2013). The database catalogs survey data by county and has two forms of data available for download: spatial and tabular data. In this study, the tabular data were analyzed in Microsoft® Access 2010, and the relevant data table (termed “component” in the database) was exported and joined to spatial data analyzed in ArcMap™ 10. The available spatial data includes several feature classes for each county, and the polygon feature class was selected for use in this analysis. In the polygon feature class, a polygon delineates the extent of each soil type, and a single county may contain thousands of soil type classifications. The Virginia SSURGO data included both single (i.e., A, B, C, D) and dual (i.e., A/B, B/C, C/D) HSG classifications while Maryland data included only the former. Urbanized impervious and ponded areas were not assigned a HSG in the SSURGO data set. Like a typical HSG class (e.g., A or B) this “null” value was treated as an additional HSG classification level in analysis. The polygon feature classes were clipped to match the watershed footprint (Figure 3-3), and the summary statistics tool was used to sum the area encompassed by each HSG type. The results of this analysis are tabulated in Table 3-3.

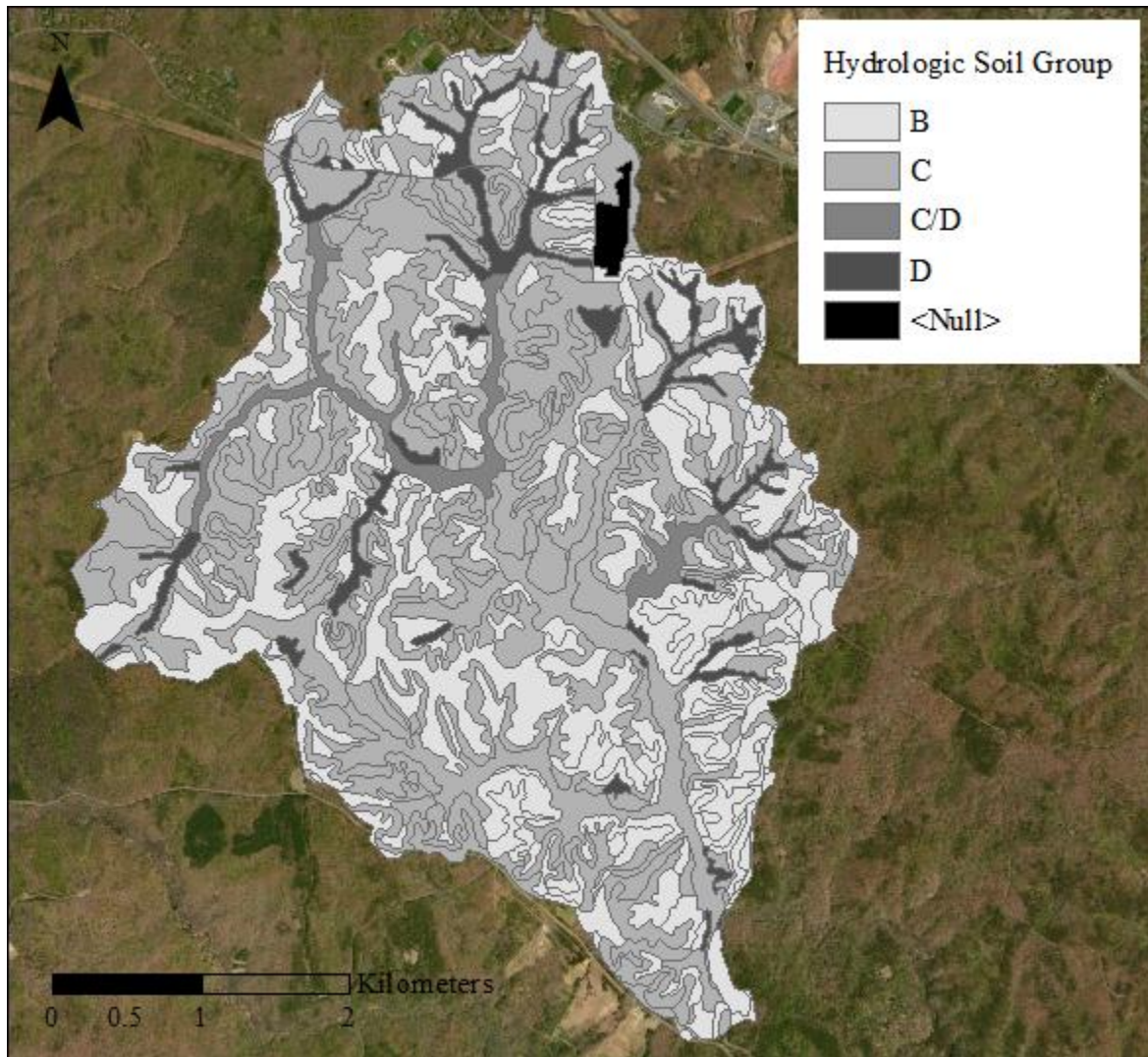


Figure 3-3. A map of hydrologic soil groups for the South Fork Quantico watershed (USGS gage no. 01658500). An urbanized area in the northeast quadrant of the watershed is classified as “<NULL>” in the SSURGO Prince William County, Virginia data set.

### 3.5 Soil Water Capacity

Volumetric field capacity and soil water saturation were also estimated using the SSURGO database. The table “chorizon” contains listings of average soil column depth (“hzdepb\_r”) and volumetric soil water content at -0.3 bar (“wthirdbar\_r”) and 0.0 bar

Table 3-3. Hydrologic soil group composition as a percent of watershed area for each of the study watersheds.

Stream Gage No.	Stream Gage Name	Watershed area encompassed by hydrologic soil group (as a percentage of total area)					
		A	B	C	C/D	D	Urban/Water
01496000	Northeast River at Leslie, MD	0.0	54.2	23.7	-	20.0	2.1
01496200	Principio Creek near Principio Furnace, MD	0.0	66.7	18.9	-	13.5	1.0
01581700	Winters Run near Benson, MD	0.6	77.5	15.8	-	5.8	0.2
01583000	Slade Run near Glyndon, MD	0.0	78.6	21.4	-	0.0	0.0
01584050	Long Green Creek at Glen Arm, MD	0.0	64.5	29.2	-	6.0	0.4
01584500	Little Gunpowder Falls at Laurel Brook, MD	0.0	77.7	17.2	-	4.6	0.4
01585500	Cranberry Branch near Westminster, MD	0.0	76.6	16.4	-	7.1	1.2
01588000	Piney Run near Sykesville, MD	0.0	78.3	10.0	-	11.8	0.0
01591000	Patuxent River near Unity, MD	0.0	78.6	15.6	-	4.6	1.1
01591400	Cattail Creek near Glenwood, MD	0.0	78.6	9.6	-	11.8	2.9
01591700	Hawlings River near Sandy Spring, MD	0.0	78.3	9.6	-	10.8	1.4
01646000	Difficult Run near Great Falls, VA	0.0	65.3	10.0	0.0	8.2	16.5
01654000	Accotink Creek near Annandale, VA	0.0	56.4	7.2	0.0	8.2	28.3
01658500	SF Quantico Creek near Independent Hill, VA	0.0	37.3	53.4	3.0	5.8	0.6
01660400	Aquia Creek near Garrisonville, VA	0.0	36.0	44.1	6.3	12.8	0.8
01671500	Bunch Creek near Boswells Tavern, VA	0.0	14.3	74.4	3.0	8.4	0.2

("wsatiated\_r"). The water content at -0.3 bar and 0.0 bar approximates the water content for the whole soil at field capacity and saturated conditions, respectively. This table was joined to the spatial data in ArcMap™, and the resulting attribute tables were exported for analysis in Excel. The soil moisture capacity was calculated by multiplying soil column depth by volumetric soil water content and taking an area-weighted average of this product. The values for soil water content at field capacity and at saturation are tabulated by watershed in Table 3-4. Soil water content data were absent from the SSURGO database for Harford County, Maryland.

Table 3-4. Maximum soil moisture content at field capacity and saturation as a depth by watershed.

Gage No.	Stream Gage Name	Field Capacity (mm water)	Maximum Saturation Soil Moisture (mm water)
01496000	Northeast River at Leslie, MD	66	644
01496200	Principio Creek near Principio Furnace, MD	62	792
01581700	Winters Run near Benson, MD	65	231
01583000	Slade Run near Glyndon, MD	54	152
01584050	Long Green Creek at Glen Arm, MD	74	311
01584500	Little Gunpowder Falls at Laurel Brook, MD	55	311
01585500	Cranberry Branch near Westminster, MD	136	152
01588000	Piney Run near Sykesville, MD	123	413
01591000	Patuxent River near Unity, MD	59	304
01591400	Cattail Creek near Glenwood, MD	73	163
01591700	Hawlings River near Sandy Spring, MD	51	791
01646000	Difficult Run near Great Falls, VA	71	163
01654000	Accotink Creek near Annandale, VA	61	1092
01658500	SF Quantico Creek near Independent Hill, VA	55	172
01660400	Aquia Creek near Garrisonville, VA	65	1092
01671500	Bunch Creek near Boswells Tavern, VA	80	404

Approximately half of the Little Gunpowder Falls watershed (gage no. 01584500) and the entire Winters Run watershed (gage no. 01581700) are within Harford County. Little Gunpowder Falls runs along the Baltimore-Harford County line, so soil water capacities calculated from Baltimore County data were used to estimate field capacity and saturation for the whole watershed. Soil water capacities for Winters Run watershed were estimated by averaging those of two neighboring watersheds, Little Gunpowder Falls and Long Green Creek (gage no. 01584050). These values were checked against soil capacity estimates of Winters Run watershed based on soil series common to both Baltimore and Harford Counties.

### 3.6 Model Description

The probability distributed model (PDM) is a conceptual continuous simulation rainfall-runoff model and was selected for this study. This model has been used successfully in many flood frequency applications worldwide [e.g., Cabus (2008) in Belgium, Lamb (1996) in the U.K., and Muncaster et al. (1997) in Australia]. In PDM, the spatial variation of soil infiltration capacity across the basin is represented by a probability distribution. Excess rainfall and groundwater recharge are routed from surface and subsurface stores, respectively, to flow at the watershed outlet. An overview of the model is shown in Figure 3-4, and more detail of these model processes follows. The following description of the model is based on the PDM users' manual (Moore, 2012), except where explicitly noted.

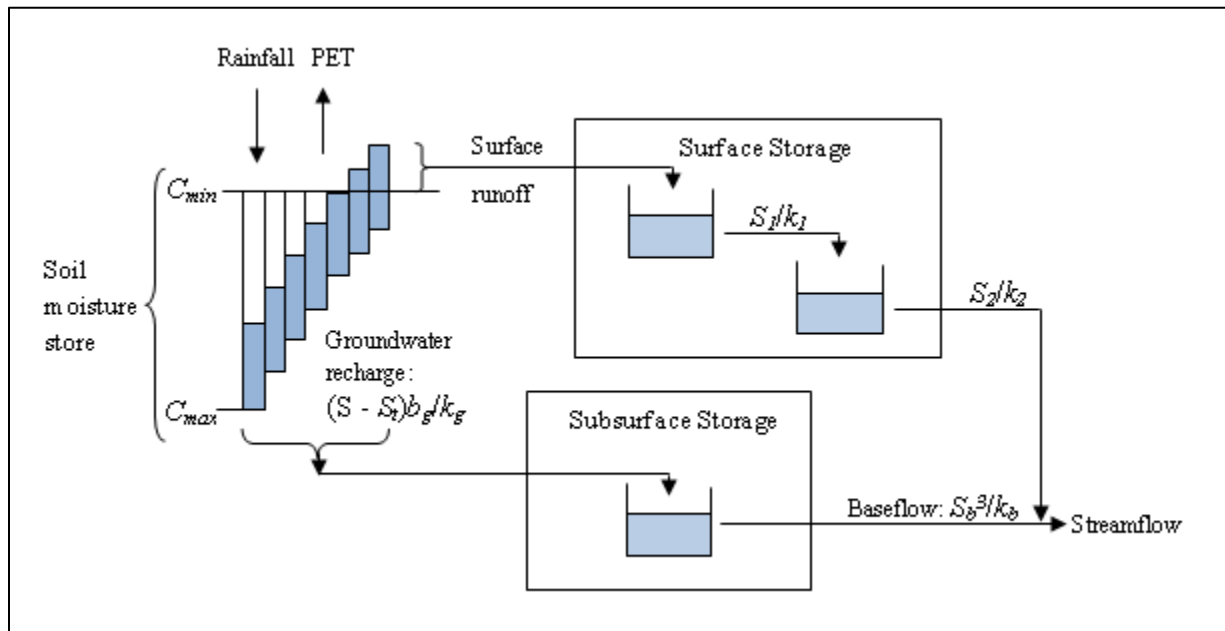


Figure 3-4. The PDM structure and parameters. Adapted from the PDM Users' Manual (Moore, 2012).

Net rainfall (precipitation minus evapotranspiration) infiltrates into a soil store. The infiltration capacity of the soil is described by a Pareto probability distribution, where the exponent of the distribution,  $b$ , controls the variability of the store capacity across the watershed. When  $b$  is less than one, there is a greater frequency of occurrence of deep stores than shallow stores in the watershed. Conversely, when  $b$  is greater than one, there is a greater frequency of occurrence of shallow stores. Also, the soil moisture capacity range is described by the parameters  $c_{min}$  and  $c_{max}$ .  $c_{min}$  can be described as the threshold value of subsurface storage required before runoff occurs, while  $c_{max}$  represents the deepest storage point in the watershed. The Pareto probability distribution of soil moisture storage can be described by the following function:

$$F(c) = 1 - \left(1 - \frac{c}{c_{max}}\right)^b \quad \text{for } 0 \leq c \leq c_{max} \quad (8)$$

where,  $F()$ = the probability distribution function;

$c$  = the storage capacity of a point in the watershed (mm);

$c_{max}$  = the maximum soil store capacity (mm); and,

$b$  = the degree spatial variability of the store capacity.

When net precipitation and accumulated soil water storage exceeds storage capacity at any point in the watershed, surface runoff begins. The accumulated rainfall excess enters the first of two surface reservoirs. The rate of release of the surface runoff is controlled by two reservoir time constants  $k_1$  and  $k_2$ . This rate and all rates in the model, denoted here by the subscript  $i$ , are calculated in the model for each interval or time-step. The rate of drainage from either reservoir is described by the following equation:

$$q_{si} = \frac{S_i}{k} \quad (9)$$

where,  $q_{si}$  = the rate drainage from the surface runoff reservoir ( $\text{mm}^3/\text{h}$ );

$S_i$  = given volume of storage in the surface runoff reservoir ( $\text{mm}^3$ ); and,

$k$  = the time constant for the surface runoff reservoir (h).

Runoff from the first reservoir flows into the second reservoir. Drainage from the second reservoir represents surface runoff at the watershed outlet. By setting  $k_2$  equal to zero, the second reservoir may be eliminated from the model.

The subsurface runoff is dependent on the volume of the soil moisture store,  $S$ . The volume of water in the store is controlled by infiltration of precipitation and losses. Losses from the soil moisture store include evapotranspiration (ET) and subsurface drainage. Calculated potential evapotranspiration (PET) is supplied to the model as an input file (or represented as a sine function if PET data are unavailable). The model uses the following ratio to estimate actual ET based on PET:

$$\frac{ET_i}{PET} = 1 - \left( \frac{S_{max} - S_i}{S_{max}} \right)^{b_e} \quad (10)$$

where,  $ET_i$  = PDM estimate of actual ET (mm);

$PET$  = calculated PET (mm);

$S_{max}$  = the total possible soil moisture storage (mm);

$S_i$  = given value of soil water storage across watershed (mm); and,

$b_e$  = exponent of evaporation function.

In addition to evaporation, water is lost from the soil moisture through subsurface drainage. This drainage is modeled as the groundwater recharge rate,  $d$ , described below:

$$d_i = \frac{(S_i - S_t)^{b_g}}{k_g} \quad (11)$$

where,  $d_i$  = rate of drainage from soil store (mm h<sup>-1</sup>);

$S_i$  = given value of soil water storage across watershed (mm);

$S_t$  = threshold basin soil water storage; water held in soil tension (mm);

$b_g$  = exponent of recharge function; and,

$k_g$  = drainage time constant (h).

The volume of groundwater recharge generated in each time step enters subsurface storage and is released according to a cubic groundwater function that follows:

$$q_{bi} = \frac{3.6 \times 10^{-6} S_{bi}^3}{k_b} \quad (12)$$

where,  $q_{bi}$  = discharge (m<sup>3</sup> s<sup>-1</sup>);

$S_{bi}$  = basin soil water storage capacity (mm); and,

$k_b$  = time constant (h).

The combination of subsurface flow and surface flow generated in each time step is the total flow from the basin outlet.

For additional model information, including non-standard model configurations, see the PDM user's manual. A summary of the model parameters described above is listed in Table 3-5.

### 3.7 Data Inputs

Three time series were used to model runoff in the study watersheds. These included daily precipitation, daily potential evapotranspiration, and daily average discharge. A daily time-

Table 3-5. Standard PDM model parameters, their function, and suggested values. Adapted from Table 1.1 of “A Practical User Guide to the PDM” (Moore, 2012).

Parameter	Unit	Description	Function	Suggested Value(s)
$f$	none	Rainfall factor	Controls runoff volume; accounts for interception or systematic error in rain gage record	1
$c_{min}$	mm	Minimum soil store capacity	Affects the time of runoff onset	0
$c_{max}$	mm	Maximum soil store capacity	Affects the time of runoff onset and soil saturation rate; feeds back to evaporation and recharge rates	75
$b$	none	Exponent of Pareto distribution	Controls the degree of spatial variability of storage capacity	0.5
$b_e$	none	Exponent in evaporation function	Affects variation between seasons or years	2.5
$k_1$	h	Time constant for release from first (or only) linear reservoir	Controls rate of rise of hydrograph	1-20
$k_2$	h	Time constant for release from second (if used) linear reservoir	Controls rate of rise of hydrograph	1-20
$k_b$	$h^{1/3}$ $mm^{2/3}$	Baseflow time constant	Controls length of hydrograph recession	5-100
$k_g$	$h\ mm^{bg-1}$	Groundwater time constant	Controls rate of aquifer recharge	10,000
$S_t$	mm	Soil tension storage capacity	Positive value prevents complete drainage of soil moisture store	0
$b_g$	none	Exponent of recharge function	Increase to magnify sensitivity of recharge rate to soil dryness	1.5
$q_c$	$m^3\ s^{-1}$	Constant flow representing a losing or gaining system	Shifts hydrograph vertically along flow axis	0
$\tau_d$	h	Time delay	Shifts hydrograph horizontally along time axis	0

step was selected due to data availability. Available historical streamflow time series from the USGS are limited to daily average flows. Likewise, the Wetbud model (Gloe, 2011), which will

eventually integrate a stream discharge frequency component based on this research, also uses a daily time step. For these reasons, all of the time series used in this model are daily values. Many previous PDM steps used a daily time step (e.g., Muncaster et al., 1997; Young and Reynard, 2004; McIntyre et al., 2005; Young, 2006), and others used hourly data (e.g., Lamb and Kay, 2004; Cabus, 2008). The selection, source, and treatment of each of these time series are described in detail below.

### 3.7.1 Measured Stream Discharge

USGS stream gages record or have recorded flow in all of the study watersheds. Daily average discharge was downloaded from the USGS National Water Information System website (USGS, 2012). Additionally, because the model was run on a non-standard time-step, each flow time series was artificially delayed one day (i.e., one time-step) by editing the streamflow data. The standard model time-step is 15 min, and in this study the model was run on a daily time-step. Because the duration of the time-step exceeded the time of concentration for the small watersheds in this study, a 24-hr delay of the observed streamflow record was necessary to match predicted and actual peaks.

### 3.7.2 Precipitation

Daily precipitation data were obtained from the National Climatic Data Center's Global Historical Climatology Network-Daily (GHCND; NCDC, 2012). Weather stations were selected based on their proximity to the centroid of the watershed of interest. The closest rain gage with a corresponding period of record was selected. Most selected weather stations were within 20 kilometers of the corresponding watersheds. Where gaps existed in the daily precipitation record

of the primary gage, the precipitation record was compared to the streamflow records. If the flow record of the adjacent stream gage(s) did not reflect an increase in discharge, the missing precipitation data point was filled with a zero. If the stream gage record did show an increase in flow, additional rain gage records were sought. These gaps were filled with either the precipitation value from the next most adjacent GHCND rain gage or the distance-weighted average of the values from the two closest rain gages. A table of the primary rain gages and the distances from the corresponding watershed centroid are listed in Table 3-6. A table (Table A-4) of additional rain gages used to fill gaps in the record of the primary gages is located in the Appendix. Additionally, a map of watersheds and the locations of all rain gages used in this study are shown in Figure 3-5 and Figure 3-6.

### 3.7.3 Potential Evapotranspiration

Potential Evapotranspiration (PET) was calculated using the Thornthwaite method (Thornthwaite, 1948):

$$PET = 16 \left( \frac{L}{12} \right) \left( \frac{N}{30} \right) \left( \frac{10T_a}{I} \right)^\alpha \quad (13)$$

where,  $PET$  = estimated potential evapotranspiration (mm/month);

$L$  = average day length (hours) of the month being calculated;

$N$  = number of days in the month being calculated;

$T_a$  = average daily temperature (degrees Celsius);

$\alpha = (6.75 * 10^{-7})I^3 - (7.71 * 10^{-5})I^2 + (1.792 * 10^{-2})I + 0.49239$ ; and,

$I = \sum_{i=1}^{12} \left( \frac{T_{ai}}{5} \right)^{1.514}$  is a heat index that depends on the 12 monthly mean temperatures,  $T_{ai}$ .

Table 3-6. Modeled stream gages and corresponding rain gages, their distance from the watershed centroid, and time periods modeled.

Stream Gage No.	Stream Gage Name	Modeled Time Periods	Primary Rain Gage(s)	Dist. from Watershed Centroid (km)
01496000	Northeast River at Leslie, MD	1957-66, 1967-76	USC00182060 Conwingo Dam	16.3
01496200	Principio Creek near Principio Furnace, MD	1967-77, 1978-87	USC00182060 Conwingo Dam	11.5
01581700	Winters Run near Benson, MD	1975-84, 1985-94	USC00180732 Benson Police	9.0
01583000	Slade Run near Glyndon, MD	1953-62, 1963-72	USC00189435 Westminster & USC00189440 Westminster 2 SSE	16.0
01584050	Long Green Creek at Glen Arm, MD	1975-84, 1985-95	USC00180732 Benson Police	9.8
01584500	Little Gunpowder Falls at Laurel Brook, MD	2002-11	USC00366289 New Park	20.6
01585500	Cranberry Branch near Westminster, MD	1962-71, 1986-95	USC00189435 Westminster & USC00189440 Westminster 2 SSE	7.5
01588000	Piney Run near Sykesville, MD	1948-57	USC00189030 Unionville	15.1
01591000	Patuxent River near Unity, MD	1969-78, 1981-90	USC00181125 Brighton Dam	15.6
01591400	Cattail Creek near Glenwood, MD	1979-88 1989-98	USC00181125 Brighton Dam USC00189750 Woodstock	13.9 17.2
01591700	Hawlings River near Sandy Spring, MD	1981-90 2000-09	USC00181125 Brighton Dam USC00182336 Damascus 3 SSW	6.2 15.1
01646000	Difficult Run near Great Falls, VA	1943-52 1984-93	USC00448737 Vienna USC00448737 Vienna	4.7 4.7
01654000	Accotink Creek near Annandale, VA	1984-93 2000-09	USC00448737 Vienna USW00013743 Washington Reagan	4.8 19.3
01658500	SF Quantico Creek near Independent Hill, VA	1989-98, 2001-10	USW00013773 Quantico MCAS	17.8
01660400	Aquia Creek near Garrisonville, VA	1987-97, 2001-10	USW00013773 Quantico MCAS	18.9
01671500	Bunch Creek near Boswells Tavern, VA	1958-67	USW00013732 Gordonsville & USC00443466 Gordonsville 3	7.6

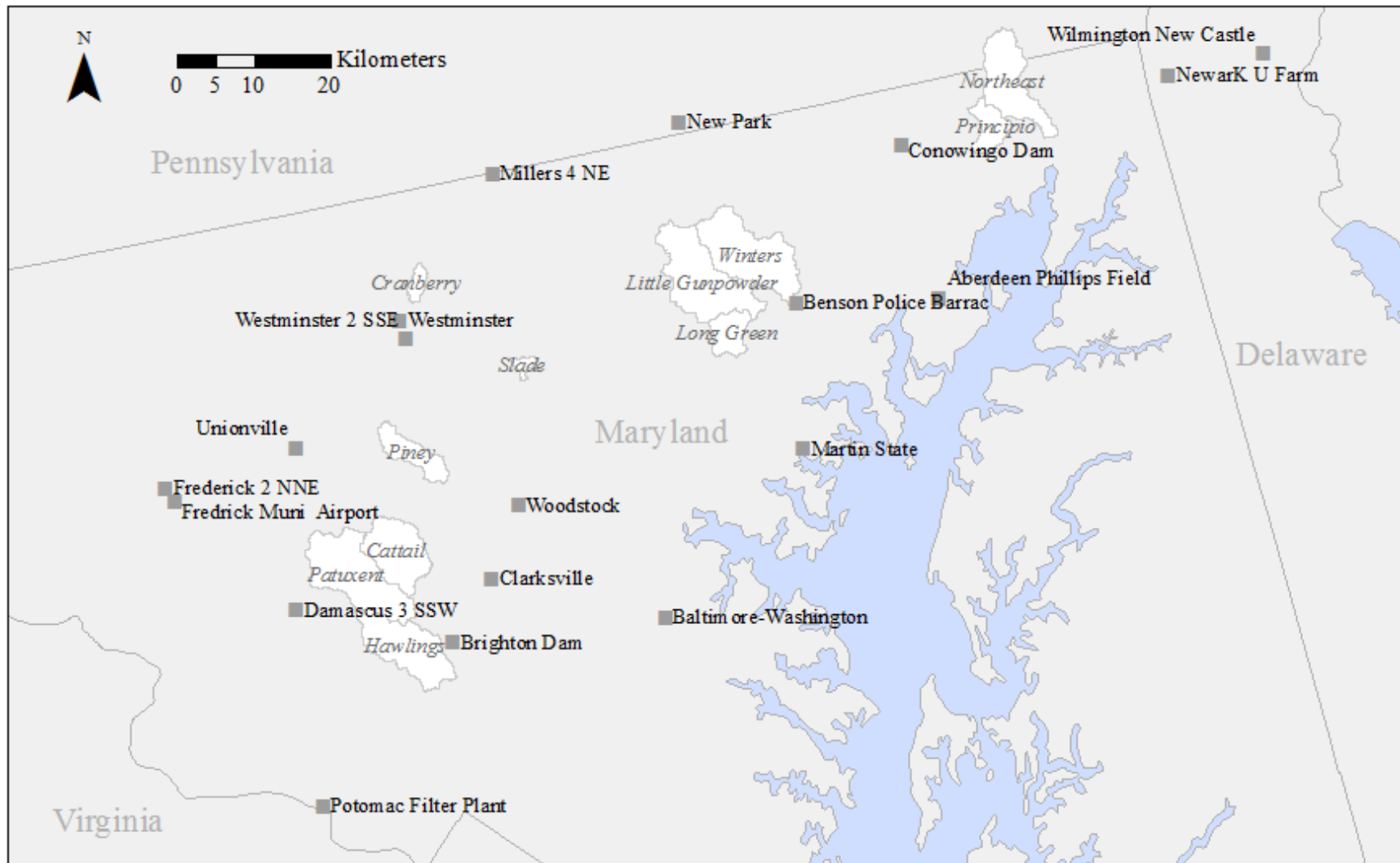


Figure 3-5. A map of Maryland watersheds with rain gages and weather stations used in this study. Watershed names are in italics and weather stations and rain gages are denoted by gray squares.

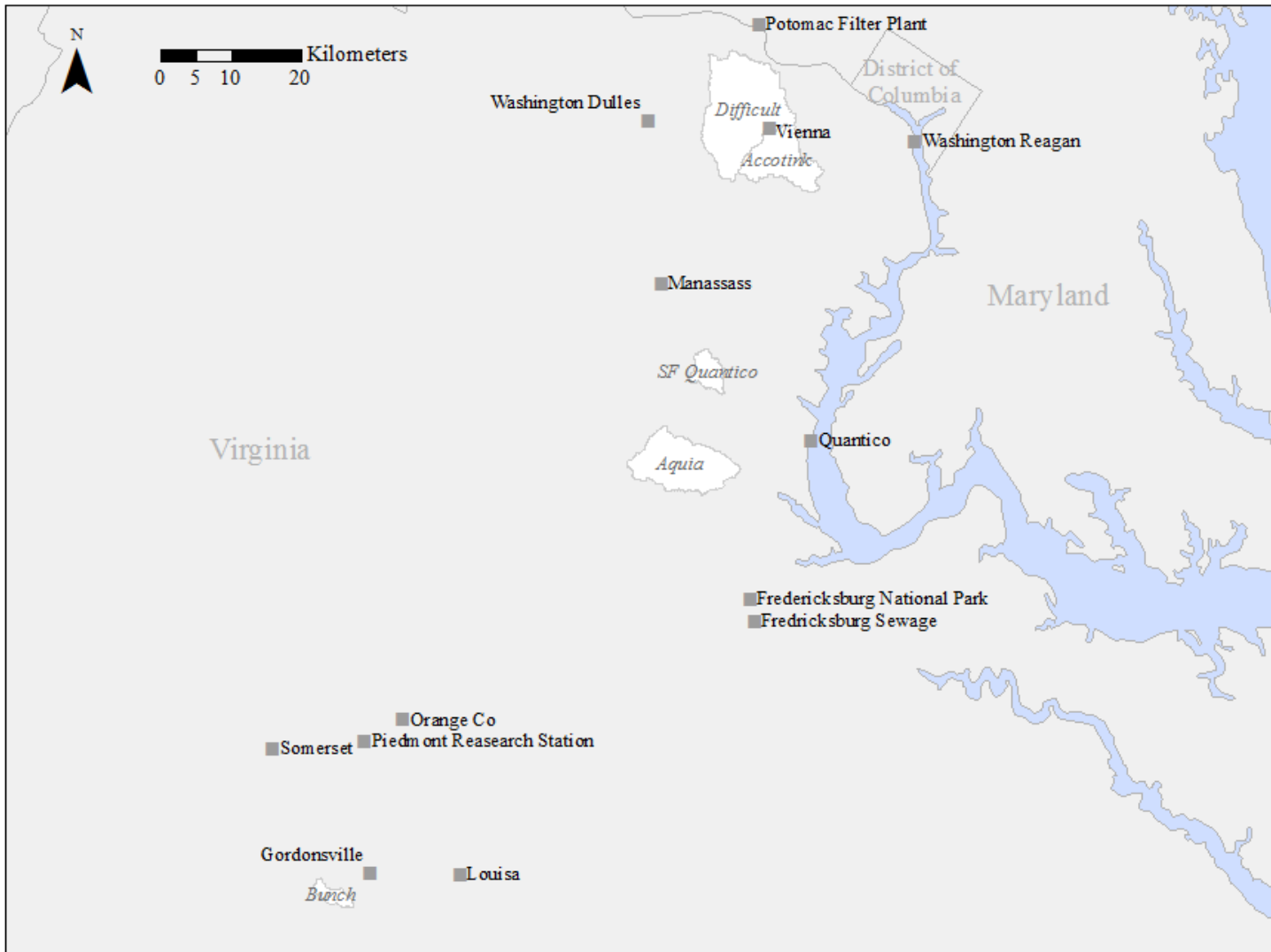


Figure 3-6. A map of Virginia watersheds with rain gauges and weather stations used in this study. Watershed names are in italics and weather stations and rain gauges are denoted by gray squares.

The limited amount of weather data available for the earlier dates modeled led to the selection of this method. The Thornthwaite method uses mean monthly temperature and site latitude to estimate monthly ET. Calculations were completed within the Wetbud model (Gloe, 2011). The weather station nearest a watershed was used to generate monthly mean temperatures and the latitude of the watershed centroid was used for the calculation. The names of the weather stations used, their distance from the respective watershed, and the latitudes of the watershed centroids are listed in Table 3-7. Additionally, maps of locations of the weather stations used for this analysis are in Figure 3-5 and Figure 3-6. Monthly values (in mm PET) were divided by the number of days in the month to produce daily PET time series.

### 3.8 Sensitivity Analysis

A sensitivity analysis was performed on two of the study watershed time periods, each on an extreme of the development spectrum. With about 64% residential and commercial development, Accotink Creek (gage no. 01654000) 1984-1993 was one of the selected watersheds for sensitivity analysis. The other watershed, South Fork Quantico Creek (gage no. 01658500), was about 96% forested during the time period of 2001-2010. Eight of the standard configuration model parameters were considered in the sensitivity analysis. These parameters include the following:  $c_{min}$ ,  $c_{max}$ ,  $b$ ,  $b_e$ ,  $k_l$ ,  $k_b$ ,  $k_g$ ,  $S_b$ ,  $b_g$ . These parameters were increased and decreased by 10%, 25%, and 50% from calibrated values. Relative sensitivity was calculated based on the following equation:

$$RS = \frac{\Delta Q}{Q_c} \quad (14)$$

Table 3-7. A summary of information used to calculate potential evapotranspiration: weather stations used for calculating mean monthly temperature, the distance between weather stations and the respective watershed, and the latitudes of the watershed centroids.

Stream Gage No.	Stream Gage Name	Weather Station Code, WBAN ID and Name	Distance from Basin Centroid (km)	Latitude of Basin Centroid (deg.)
01496000	Northeast River at Leslie, MD	724089 13781 Wilmington New Castle	33.5	N 39.70
01496200	Principio Creek near Principio Furnace, MD	724089 13781 Wilmington New Castle	37.4	N 39.66
01581700	Winters Run near Benson, MD	724067 93744 Martin State	26.6	N 39.57
01583000	Slade Run near Glyndon, MD	724060 93721 Baltimore-Washington	38.0	N 39.50
01584050	Long Green Creek at Glen Arm, MD	724067 93744 Martin State	18.1	N 39.48
01584500	Little Gunpowder Falls at Laurel Brook, MD	724067 93744 Martin State	26.1	N 39.55
01585500	Cranberry Branch near Westminster, MD	724060 93721 Baltimore-Washington	39.6	N 39.61
		724066 99999 Hagerstown Regional	67.1	
01588000	Piney Run near Sykesville, MD	999999 13730 Frederick	31.5	N 39.42
01591000	Patuxent River near Unity, MD	724060 93721 Baltimore-Washington	41.1	N 39.29
01591400	Cattail Creek near Glenwood, MD	724060 93721 Baltimore-Washington	36.3	N 39.31
01591700	Hawlings River near Sandy Spring, MD	724060 93721 Baltimore-Washington	34.2	N 39.20
01646000	Difficult Run near Great Falls, VA	724050 13743 Washington Reagan	25.5	N 38.93
		724030 93738 Washington Dulles	12.3	
01654000	Accotink Creek near Annandale, VA	724030 93738 Washington Dulles	18.8	N 38.86
01658500	SF Quantico Creek near Independent Hill, VA	724035 13773 Quantico MCAF	17.8	N 38.61
01660400	Aquia Creek near Garrisonville, VA	724035 13773 Quantico MCAF	18.9	N 38.50
01671500	Bunch Creek near Boswells Tavern, VA	722167 99999 Orange County	27.1	N 38.05

where,  $RS$  = relative sensitivity;

$\Delta Q$  = change in discharge corresponding to a specified change in model parameter value ( $\text{m}^3/\text{s}$ ); and,

$Q_c$  = discharge corresponding to calibrated parameter set ( $\text{m}^3/\text{s}$ ).

The resulting values for a representative baseflow, small peak (approximately a  $Q_2$ ), and large peak (approximately a  $Q_5$ ) were recorded and used to tabulate relative sensitivity.

### 3.9 Calibration

Of the 13 model parameters in the standard PDM configuration, four (i.e.,  $k_g$ ,  $k_l$ ,  $k_b$ ,  $b$ ) were calibrated by comparing simulated flows to observed discharge. These parameters were selected based on a sensitivity analysis, previous studies (e.g., Lamb, 1999; Lamb and Kay, 2004; Young and Reynard, 2004; Young, 2006), and local hydrologic considerations. Two additional parameters were estimated based on soil characteristics of the study watersheds. The maximum soil moisture storage depth,  $c_{max}$ , and the threshold soil storage,  $S_t$ , were estimated using soil survey data.  $S_t$ , the quantity of water that cannot be drained to groundwater, was initially set to the watershed average field capacity as a depth. Likewise,  $c_{max}$  was initially set to the maximum watershed soil moisture saturation depth. A description of the calculation of these values is in Section 3.5.

The remaining seven parameters were unchanged from their default recommended values. The rainfall factor,  $f$ , used to correct for a systematic error of a rain gage or interception, was unchanged from the recommended value of 1. The shallowest depth of subsurface storage at any point in the watershed,  $c_{min}$ , was also held constant. All of the study watersheds have impervious areas, which allow no storage before runoff commences; therefore,  $c_{min}$  was set to zero (Lamb,

1999; Lamb and Kay, 2004; Young and Reynard, 2004; Young, 2006). Additionally, because less than 10% of the drainage area of any of the study watersheds is impounded, the watersheds were modeled as having a single surface runoff reservoir. To remove the second reservoir  $k_2$  was set to zero. The constant flow parameter,  $q_c$ , which accounts for systematic gains or losses of stream discharge was also kept constant at zero for model calibration. Likewise, the time delay parameter,  $\tau_d$ , was also held constant at zero. The exponent of the groundwater recharge function,  $b_g$ , was unchanged from its default value of 1.5. Although a sensitivity analysis showed  $b_g$  to have an effect on baseflow, the calibration of the parameter did not significantly improve the model fit (i.e., decrease the objective function). Additionally, in none of the previously mentioned studies was  $b_g$  calibrated. Lastly, a sensitivity analysis showed that the parameter  $b_e$  had little effect on mid-range flows, which are the focus of this study.

Calibration of simulated flows to observed flows begins with calibrating the parameters that govern long term watershed hydrologic response. Baseflow parameters (i.e.,  $c_{max}$ ,  $k_g$ ,  $S_b$ , and  $b$ ) were either set based on soil moisture characteristics or manually calibrated per the suggestion of the PDM User's Manual. Calibration to baseflow was done visually by comparing predicted and observed flows. The model parameters that primarily govern short term hydrologic response or peak flows (i.e.,  $k_1$ ,  $k_b$ , and  $b$ ) were calibrated using an automatic optimization routine provided within the PDM calibration shell.

### 3.9.1 Objective Function

The objective function selected for automatic optimization of the model was root mean square error (RMSE). Of the objective functions considered (e.g., RMSE, RMSE of  $\log_{10}$  error,

RMSE of error in square roots), RMSE gave the most weight to higher flows; whereas the other options were sensitive to baseflow. The equation describing RMSE follows:

$$RMSE = \sqrt{n^{-1} \sum e_t^2} \quad (13)$$

where,  $n$  = number of observations; and,

$e_t$  = difference between observed and simulated flow at time  $t$ .

### 3.9.2 Calibration to Baseflow

Baseflow calibration was done through the manual adjustment of several parameters:  $c_{max}$ ,  $k_g$ ,  $S_b$  and  $b$ . The initial values of two of these were based on estimates from soil survey data.  $S_t$  and  $c_{max}$  were initially set to the watershed average field capacity and maximum soil moisture capacity, respectively. The remaining two baseflow parameters,  $k_g$  and  $b$ , were adjusted manually to fit observed flow. In some cases the initial  $c_{max}$  value was too large to obtain a good baseflow fit. This was the case for several watersheds where the maximum soil moisture store calculated from SSURGO data was in excess of 1000 mm. The default  $c_{max}$  value is 75 mm, but in the few instances where calibrated values have been published,  $c_{max}$  has exceeded 200 mm (Young and Reynard, 2004). In the cases where the initial  $c_{max}$  was too great to obtain a good fit, the parameter value was reduced until a good visual fit was obtained. The parameters  $k_g$  and  $b_g$  were adjusted until the best visual fit was obtained.

### 3.9.3 Calibration to Peak Flow

Automatic optimization was used to calibrate the parameters dominating peak flow. The objective function used for this calibration was RMSE (Equation 15). The calculation of the

objective function used only a range of peak discharge values, the selection of which is described in the subsequent section. Three parameters were considered in this calibration:  $k_I$ ,  $k_b$ , and  $b$ . These parameters were calibrated using automatic optimization within the PDM Calibration Shell. They were calibrated one at a time in descending order of sensitivity:  $k_I$ ,  $b$ , and  $k_b$ .

Optimization was run in the PDM Calibration Shell, and the optimized value of each parameter was considered for feasibility. If the optimized parameter for any of the calibrated time series fell outside of the range of values suggested by the PDM User's Manual, the time series of observed and simulated flows were examined for large discrepancies that could contribute to large errors in the objective function. For several gages, summer storms events recorded by the stream gage were misrepresented by the precipitation captured at the rain gage. In the case that a large storm event measured at the rain gage was not reflected in a significant increase in streamflow, the precipitation value was removed from the record. In the case when streamflow increased dramatically without significant precipitation being recorded by the rain gage, the stream discharge value was removed from the record and streamflow was set equal to that of the previous day. A record of these changes is available in Table A-5 in the Appendix.

In some cases the parameter  $k_b$  optimized beyond the suggested maximum of the value. This parameter controls the rate of groundwater discharge. A high  $k_b$  value relates to a fast release rate of groundwater and is indicative of a flashy hydrograph. Because sensitivity analysis revealed baseflow discharges to be sensitive to changes in  $k_b$  with values in excess of the suggested value (i.e., 100), the parameter was allowed to optimize beyond this value. In a study by Young and Reynard (2004) using PDM for a parameter regionalization in the U.K., they also calibrated  $k_b$  to values well above (e.g., 683, 1673) the values suggested in the PDM user manual.

### 3.9.4 Specifying a Range of Flows

The PDM Calibration Shell allows the user to specify a range of observed flows to use in the calculation of the objective function. Observed discharge values outside the specified range do not contribute to the objective function. The selected endpoints (i.e.,  $q_{\min}$  and  $q_{\max}$ ) of this range for this study correspond to the discharge with twice the magnitude of baseflow (i.e.,  $Q_{2xBF}$ ) and the discharge with an average return period of ten years (i.e.,  $Q_{10}$ ), respectively. This specific range of flows was selected because they bracket those flows that are generally accepted as responsible for shaping channel geometry (bankfull or effective discharge). Since the final application of this modeling procedure will be for stream and wetland restoration design, this range of flows was considered the most important to accurately capture. The value of  $Q_{2xBF}$  was estimated by visually examining the stream hydrograph of the decade to be modeled. For each watershed, spring baseflow was estimated and doubled to generate the  $Q_{2xBF}$ . Statistical analysis was used to generate the  $Q_{10}$  values for each study watershed.

The U.S. Army Corps of Engineers Statistical Software Package (HEC-SSP) was used to perform a peak flow analysis of daily average flows (Brunner and Fleming, 2010). The full period of record of daily average discharge for each USGS gage was downloaded and used in a volume-frequency analysis of peaks of one day duration. The analyses used annual maxima for each calendar year and station skew, and the maxima were fitted to a log-Pearson Type III distribution. The discharges with an annual exceedance probability of 10% or the  $Q_{10}$  values were tabulated and are presented in Table 3-8 along with the  $Q_{2xBF}$  for each of the study gages.

Table 3-8. Discharge values of twice that of baseflow ( $Q_{2xBF}$ ) and of an average annual exceedance probability of ten percent ( $Q_{10}$ ) for each of the study gages.

Stream Gage No.	Stream Gage Name	$Q_{2xBF}$ ( $m^3/s$ )	$Q_{10}$ ( $m^3/s$ )
01496000	Northeast River at Leslie, MD	3.0	52
01496200	Principio Creek near Principio Furnace, MD	1.0	19
01581700	Winters Run near Benson, MD	6.0	63
01583000	Slade Run near Glyndon, MD	0.3	2
01584050	Long Green Creek at Glen Arm, MD	2.0	12
01584500	Little Gunpowder Falls at Laurel Brook, MD	6.0	49
01585500	Cranberry Branch near Westminster, MD	0.6	5
01588000	Piney Run near Sykesville, MD	1.6	16
01591000	Patuxent River near Unity, MD	6.0	53
01591400	Cattail Creek near Glenwood, MD	2.6	30
01591700	Hawlings River near Sandy Spring, MD	4.0	44
01646000	Difficult Run near Great Falls, VA	6.0	109
01654000	Accotink Creek near Annandale, VA	2.0	58
01658500	SF Quantico Creek near Independent Hill, VA	0.8	13
01660400	Aquia Creek near Garrisonville, VA	5.0	62
01671500	Bunch Creek near Boswells Tavern, VA	0.8	10

### 3.10 Regionalization of Model Parameters by Regression

To apply the PDM to ungaged watersheds in the Piedmont physiographic province, the calibrated model parameters were related to watershed characteristics using regression analysis.

All of the statistical analyses were performed in R, and a copy of the code used is available in the Appendix. The calibrated model parameters were checked for correlation using both the Spearman and Kendall tests. Each parameter calibrated (i.e., not definitely set based on soil properties;  $c_{max}$ ,  $b$ ,  $k_l$ ,  $k_b$ ,  $k_g$ ) was plotted against all potential explanatory variables (i.e., watershed characteristics).

The watershed characteristics considered include watershed area (in  $km^2$ ), watershed slope, channel slope, a numerical index of the HSG, and percent of watershed area encompassed by urban, agricultural, forested, or open water land use. The numerical index representing HSG was calculated by assigning each class a numerical value where HSG A was represented by 1, HSG

A/B was represented by 1.5, HSG B was assigned 2, etc. The impervious lands classified as “NULL” in the SSURGO data set were assigned a 5. These indexed HSG values were area-weighted for each watershed to yield a single HSG index for each watershed.

The presence and shape of trends were noted prior to conducting regression analysis. Each model parameter and watershed characteristic was tested for normality and transformed until a normal or near-normal distribution was obtained. Stepwise regressions were performed using the MASS package in R (Venables and Ripley, 2002). The results of the stepwise regression were checked for over-parameterization. When multiple correlated explanatory variables were present in a regression model, all but the variable with the most statistically significant relationship was removed. The Prediction Error Sum of Squares (PRESS) statistics of models using the remaining explanatory variables were compared using the package MPV in R (Montgomery et al., 2001). The PRESS statistic is a “leave one out” validation-type estimator of error, and a lower value indicates better quality model (Helsel and Hirsch, 1992). The model with the lowest PRESS statistic was selected, and diagnostic plots of model residuals were generated to check for normality, homoscedasticity, and leverage points.

Once a best general model was selected, it was used to generate watershed-specific regression equations in a “leave one out” regression analysis. Each watershed was removed in turn from the pool of all watersheds and a set of regression models independent of that watershed was calculated. Additionally the model coefficients, adjusted correlation coefficient ( $R^2$ ), regression p-value, and PRESS statistic were tabulated. This was repeated for all watersheds. The regression equations generated for each parameter were ranked one through sixteen based on PRESS statistics, where the lowest PRESS value was ranked superior (i.e., 1). The set of equations with the lowest sum of ranked values was selected as the best, most robust model set. The resulting set

of equations relating PDM parameters to watershed characteristics was used for model evaluation. Also, by using “leave one out” regression analysis, one watershed (and two time series) was available for independent model evaluation.

### 3.11 Model Evaluation

The regionalized model parameters were used for model evaluation. The best set of regression equations were used to calculate PDM parameters  $c_{max}$ ,  $b$ ,  $k_I$ , and  $k_g$  for each watershed. The regional average or average calibration value was used to calculate  $k_b$ . The model parameter  $S_t$  was set to the watershed area-averaged field capacity in mm water. For each time series analyzed, values for  $c_{max}$ ,  $b$ ,  $k_I$ ,  $k_b$ ,  $k_g$ , and  $S_t$  were calculated based on watershed properties. These values were entered into the corresponding PDM input file, and the resulting hydrographs were analyzed for goodness-of-fit measures.

### 3.12 Goodness-of-Fit Measures

Goodness-of-fit measures were calculated to provide an indication of how well the modeled data fit observed data for the calibration and evaluation simulations. The measures considered included the RMSE, the Nash Sutcliffe Efficiency (NSE) rating, and a FFA of annual maxima of daily mean discharge for observed and simulated flows. The equation for NSE model efficiency rating follows (Nash and Sutcliffe, 1970):

$$NSE = 1 - \frac{\sum_{t=1}^T (Q_o^t - Q_m^t)^2}{\sum_{t=1}^T (Q_o^t - \bar{Q}_o)^2} \quad (16)$$

where,  $Q_o$  = observed discharge ( $m^3/s$ );

$Q_m^t$  = modeled discharge ( $m^3/s$ ) at time  $t$ ; and,

$Q_o^t$  = observed discharge ( $m^3/s$ ) at time  $t$ .

A NSE rating can range from negative infinity to one. A NSE of one is indicative of a perfect model; a NSE rating of zero indicates that model predictions are as accurate as the mean of the observed data. A negative NSE indicates that the mean of the observed data is a better predictor than the model.

The RSME was calculated within the PDM calibration shell, and the NSE rating was calculated in R using the HydroGOF package (Zambrano-Bigiarin, 2012). Finally, the evaluation time series was evaluated in terms of flood frequency prediction. The partial duration series with an average of two independent flood peaks per year for the observed and model evaluation flows were compared using the Kolmogorov–Smirnov test. Additionally a FFA was performed on the observed and model evaluation time series. The annual peak discharges for both time series were fit to a log Pearson Type III distribution using station skew in HEC-SSP Version 2.0, and discharges of standard return periods (i.e., 2, 5, 10, 25, 50, and 100 yrs) were calculated. These were compared to discharges for the same return periods calculated from USGS peak discharge regional regression equations (Thomas and Moglen, 2010; Austin et al., 2011).

## **Chapter 4 Results and Discussion**

### *4.1 Calibration*

PDM was calibrated for one or two decades of streamflow for each of the selected study watersheds. The number (i.e., one or two) of time series evaluated for each watershed was dependent upon the availability of data (e.g., land use, precipitation, streamflow). The four (of 16) watersheds that were evaluated for only one time period include: Little Gunpowder Falls (gage no.

01584500), Cranberry Branch (gage no. 01585500), Piney Run (gage no. 01588000), and Bunch Creek (gage no. 01671500). Two decades of discharge were evaluated for each of the remaining 12 watersheds. The calibrated model parameters are shown in Table 4-1. The hydrograph of observed and PDM simulated flow in Accotink Creek near Annandale, VA (gage no. 01654000) from February through June of 1984 is in Figure 4-1. The calibration of this flow time series was fairly successful due to the quality of the precipitation data. The rain gage was located within the 0.5 km of the watershed boundary and had no data gaps for the time periods used. This successful calibration is evident in the segment of the 10 yr hydrograph depicted in Figure 4-1.

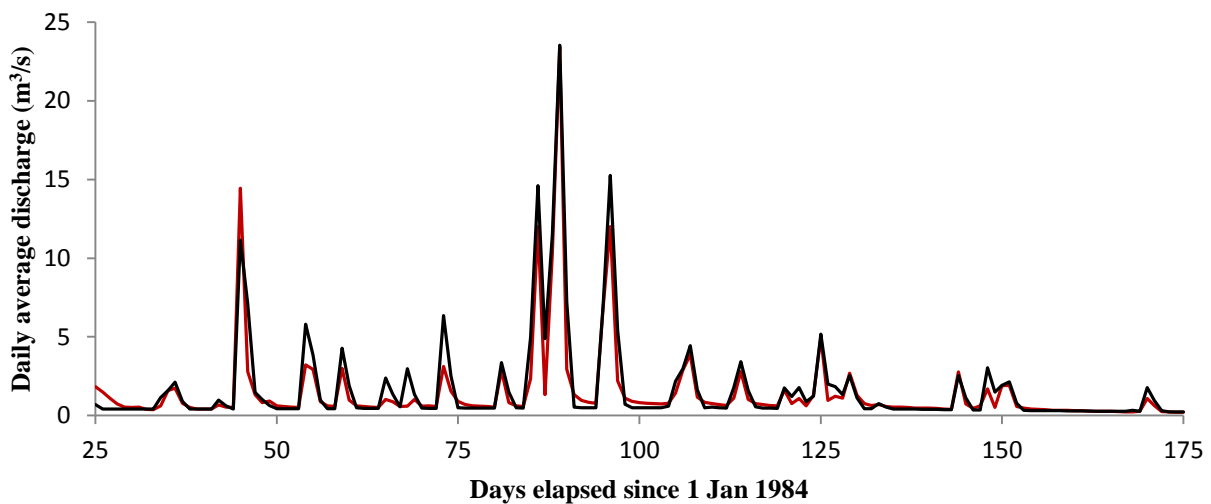


Figure 4-1. A hydrograph of observed (red) and PDM calibrated simulated (black) flow in Accotink Creek near Annandale, VA (gage no. 01654000) from February through June of 1984.

The calibrated PDM parameters for the study watersheds were similar to values published in other studies. The values for  $c_{max}$  and  $b$  fall well within the range of parameter values (0-500 and

Table 4-1. Calibrated model parameters for all of the study watershed time series. The watershed time series are described by both USGS stream gage number and time period modeled.

Stream Station No.	Stream Station Name	Modeled Time Period	Calibrated Parameter Value					
			$c_{max}$	$b$	$k_I$	$k_b$	$k_g$	$S_t$
01496000	Northeast River at Leslie, MD	1/1/1957 - 12/31/1966	240	0.45	6.6	6	25000	66
01496000	Northeast River at Leslie, MD	1/1/1967 - 12/31/1976	300	0.79	13.6	3	16000	66
01496200	Principio Creek near Principio Furnace, MD	6/1/1968 - 5/31/1977	310	0.51	11.6	223	18000	62
01496200	Principio Creek near Principio Furnace, MD	1/1/1978 - 12/31/1987	225	0.59	18.1	171	17000	62
01581700	Winters Run near Benson, MD	1/1/1975 - 12/31/1984	231	0.61	20.0	243	7000	65
01581700	Winters Run near Benson, MD	1/1/1985 - 12/31/1994	231	0.58	16.4	168	10000	65
01583000	Slade Run near Glyndon, MD	1/1/1953 - 12/31/1962	311	0.70	5.2	324	5000	54
01583000	Slade Run near Glyndon, MD	1/1/1963 - 12/31/1972	311	0.96	2.9	68	7000	54
01584050	Long Green Creek at Glen Arm, MD	10/1/1975 - 9/30/1985	311	0.40	18	313	15000	74
01584050	Long Green Creek at Glen Arm, MD	10/1/1985 - 9/30/1995	311	0.48	15	270	21000	74
01584500	Little Gunpowder Falls at Laurel Brook, MD	1/1/2002 - 12/31/2011	152	0.34	37	66	8000	55
01585500	Cranberry Branch near Westminster, MD	1/1/1986 - 12/31/1995	413	0.54	18	389	11500	136
01588000	Piney Run near Sykesville, MD	1/1/1948 - 12/31/1957	304	0.38	14	347	3000	123
01591000	Patuxent River near Unity, MD	1/1/1969 - 12/31/1978	163	0.17	28	242	12000	59
01591000	Patuxent River near Unity, MD	1/1/1981 - 12/31/1990	163	0.44	26	217	9000	59
01591400	Cattail Creek near Glenwood, MD	1/1/1979 - 12/31/1988	240	0.55	22	276	15000	73
01591400	Cattail Creek near Glenwood, MD	1/1/1989 - 12/31/1998	280	0.34	17	235	17000	73
01591700	Hawlings River near Sandy Spring, MD	1/1/1981 - 12/31/1990	163	0.48	22	107	13000	51
01591700	Hawlings River near Sandy Spring, MD	1/1/2000 - 12/31/2009	163	0.38	25	108	15000	51
01646000	Difficult Run near Great Falls, VA	1/1/1943 - 12/31/1952	270	0.52	28	299	18000	71
01646000	Difficult Run near Great Falls, VA	1/1/1984 - 12/31/1993	264	0.44	19	330	22000	71
01654000	Accotink Creek near Annandale, VA	1/1/1984 - 12/31/1993	153	0.38	4	286	10000	61
01654000	Accotink Creek near Annandale, VA	1/1/2000 - 12/31/2009	230	0.75	4	287	15000	61

Table 4-1. (cont.) Calibrated model parameters for all of the study watershed time series. The watershed time series are described by both USGS stream gage number and time period modeled.

Stream Station No.	Stream Station Name	Modeled Time Period	Calibrated Parameter Value					
			$c_{max}$	$b$	$k_I$	$k_b$	$k_g$	$S_t$
01658500	SF Quantico Creek near Independent Hill, VA	1/1/1989 - 12/31/1998	172	0.44	12	293	9000	55
01658500	SF Quantico Creek near Independent Hill, VA	1/1/2001 - 12/31/2010	172	0.78	19	107	8000	55
01660400	Aquia Creek near Garrisonville, VA	10/17/1987 - 10/16/1997	200	0.58	5	127	10000	66
01660400	Aquia Creek near Garrisonville, VA	1/1/2001 - 12/31/2010	230	0.45	4	4	15000	66
01671500	Bunch Creek near Boswells Tavern, VA	1/1/1958 - 12/31/1967	240	0.53	13	10	10000	80

0-2, respectively) reported by McIntyre et al. (2005) in a study of U.K. watersheds using PDM with a daily time-step. Likewise, Young and Reynard (2004) reported calibrated values for  $c_{max}$  ranging from 102 to 217 and values of  $b$  ranging from 0.1 to 3.8 for five catchments also modeled with a daily time-step in the U.K. The calibration values for the Virginia and Maryland watersheds fall within the range reported by McIntyre and are a little greater than those reported by Young and Reynard, suggesting that the Virginia and Maryland watersheds have a slightly greater soil moisture storage capacity. Young and Reynard (2004) published values of the fast release storage constant,  $k_I$ , ranging from 49 to 117. All of the  $k_I$  values for the Virginia and Maryland watersheds are below this range for the U.K. watersheds, indicating a much larger magnitude of flow for a given precipitation depth. This difference could be attributed to climatic differences and land development. In general precipitation events in the eastern U.S. tend to be relatively shorter and more intense than those in the U.K, so a greater runoff potential for the Virginia and Maryland watersheds is expected. Also, the

U.K. studies do not mention the presence or extent of land development in their study watersheds. The calibrated values for  $k_b$  and  $k_g$  are consistent with those reported by Cabus (2008) and Young and Reynard (2004). Finally, none of the studies using PDM reported a non-zero value for  $S_t$ , the quantity water, as a depth, held in soil tension.

The calibrated flow time series were checked for goodness-of-fit using the RMSE and NSE ratings (Table 4-2). The NSE was evaluated for all flows and peak flows with a magnitude greater than twice baseflow but less than a ten-year flood, based on daily average discharge. The NSE ratings were generally poor for the calibrated watersheds. In several cases, however, the model performed favorably, having NSE ratings of 0.5 or greater. Two examples are Accotink Creek (gage no. 01654000) and Difficult Run (gage no. 01646000). Both of these watersheds have rain gages inside of or within 0.5 km of the watershed boundary. This proximity to the rain gage may have had a large impact on model performance as measured by the NSE rating. However, when the entire data set is considered, no correlation between NSE and distance to primary rain gage is detected. The negative NSE ratings reflect poor model performance. A NSE less than zero indicates that the mean of observed discharges is a better predictor of flow than the model. The long model time-step could have also contributed to poor model performance. Because the watersheds selected in this study are small, the lack of temporal resolution in the precipitation record may have been an issue.

The Cabus (2008) study of 98 Flemish watersheds reported an average NSE of 0.58. Summer months were not considered in the calculation of the NSE, and ten of the watersheds were removed from the study because an adequate NSE value (0.35) could not be obtained through calibration. Having much larger watersheds, ranging up to 800 km<sup>2</sup> compared to 150 km<sup>2</sup> in this

Table 4-2. Goodness-of-fit measure for the calibrated time series. The RMSE was calculated for all flows (All Q) and flows between two times baseflow ( $Q_{2 \times \text{BF}}$ ) and a ten-yr discharge ( $Q_{10}$ ). The Nash Sutcliffe Efficiency rating was evaluated for all flows and peak flows, those exceeding  $Q_{2 \times \text{BF}}$ .

Stream Station No.	Stream Station Name	Modeled Time Period	RMSE ( $\text{m}^3/\text{s}$ )		Nash Sutcliffe Efficiency	
			$Q_{2 \times \text{BF}} - Q_{10}$	All Q	$> Q_{2 \times \text{BF}}$	All Q
01496000	Northeast River at Leslie, MD	1/1/1957 - 12/31/1966	5.5	1.4	-0.48	0.37
01496000	Northeast River at Leslie, MD	1/1/1967 - 12/31/1976	5.8	2.0	0.33	0.50
01496200	Principio Creek near Principio Furnace, MD	6/1/1968 - 5/31/1977	2.4	0.6	0.21	0.42
01496200	Principio Creek near Principio Furnace, MD	1/1/1978 - 12/31/1987	3.4	0.7	-0.26	-0.02
01581700	Winters Run near Benson, MD	1/1/1975 - 12/31/1984	9.2	2.3	-0.24	-0.03
01581700	Winters Run near Benson, MD	1/1/1985 - 12/31/1994	8.2	2.2	-0.08	-0.12
01583000	Slade Run near Glyndon, MD	1/1/1953 - 12/31/1962	0.5	0.1	-0.53	0.17
01583000	Slade Run near Glyndon, MD	1/1/1963 - 12/31/1972	0.7	0.1	-0.14	0.32
01584050	Long Green Creek at Glen Arm, MD	10/1/1975 - 9/30/1985	3.0	0.6	-1.02	0.01
01584050	Long Green Creek at Glen Arm, MD	10/1/1985 - 9/30/1995	2.2	0.6	-1.17	-1.13
01584500	Little Gunpowder Falls at Laurel Brook, MD	1/1/2002 - 12/31/2011	9.2	2.7	-0.38	-0.83
01585500	Cranberry Branch near Westminster, MD	1/1/1986 - 12/31/1995	0.7	0.2	-0.58	-0.23
01588000	Piney Run near Sykesville, MD	1/1/1948 - 12/31/1957	1.9	0.5	-0.26	0.11
01591000	Patuxent River near Unity, MD	1/1/1969 - 12/31/1978	11.0	2.3	0.10	-0.02
01591000	Patuxent River near Unity, MD	1/1/1981 - 12/31/1990	7.7	2.0	-0.31	-0.76
01591400	Cattail Creek near Glenwood, MD	1/1/1979 - 12/31/1988	4.7	1.3	0.27	-0.02
01591400	Cattail Creek near Glenwood, MD	1/1/1989 - 12/31/1998	4.6	1.3	-0.08	0.13
01591700	Hawlings River near Sandy Spring, MD	1/1/1981 - 12/31/1990	5.7	1.7	0.24	-0.39
01591700	Hawlings River near Sandy Spring, MD	1/1/2000 - 12/31/2009	6.9	1.9	-0.20	-0.43
01646000	Difficult Run near Great Falls, VA	1/1/1943 - 12/31/1952	6.4	2.4	-0.43	-0.22

Table 4-2. (cont.) Goodness-of-fit measure for the calibrated time series. The RMSE was calculated for all flows (All Q) and flows between two times baseflow ( $Q_{2 \times \text{BF}}$ ) and a ten-yr discharge ( $Q_{10}$ ). The Nash Sutcliffe Efficiency rating was evaluated for all flows and peak flows, those exceeding  $Q_{2 \times \text{BF}}$ .

Stream Station No.	Stream Station Name	Modeled Time Period	RMSE ( $\text{m}_3/\text{s}$ )		Nash Sutcliffe Efficiency	
			$Q_{2 \times \text{BF}} - Q_{10}$	All Q	$> Q_{2 \times \text{BF}}$	All Q
01646000	Difficult Run near Great Falls, VA	1/1/1984 - 12/31/1993	6.6	2.8	0.47	0.13
01654000	Accotink Creek near Annandale, VA	1/1/1984 - 12/31/1993	3.1	1.2	0.71	0.67
01654000	Accotink Creek near Annandale, VA	1/1/2000 - 12/31/2009	4.9	2.1	0.32	0.49
01658500	SF Quantico Creek near Independent Hill, VA	1/1/1989 - 12/31/1998	1.6	0.5	0.15	0.22
01658500	SF Quantico Creek near Independent Hill, VA	1/1/2001 - 12/31/2010	1.6	0.6	0.43	0.37
01660400	Aquia Creek near Garrisonville, VA	10/17/1987 - 10/16/1997	12.4	2.5	-0.63	-0.24
01660400	Aquia Creek near Garrisonville, VA	1/1/2001 - 12/31/2010	11.5	2.3	-1.71	-0.37
01671500	Bunch Creek near Boswells Tavern, VA	1/1/1958 - 12/31/1967	1.0	0.2	-0.73	0.29

study, by eliminating summer months from the simulations, and removing watersheds that calibrated poorly, the Flemish study was able to achieve better NSE coefficients.

#### 4.2 Sensitivity Analysis

A sensitivity analysis for a highly urban watershed, Accotink Creek (gage no. 01654000), and a largely forested watershed, South Fork Quantico Creek (gage no. 01658500), was performed. The model parameters were increased and decreased by factors of 0.1, 0.25, and 0.5 and the relative sensitivity of baseflow, a small peak (roughly a  $Q_2$ ), and a large peak (about a  $Q_{10}$ ) were recorded.

The sensitivity analysis revealed that the parameters with the greatest effect on baseflow include  $c_{min}$ ,  $c_{max}$ ,  $b_g$ ,  $b$ , and  $S_t$ . Increases in the minimum or maximum soil moisture capacity (i.e.,  $c_{min}$  or  $c_{max}$ , respectively), the relative proportion of deeper soil moisture stores (i.e.,  $b$ ), and the exponent of the groundwater recharge rate function (i.e.,  $b_g$ ) and decreases in the parameter related to soil moisture storage  $S_t$ , all increased baseflow in the urban watershed Accotink Creek (Table 4-3) Similar results were seen in the rural, forested watershed South Fork Quantico Creek (Table 4-4) with the addition of the baseflow time constant,  $k_b$ , showing an effect on baseflow. As  $k_b$  increases, baseflow also increases.

Table 4-3. A sensitivity analysis on baseflow (at 860 days) for Accotink Creek (gage no. 01654000) watershed. The model parameters listed were increased and decreased by 10, 25, and 50%. The table lists the relative sensitivity of simulated flow for each change in parameter value.

Model Parameter	Relative sensitivity of baseflow to the following change in parameter					
	-50%	-25%	-10%	+10%	+25%	+50%
$c_{min}$	--	--	--	0.0	1.0	2.0
$c_{max}$	-1.0	-1.0	0.0	0.0	1.0	2.0
$b$	1.0	1.0	0.0	0.0	0.0	0.0
$b_e$	0.0	0.0	0.0	0.0	0.0	0.0
$k_I$	0.0	0.0	0.0	0.0	0.0	0.0
$k_b$	0.0	0.0	0.0	0.0	0.0	0.0
$k_g$	0.0	0.0	0.0	0.0	0.0	0.0
$S_t$	3.0	1.0	0.0	0.0	-1.0	-1.0
$b_g$	-1.0	0.0	0.0	0.0	0.0	1.0

The sensitivity analyses of small peaks (roughly a  $Q_2$ ) in the flow time series for both watersheds showed very similar results (Tables 4-5 and 4-6). The magnitude of the small peak was affected by parameters that control both baseflow and peak flow. Increases in the minimum and maximum soil moisture capacity,  $c_{min}$  and  $c_{max}$ , resulted in lower small peaks. Likewise, the magnitude of small peaks decreased with increases in  $k_I$  and  $b_g$ . Meanwhile, increases in  $b$  and  $S_t$

Table 4-4. A sensitivity analysis on baseflow (at 3505 days) for South Fork Quantico Creek (gage no. 01658500) watershed. The model parameters listed were increased and decreased by 10, 25, and 50%. The table lists the relative sensitivity of simulated flow for each change in parameter value.

Model Parameter	Relative sensitivity of baseflow to the following change in parameter					
	-50%	-25%	-10%	+10%	+25%	+50%
$c_{min}$	--	--	--	0.0	1.0	2.0
$c_{max}$	-1.0	0.0	0.0	0.0	0.0	1.0
$b$	0.0	0.0	0.0	0.0	0.0	0.0
$b_e$	0.0	0.0	0.0	0.0	0.0	0.0
$k_l$	0.0	0.0	0.0	0.0	0.0	0.0
$k_b$	0.0	0.0	0.0	0.0	1.0	1.0
$k_g$	0.0	0.0	0.0	0.0	0.0	0.0
$S_t$	1.0	0.0	0.0	0.0	0.0	0.0
$b_g$	-1.0	0.0	0.0	0.0	0.0	0.0

increased the magnitude of small hydrograph peaks in both of the watersheds evaluated. As with the baseflow sensitivity analysis, storm flows in South Fork Quantico Creek are more sensitive to changes in the groundwater time constant  $k_g$  than for the Accotink Creek model. As  $k_g$  increases so does the discharge for the small peak analyzed.

Table 4-5. A sensitivity analysis on a small peak (at 2511 days) for Accotink Creek (gage no. 01654000) watershed. The model parameters listed were increased and decreased by 10, 25, and 50%. The table lists the relative sensitivity of simulated flow for each change in parameter value.

Model Parameter	Relative sensitivity of peak to the following change in parameter					
	-50%	-25%	-10%	+10%	+25%	+50%
$c_{min}$	--	--	--	0.0	0.0	-0.1
$c_{max}$	0.2	0.2	0.1	-0.1	-0.2	-0.4
$b$	-0.1	0.0	0.0	0.0	0.0	0.1
$b_e$	0.0	0.0	0.0	0.0	0.0	0.0
$k_l$	0.5	0.2	0.1	-0.1	-0.2	-0.3
$k_b$	0.0	0.0	0.0	0.0	0.0	0.0
$k_g$	0.0	0.0	0.0	0.0	0.0	0.0
$S_t$	-0.4	-0.2	0.0	0.0	0.1	0.1
$b_g$	0.1	0.1	0.0	0.0	-0.1	-0.1

Table 4-6. A sensitivity analysis on a small peak (at 1480 days) for South Fork Quantico Creek (gage no. 01658500) watershed. The model parameters listed were increased and decreased by 10, 25, and 50%. The table lists the relative sensitivity of simulated flow for each change in parameter value.

Model Parameter	Relative sensitivity of peak to the following change in parameter					
	-50%	-25%	-10%	+10%	+25%	+50%
$c_{min}$	--	--	--	0.0	0.0	-0.1
$c_{max}$	0.2	0.2	0.1	-0.1	-0.3	-0.7
$b$	-0.1	0.0	0.0	0.0	0.0	0.1
$b_e$	0.0	0.0	0.0	0.0	0.0	0.0
$k_l$	0.9	0.4	0.1	-0.1	-0.2	-0.3
$k_b$	0.0	0.0	0.0	0.0	0.0	0.0
$k_g$	-0.2	-0.1	0.0	0.0	0.1	0.3
$S_t$	-0.3	-0.1	0.0	0.1	0.1	0.2
$b_g$	0.2	0.2	0.1	-0.1	-0.4	-0.5

Finally, the sensitivity of the magnitude of a large peak to changes in model parameters was evaluated for the Accotink and South Fork Quantico Creek watersheds (Tables 4-7 and 4-8). The large peak analyzed in each time series correlated to roughly a  $Q_{10}$ . The large peaks showed sensitivity to changes in few of the model parameters. Changes in the surface storage time constant,  $k_l$ , had the greatest effect on the magnitude of the large peaks. Increases in  $k_l$  decreased magnitude of the large peak.  $c_{max}$  had a similar but slightly smaller effect in both watersheds. Lastly, the effect of changes in the exponent of the groundwater recharge function,  $b_g$ , on large peak flows was limited to the rural forested watershed.

Although others studies in which PDM was used did not publish results from a sensitivity analysis, these results are not unexpected. Peaks corresponding to a 10-yr flood showed the greatest sensitivity to parameters that control peak flow, while baseflow was affected by parameters that related to soil moisture storage. Small peaks exhibited sensitivity to both of these groups, slow- and fast- response parameters. These results follow from hydrologic principles.

Table 4-7. A sensitivity analysis on a large peak (at 2493 days) for Accotink Creek (gage no. 01654000) watershed. The model parameters listed were increased and decreased by 10, 25, and 50%. The table lists the relative sensitivity of simulated flow for each change in parameter value.

Model Parameter	Relative sensitivity of peak to the following change in parameter					
	-50%	-25%	-10%	+10%	+25%	+50%
$c_{min}$	--	--	--	0.0	0.0	0.0
$c_{max}$	0.3	0.1	0.1	-0.1	-0.1	-0.3
$b$	0.0	0.0	0.0	0.0	0.0	0.0
$b_e$	0.1	0.0	0.0	0.0	0.0	-0.1
$k_l$	0.4	0.2	0.1	-0.1	-0.2	-0.3
$k_b$	0.0	0.0	0.0	0.0	0.0	0.0
$k_g$	0.0	0.0	0.0	0.0	0.0	0.0
$S_t$	-0.1	0.0	0.0	0.0	0.0	0.0
$b_g$	0.0	0.0	0.0	0.0	0.0	0.0

Table 4-8. A sensitivity analysis on a large peak (at 2494 days) South Fork Quantico Creek (gage no. 01658500) watershed. The model parameters listed were increased and decreased by 10, 25, and 50%. The table lists the relative sensitivity of simulated flow for each change in parameter value.

Model Parameter	Relative sensitivity of peak to the following change in parameter					
	-50%	-25%	-10%	+10%	+25%	+50%
$c_{min}$	--	--	--	0.0	0.0	0.0
$c_{max}$	0.0	0.0	0.0	0.0	0.0	-0.2
$b$	0.0	0.0	0.0	0.0	0.0	0.0
$b_e$	0.0	0.0	0.0	0.0	0.0	0.0
$k_l$	0.9	0.4	0.1	-0.1	-0.2	-0.4
$k_b$	0.0	0.0	0.0	0.0	0.0	0.0
$k_g$	0.0	0.0	0.0	0.0	0.0	0.0
$S_t$	0.0	0.0	0.0	0.0	0.0	0.0
$b_g$	0.0	0.0	0.0	0.0	-0.1	-0.2

### 4.3 Correlation of Model Variables

Both the calibrated model parameters and watershed characteristics were checked for correlation.

Using the non-parametric Spearman and Kendall tests, both tests provided similar results.

Among the model parameters only  $S_t$  and  $c_{max}$  were significantly correlated ( $p < 0.01$ ). A matrix of Spearman's  $\rho$  and Kendall's  $\tau$  correlation coefficients for all calibrated model pairs is shown in Table 4-9.

Table 4-9. Spearman's  $\rho$  (upper right) and Kendall's  $\tau$  (lower left) correlation coefficients for the calibrated model parameters. Highlighted cell indicate that the pair is significantly correlated at an alpha level of 5%.

	$c_{max}$	$b$	$k_l$	$k_b$	$k_g$	$S_t$
$c_{max}$		0.31	-0.30	0.24	0.20	0.57
$b$	0.20		-0.34	-0.13	-0.12	0.08
$k_l$	-0.22	-0.23		-0.01	0.07	-0.04
$k_b$	0.18	-0.11	-0.01		-0.04	0.24
$k_g$	0.16	0.10	0.04	-0.02		0.35
$S_t$	0.48	-0.07	-0.02	0.17	0.27	

There are many significant ( $p < 0.05$ ) correlated pairs among the characteristics of the study watersheds (Table 4-10). Channel slope and basin slope for the study watersheds are positively correlated, which is to be expected. Both of these variables are also negatively correlated with the watershed area-weighted HSG numerical representation and positively correlated with the fraction of watershed area in agricultural land use. The negative correlation between HSG and slope is logical. A smaller HSG numerical representation corresponds to a watershed with a greater prevalence of HSG A or B soils. Due to the weathering and transport of soils, upland areas tend to have a greater prevalence of B soils whereas flatter alluvial plains have a greater prevalence of HSG C and D soils. A steeper watershed would be expected to have more upland areas comprised of HSG B soils than a less steep watershed where more weathered HSG C and D prevail. The positive correlation between agricultural land use and steep slopes is not as logical. The most favorable farm land tends have gentle slope, but this correlation suggests

that steeper watersheds have a greater proportion of agriculture. The correlation may be explained by the fact that areas of gentle slope are also favorable for development, and in nearly all of the study watersheds urban development has succeeded agricultural development. Lastly, the channel slope is also negatively correlated with basin area: the smaller the drainage area, the steeper the stream slope is.

Correlation analysis also revealed that as urban land use increases, so does agricultural land use and open water ( $0.01 < p < 0.05$ ). The last statistically significant correlation pair indicates that as agricultural lands increase, forested lands decrease. The time periods evaluated in this study include periods of development that saw forested lands converted to agricultural lands and agricultural lands in turn developed into urban areas. A negative correlation between forested and agricultural lands fits this pattern. The positive correlation between urban area and agriculture does not fit the development pattern. However, having increased areas of open water in more developed watersheds is a logical trend. Many of the areas of open water are the remnants of old farm ponds established in areas that have since been urbanized while some are urban retention ponds. All of these statistically significant correlation pairs were taken into account during regression analysis.

#### *4.4 Regionalization of Model Parameters*

Calibrated model parameters  $c_{max}$ ,  $b$ ,  $k_I$ , and  $k_g$  were predicted based on watershed characteristics using regression analysis. The most robust set of equations in predicting a calibrated model parameter based on physical characteristics of watersheds in the Virginia and Maryland Piedmont physiographic province is in Table 4-11. This equation set was generated when the Northeast River watershed (gage no. 01496000) was removed from the data set in

Table 4-10. Spearman’s *rho* (upper right) and Kendall’s *tau* (lower left) correlation coefficients for the studied watershed characteristics. Highlighted cell indicate that the pair is significantly correlated at an alpha level of 5%.

	Area	Basin Slope	Channel Slope	HSG	LU_Urban	LU_Ag	LU_For	LU_Water
Area		-0.07	-0.67	0.08	0.29	-0.08	0.05	0.31
BasinSlope	-0.01		0.67	-0.87	-0.16	0.53	-0.22	-0.09
ChannelSlope	-0.48	0.49		-0.66	-0.23	0.51	-0.34	-0.26
HSG	0.01	-0.72	-0.51		0.03	-0.36	0.14	0.11
LU_Urban	0.19	-0.14	-0.17	-0.02		-0.39	-0.10	0.44
LU_Ag	-0.07	0.38	0.34	-0.13	-0.32		-0.76	-0.02
LU_For	0.13	-0.14	-0.23	0.02	-0.06	-0.63		0.04
LU_Water	0.26	-0.07	-0.21	0.09	0.38	-0.04	0.01	

the “leave one out” regression analysis. Of the equation sets generated in the “leave one out” regression analysis, this set had the lowest collective PRESS statistic values, indicating a robust predictive power. These models are statistically significant at a 98.5% confidence level. Residual plots for the selected regression models are in the Appendix in Figure A-2 through Figure A-5. No model was found to satisfactorily fit the parameter  $k_b$ . Instead the average value of the calibrated parameter or regional mean was used. The full equation list of “leave one out” regression equations and associated  $R^2$ , p- values, and PRESS statistics for model parameters  $b$ ,  $c_{max}$ ,  $k_l$ , and  $k_g$  are located in the Appendix in Table A-6.

The most significant and robust regression relationship for predicting  $b$  was based on watershed area.  $b$  controls the variability of soil moisture store capacity. A smaller value of  $b$  represents a watershed with relatively deeper soil stores. This relationship explains only 22% of the variation in the data, but has a physical explanation. As watershed area increases, soils become deeper and a larger watershed allows for greater variability of soils. A previous study by Young (2006) of 260 U.K. watersheds modeled with a daily time-step found HSG to be the best

Table 4-11. Regression equations relating predicted model parameters  $b$ ,  $c_{max}$ ,  $k_1$ , and  $k_g$  (i.e.,  $\hat{b}$ ,  $\hat{c}_{max}$ ,  $\hat{k}_1$ , and  $\hat{k}_g$ ) to watershed characteristics and the statistical significance (p-value) and correlation coefficient ( $R^2$ ) for each regression relationship. [*Watershed characteristic* = definition (hull, or range of values used in this study): *Area* = basin area (2.0-93.3 km<sup>2</sup>), *ChS* = channel slope (0.0026-0.0183 km/km), *Water* = fraction of basin area covered by open water (0.0-0.8), *HSG* = hydrologic soil group index (2.21-3.09), *Urban* = fraction of basin area in urban land (0.8-66.3), *Ag* = fractional extent of watershed in agricultural land use (0.2-76.5)].

Regression Equations	Regression P-Values	Regression Adjusted R <sup>2</sup>
$\hat{b} = 0.740 - 0.0815 \ln (Area)$	0.0072	0.23
$\hat{c}_{max} = 674 + 87.9 \ln (ChS) + 203 \ln (Water + 1)$	0.0003	0.46
$\hat{k}_1 = 38.3 + 5.57 \ln (Area) - 36.7 \ln (HSG) - 2.10 \ln (Urban)$	0.0003	0.51
$\hat{k}_g = -27334 + 37234 \ln (HSG) + 136 Ag$	0.0140	0.25

explanatory variable with an  $R^2$  of 0.66. However, Young states that the relationship does not give a major improvement over using the regional mean of  $b$ .

The best regression relationship for predicting maximum soil moisture depth relates  $c_{max}$ , to channel slope and fractional extent of open water in catchment. In the relationship, increasing slope is related to increasing maximum soil moisture storage depth, which does not have a straightforward explanation. However, the correlation of channel and watershed slope with HSG and the possible occurrence of fracture bedrock may offer some explanation. However, the relationship between more surface water storage and greater soil moisture depths is reasonable. Slow release of water held in ponds may mimic deep soil moisture stores. Other studies found different explanatory watershed characteristics for predicting  $c_{max}$ . Young (2006) found  $c_{max}$  related to HSG ( $R^2=0.99$ ). Lamb and Kay (2004) in a study modeling 40 U.K. catchments with an hourly time-step found a variety of explanatory variables, including the skew of the

distribution of logarithm of watershed slope divided by drainage area index, length of the mean drainage path, average annual rainfall ( $R^2=0.7$ ).

The most robust regression equation for predicting the surface store time constant,  $k_I$ , was based on drainage area, HSG, and fractional extent of urban area in the watershed. This relationship has a strong physical basis and incidentally has the best  $R^2$  value of the regression set. As  $k_I$  decreases, flood peaks increase in magnitude. This relationship suggests that watersheds with a greater relative abundance of HSG type D soils and more urbanization have a smaller  $k_I$  time constant, resulting in peak flows of greater magnitude. Both the Young (2006) and Lamb and Kay (2004) studies had regressions based on soil attributes and had  $R^2$  values of 0.99 and 0.7, respectively.

No satisfactory regression relationship was found for baseflow reservoir time constant,  $k_b$ . Instead the regional mean was used to predict  $k_b$ . Young (2006) found the best explanatory relationship based on watershed area and HSG ( $R^2=0.51$ ). The final parameter considered, the groundwater time constant  $k_g$ , was best predicted by HSG and the fractional extent of the watershed area in agricultural production. This relationship also has a physical basis. The sensitivity analysis shows that more runoff is generated with increases in  $k_g$ . The regression relationship shows that  $k_g$  increases with the relative abundance of HSG type D soils and agricultural land. Runoff potential may increase with ditched or tiled agricultural lands. Young (2006) found  $k_g$  to be best predicted by a precipitation index, the longest drainage path, and the regression residuals from a regression between two indices of soil runoff potential ( $R^2=0.58$ ).

The small number of watersheds considered in this study and the variability of the watersheds, especially in terms of land use composition, may have contributed to the low coefficients of determination. The  $R^2$  values calculated for the regression relationships were

lower than both the Young (2006) and Lamb and Kay (2004) studies. The sample sizes were larger in both of these studies, and watershed land use composition was not discussed in either study.

#### *4.5 Model Evaluation*

The set of regression equations in Table 5-10 were used to calculate values for  $c_{max}$ ,  $b$ ,  $k_I$ , and  $k_g$  based on watershed properties for model evaluation. Threshold soil moisture storage,  $S_t$ , was set to the area-weighted average field capacity and  $k_b$  was set to the regional average of 197 h. Due to the small number of watersheds that fit study criteria, the same watersheds and time series used in model calibration were used for model evaluation. However, because “leave one out” regression analysis was employed, one watershed was available for independent model evaluation. This watershed is the Northeast River watershed (gage no. 01496000). Hydrographs from the evaluation flow time series for this watershed are in Figures 4-2 and 4-3.

#### *4.6 Goodness-of-Fit*

Several indicators of goodness-of-fit were considered to evaluate model performance. These indicators include RMSE and NSE and are included in the Appendix in Table A-7. In general the hydrographs generated during model evaluation had slightly poorer RMSE and NSE values than those corresponding to calibration, which is an expected result. Additionally, a Kolmogorov–Smirnov test was used to compare a partial duration series of two peaks per year of both the observed and simulated flows of the evaluation time series. The results (Table A-7) of this analysis show that the simulated flows are not from the same distribution as observed flows for either of the evaluation watershed time series ( $p < 0.05$ ). This could be a result of calibrating

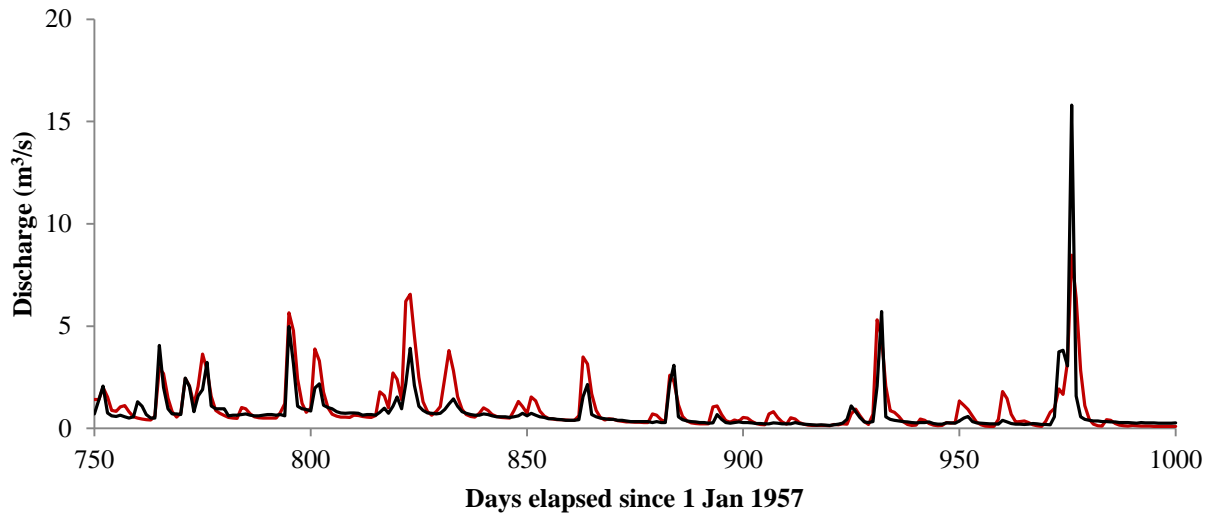


Figure 4-1. A hydrograph of observed (red) and PDM model evaluation (black) flow in Northeast River watershed (gage no. 01496000) from April through September of 1959.

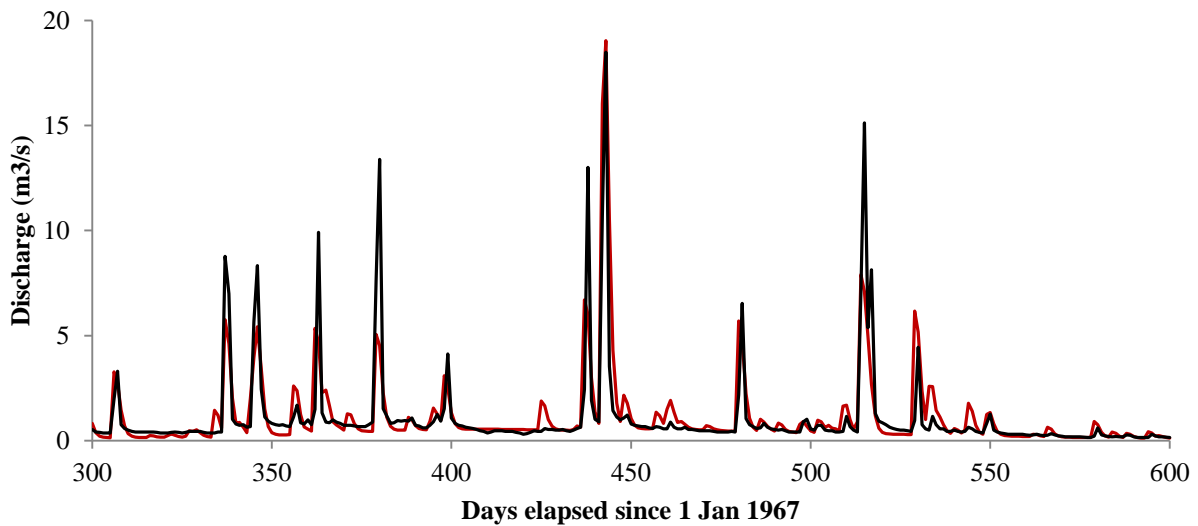


Figure 4-2. A evaluation hydrograph of observed (red) and PDM model evaluation (black) flow in Northeast River watershed (gage no. 01496000) from November 1967 through August of 1968.

strictly to lower peak flows. Higher flows were sometimes poorly replicated during the model evaluation simulations. As a result, the complete distribution of flows may have been poorly represented due to the selected calibration method.

In addition to statistical measures of model performance, peak discharges of standard return periods for observed and simulated flows were calculated and plotted for visual comparison. Peak discharges were calculated using a log-Pearson Type III flood frequency analysis of annual maxima of the observed and simulated time series. These discharges for each time series are tabulated in the Appendix in Table A-8 and Table A-9. Because mean daily discharge time series were evaluated, they cannot be directly compared to instantaneous peak flow discharges calculated from USGS regional regression equations. However, for reference, instantaneous peak flow discharges using USGS peak flow regional regression equations for the Maryland and Virginia piedmont were calculated (Table A-10; Thomas and Moglen, 2010; Austin et al., 2011). As expected, the instantaneous peak flow discharges calculated from regional regression equations are 40% to 200% larger than both observed and modeled daily mean peak flow values determined with the FFA.

Plots comparing peak discharges of standard return periods for observed and simulated daily average flows were made to examine trends and to visually compare values. Bar plots of the independent evaluation watershed, Northeast River watershed (gage no. 01496000), are shown below. Figure 4-3 shows that for the 1957-1966 time series the model simulated observed flows of the lower return periods very well, within  $3 \text{ m}^3/\text{s}$  (13%) for the  $Q_5$ . This result reflects that the model was calibrated to lower flows, specifically those between two times baseflow and a  $Q_{10}$ . Figure 4-4 shows that the simulated flows under-predicted flows by 40% for the 2-yr flow and 70% for the 100-yr flood. Bar plots comparing observed and simulated flows from model

evaluation for all of the watersheds in the study are in Figure A-6 in the Appendix. In general, lower flows were better simulated than higher flows. This trend is indicative of the calibration method used.

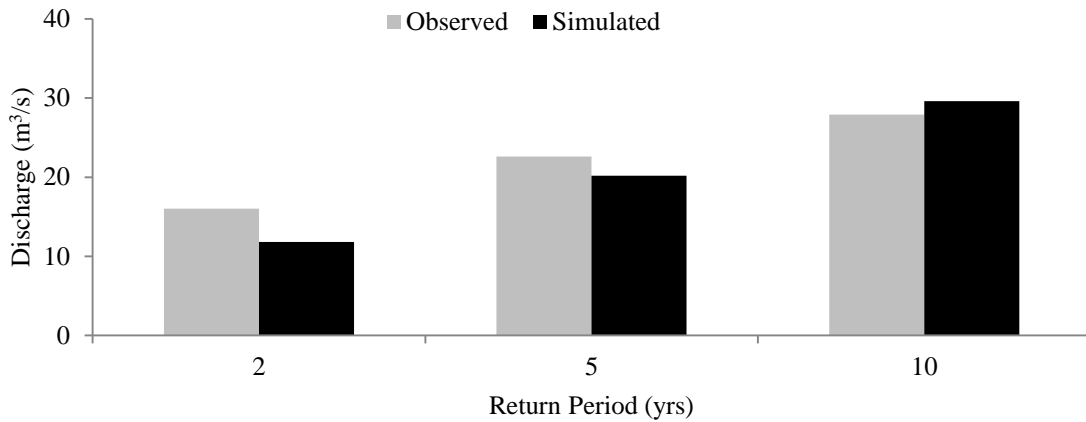


Figure 4-3. Peak discharge values of standard return intervals for observed and simulated daily average flows in Northeast River watershed (gage no. 01496000) from 1957-1966.

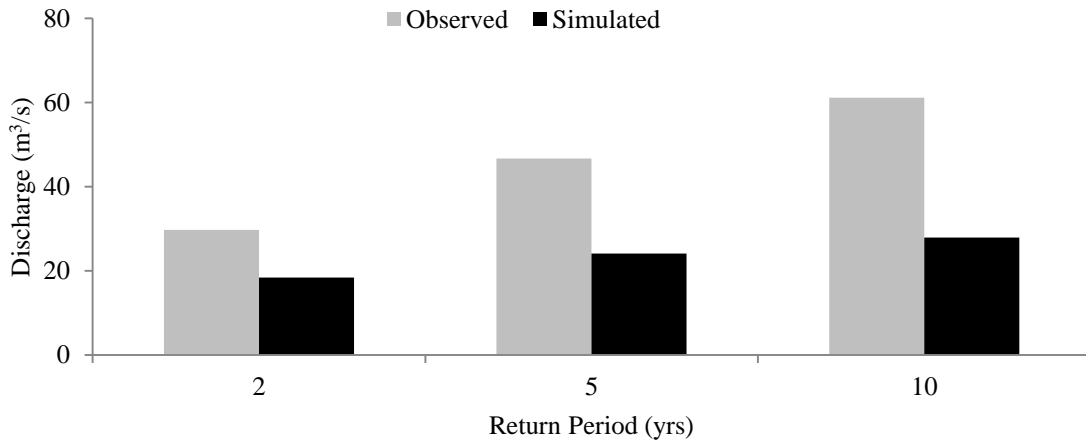


Figure 4-4. Peak discharge values of standard return intervals for observed and simulated daily average flows in Northeast River watershed (gage no. 01496000) from 1967-1976.

Scatter plots were used as another way to compare simulated peak discharges to observed peak flows. Peak discharges of standard return periods for simulated flows were plotted against those for daily average observed flows, so that a line with a slope of one and intercept of zero (a 1:1 line”) represents a distribution of hypothetical simulated flows that matches the distribution of observed flows. As a result, the distance a point lies from this 1:1 line is an indicator of the accuracy of that discharge value, where a shorter distance represents better accuracy. These plots were used to investigate trends in prediction accuracy related to watershed characteristics. The time series were sorted based on values related to watershed characteristics (e.g., drainage area, channel slope, HSG, and land use) and formed into three to five groups per variable considered based on natural breaks in values of the watershed characteristics. Each group was graphed on a single plot, and the series of plots were inspected for trends. The series of plots corresponding to increasing watershed area follows in Figures 4-6 through 4-8.

As with all other watershed characteristics considered, these plots reveal no trends in prediction accuracy. However, all of the following line plots, like the bar plots, show that peak flow estimates for lower flows were more accurate than for higher flows. This trend can be attributed to calibration techniques.

Lastly, the flood prediction estimates of this study were compared to the 95% confidence interval of bankfull discharge estimates from a Virginia regional curve (Lotspeich, 2009; Table 4-12) to assess the quality of the study results. For more than a third of the watersheds, the  $Q_2$  through  $Q_{100}$  estimates for both observed and predicted daily average flow fell within the 95% confidence interval of bankfull discharge estimate. Generally, for the Virginia watersheds the  $Q_2$  through  $Q_{25}$  of observed and predicted daily average streamflow fell within the 95% confidence interval of bankfull discharge. For about half of the Maryland watersheds, the modeled  $Q_2$  was

outside the 95% confidence interval for the bankfull discharge predicted in the Maryland regional curve. Although the predicted flood frequency estimates in this study were not consistently accurate, they represent a great improvement to current techniques.

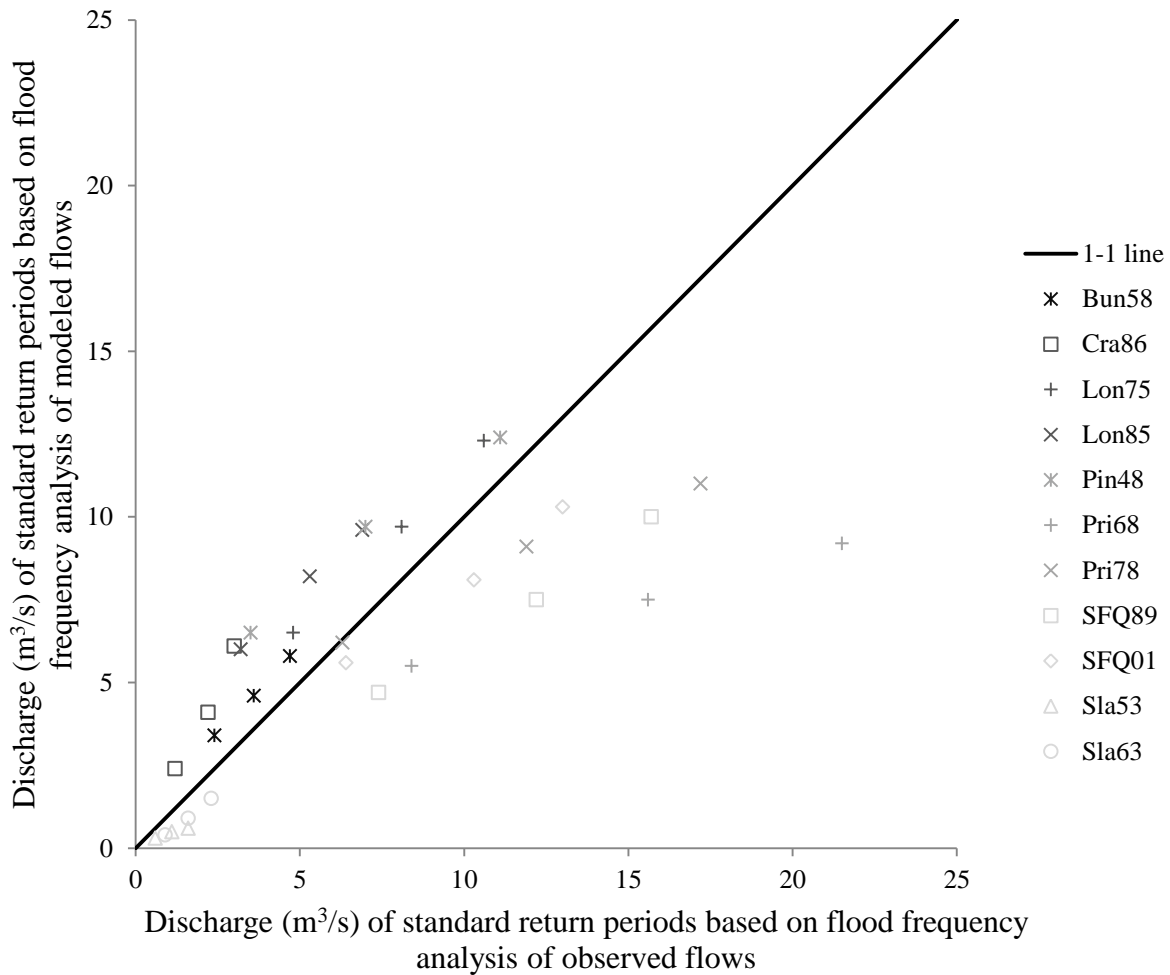


Figure 4-5. Peak discharges of standard return intervals (i.e., 2-, 5-, and 10-yrs) of daily average flows simulated during model evaluation and were plotted against discharges of standard return intervals of observed daily average streamflow. This plot is specific for the seven smallest watersheds (5.3 – 11.4 km<sup>2</sup>) in the study. Calculated discharge values are denoted by a symbol. The 1-1 line represents a hypothetical, perfectly reproduced flow distribution.

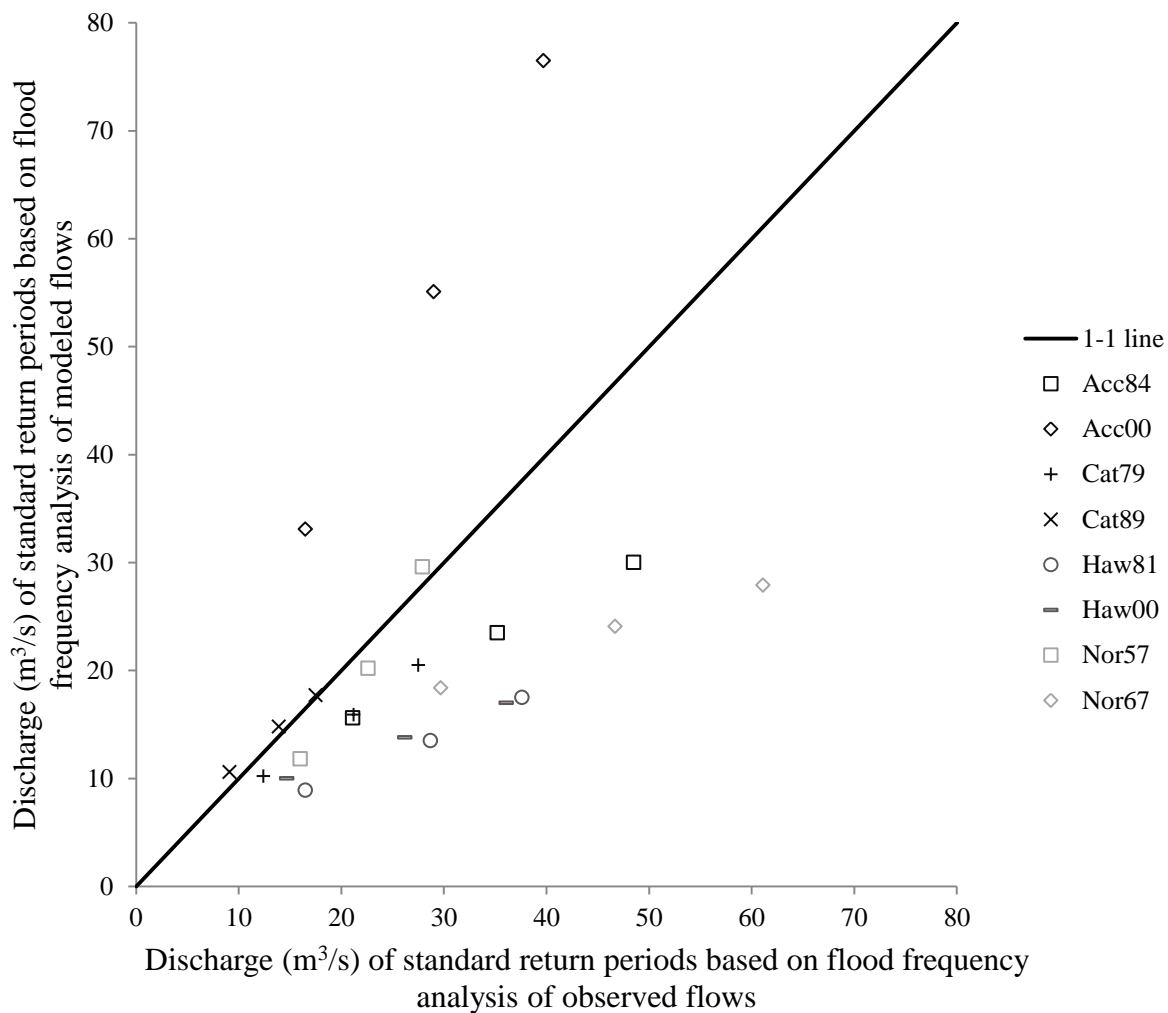


Figure 4-6. Peak discharges of standard return intervals (i.e., 2-, 5-, and 10-yrs) of daily average flows simulated during model evaluation and were plotted against discharges of standard return intervals of observed daily average streamflow. This plot is specific for four watersheds of intermediate size (22.9 – 67.7 km<sup>2</sup>) in the study. Calculated discharge values are denoted by a symbol. The 1-1 line represents a hypothetical, perfectly reproduced flow distribution.

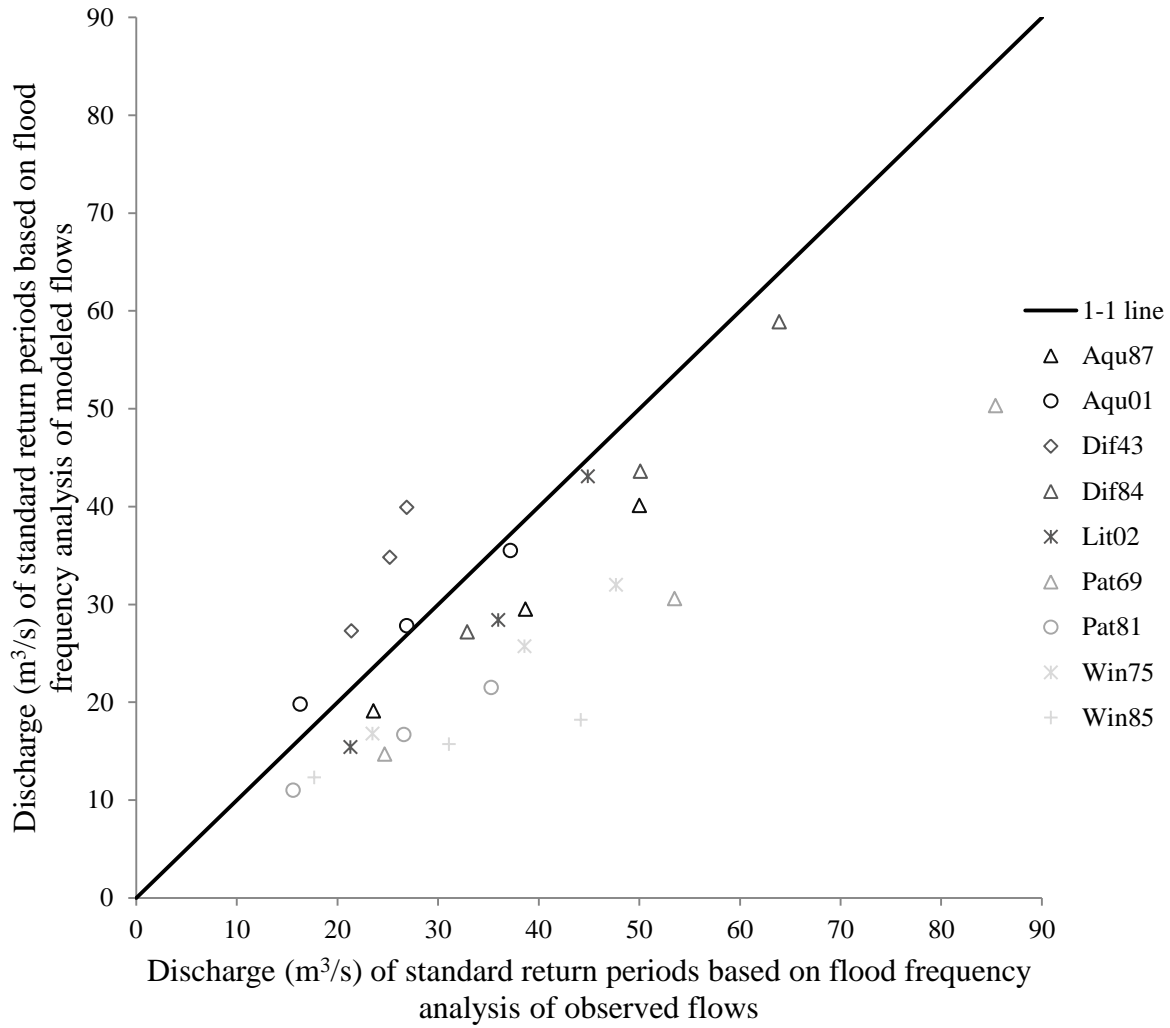


Figure 4-7. Peak discharges of standard return intervals (i.e., 2-, 5-, and 10-yr) of daily average flows simulated during model evaluation and were plotted against discharges of standard return intervals of observed daily average streamflow. This plot is specific for the five largest watersheds (89.8 –149.7 km<sup>2</sup>) in the study. Calculated discharge values are denoted by a symbol. The 1-1 line represents a hypothetical, perfectly reproduced flow distribution.

Table 4-12. Bankfull discharge estimates for the study stream based on Virginia Piedmont and Maryland Piedmont regional curves (Lotspeich, 2009; McCandless and Everett, 2002). Calculated  $Q_2$  estimates based on simulated model flow are listed for comparison. [*CI* = *confidence interval*].

Stream Gage No.	Stream Gage Name	Simulated	Discharge ( $m^3/s$ )	
		$Q_2$ ( $m^3/s$ )	Lower 95% CI	Upper 95% CI
01496000	Northeast River at Leslie, MD	15	13	60
01496200	Principio Creek near Principio Furnace, MD	6	6	28
01581700	Winters Run near Benson, MD	15	16	78
01583000	Slade Run near Glyndon, MD	0.4	2	9
01584050	Long Green Creek at Glen Arm, MD	6	6	29
01584500	Little Gunpowder Falls at Laurel Brook, MD	15	17	80
01585500	Cranberry Branch near Westminster, MD	2	3	13
01588000	Piney Run near Sykesville, MD	7	7	33
01591000	Patuxent River near Unity, MD	13	16	78
01591400	Cattail Creek near Glenwood, MD	10	12	57
01591700	Hawlings River near Sandy Spring, MD	9	13	63
01646000	Difficult Run near Great Falls, VA	27	23	147
01654000	Accotink Creek near Annandale, VA	24	10	64
01658500	SF Quantico Creek near Independent Hill, VA	5	3	22
01660400	Aquia Creek near Garrisonville, VA	19	14	92
01671500	Bunch Creek near Boswells Tavern, VA	3	2	13

## Chapter 5 Conclusions

The regionalized PDM was moderately successful in reproducing flows of lower return periods. This is an encouraging result for the application of this technique to stream restoration. Additionally, as opposed to other methods for estimating a design discharge in ungaged streams, this method yields a full hydrograph rather than single peak flow. Hydrographs are useful not only for stream restoration design but also in wetland design applications. However, this method for design flow estimation could be improved.

Future research may improve upon this technique used during this study. Because of the variability in the study data set and insufficient number of evaluation watersheds, adding more watersheds may allow for better regression relationships and provide more independent evaluations. Also as the USGS makes more instantaneous discharge time series available, it could be beneficial to model instantaneous flow rather than daily average flow to allow for comparison to regional regression equations. Additionally, these values would have more practical use in design as design flows are typically based on instantaneous shear stresses or velocities rather than mean stresses or velocities. Also, selecting watersheds with rain gages in close proximity may also improve study results.

Another recommendation for future studies is to explore other objective functions for calibration. During one of the evaluation runs, several hydrographs resulting from the parameters sets tested led to better NSE ratings than those achieved during calibration. Using NSE ratings as the objective function or calibrating to a flow-duration curve may improve model performance. Lastly, using other methods for model regionalization may yield superior results. Two of the regionalization methods discussed in the literature review but not explored in this study include the site-similarity and spatial proximity approaches. These methods have been successful in other model regionalization studies, and may produce better results than regression, especially if more watersheds are included in the study. Another option for future studies has already been applied by Cabus (2008), who removed summer months from the modeled time series. By omitting summer months from the modeled time series, isolated convective storms can be avoided and accurate ET calculations are less crucial to the water budget. However, for the

## Chapter 6 References

- Anderson, J. R., E. E. Hardy, J. T. Roach, and R. E. Witmer. 1976. A land use and land cover classification system for use with remote sensor data. Geological Survey Professional Paper 964. A revision of the land use classification system as presented in U.S. Geological Survey Circular 671. Reston, Va.: USGS.
- Arnaud, P., and J. Lavabre. 2002. Coupled rainfall model and discharge model for flood frequency estimation. *Water Resources Research* 38(6).
- Aronica, G. T., and A. Candela. 2007. Derivation of flood frequency curves in poorly gauged Mediterranean catchments using a simple stochastic hydrological rainfall-runoff model. *Journal of Hydrology* 347(1-2): 132-142.
- Austin, S. H., J. L. Krstolic, and U. Wiegand. 2011. *Peak-Flow Characteristics of Virginia Streams*. Scientific investigations report No. 2011-5144. Reston, Va.: U.S. Dept. of the Interior, USGS.
- Bardossy, A. 2007. Calibration of hydrological model parameters for ungauged catchments. *Hydrology and Earth System Sciences* 11(2): 703-710.
- Bedient, P. B., and W. C. Huber. 1992. *Hydrology and Floodplain Analysis*. 2nd ed. Reading, Mass.: Addison-Wesley.
- Bernhardt, E. S., M. A. Palmer, J. D. Allan, G. Alexander, K. Barnas, S. Brooks, J. Carr, S. Clayton, C. Dahm, J. Follstad-Shah, D. Galat, S. Gloss, P. Goodwin, D. Hart, B. Hassett, R. Jenkinson, S. Katz, G. M. Kondolf, P. S. Lake, R. Lave, J. L. Meyer, T. K. O'Donnell, L. Pagano, B. Powell, and E. Sudduth. 2005. Synthesizing US river restoration efforts. *Science* 308(5722): 636-637.
- Beven, K., and J. Freer. 2001. A dynamic TOPMODEL. *Hydrological Processes* 15(10): 1993-2011.
- Beven, K. J. 2012. *Rainfall-Runoff Modeling: The Primer*. 2nd ed. Hoboken, N.J.: Wiley-Blackwell.
- Bicknell, B. R., J. C. Imhoff, J. L. Kittle, Jr., A. S. Donigian, Jr., and R. C. Johanson. 1997. Hydrological Simulation Program--Fortran, User's manual for version 11. EPA/600/R-97/080. Athens, Ga.: USEPA.
- Biedenharn, D. S., C. R. Thorne, P. J. Soar, R. D. Hey, and C. C. Watson. 2001. Effective discharge calculation guide. *International Journal of Sediment Research* 16(4): 445-459.
- Bisese, J. A. 1995. Methods for Estimating the Magnitude and Frequency of Peak Discharges of Rural, Unregulated Streams in Virginia. U.S. Geological Survey 94-4148. Richmond, Va.: USGS.

- Boughton, W., and O. Droop. 2003. Continuous simulation for design flood estimation - a review. *Environmental Modelling & Software* 18(4): 309-318.
- Cabus, P. 2008. River flow prediction through rainfall-runoff modelling with a probability-distributed model (PDM) in Flanders, Belgium. *Agricultural Water Management* 95(7): 859-868.
- Calver, A., and R. Lamb. 1996. Flood frequency estimation using continuous rainfall-runoff modelling. *Physics and Chemistry of The Earth* 20(5-6): 479-483.
- Cameron, D. S., K. J. Beven, J. Tawn, S. Blazkova, and P. Naden. 1999. Flood frequency estimation by continuous simulation for a gauged upland catchment (with uncertainty). *Journal of Hydrology* 219(3-4): 169-187.
- Castro, J. M., and P. L. Jackson. 2001. Bankfull discharge recurrence intervals and regional hydraulic geometry relationships: Patterns in the Pacific Northwest, USA. *Journal of the American Water Resources Association* 37(5): 1249-1262.
- Dillow, J. J. A., Geological Survey (U.S.), and Maryland State Highway Administration. 1996. *Technique for estimating magnitude and frequency of peak flows in Maryland*. Water-Resources Investigations Report No. 95-4154. Towson, Md.: USGS.
- Dury, G. H. 1973. Magnitude-frequency analysis and channel morphology. In *Fluvial Geomorphology*, 91-121. M. Morisawa, ed. Binghamton, N.Y.: State University of New York.
- Fenneman, N. M., and D. W. Johnson. 1946. Physiographic divisions of the conterminous U. S. Reston, Va.: USGS. Available at: <http://water.usgs.gov/GIS/metadata/usgswrd/XML/physio.xml>. Accessed 18 January 2013.
- Gloe, M. 2011. Evaluating a Process-based Mitigation Wetland Water Budget Model. MS thesis. Blacksburg, Va.: Virginia Polytechnic and State University, Department of Biological Systems Engineering.
- Grover, P. L., D. H. Burn, and J. M. Cunderlik. 2002. A comparison of index flood estimation procedures for ungauged catchments. *Canadian Journal of Civil Engineering* 29(5): 734-741.
- Haberlandt, U., A. D. E. von Eschenbach, and I. Buchwald. 2008. A space-time hybrid hourly rainfall model for derived flood frequency analysis. *Hydrology and Earth System Sciences* 12(6): 1353-1367.
- Helsel, D. R., and R. M. Hirsch. 1992. *Statistical Methods in Water Resources*. Amsterdam, The Netherlands: Elsevier.
- Hey, R. D. 1975. Design discharge for natural channels. In *Science, Technology and Environmental Management*. R. D. Hey, and T. D. Davies, eds. Farnborough, U.K.: Saxon House.

- Hey, R. D. 1997. Channel response and channel forming discharge: Literature review and interpretation. Final report for the US Army contract number R&D 6871-EN-01. 108 p.
- Interagency Advisory Committee on Water Data. 1982. Guidelines for determining flood-flow frequency: Bulletin 17B. Hydrology Subcommittee, Office of Water Data Coordination. Reston, Va.: USGS.
- Kay, A. L., D. A. Jones, S. M. Crooks, A. Calver, and N. S. Reynard. 2006. A comparison of three approaches to spatial generalization of rainfall-runoff models. *Hydrological Processes* 20(18): 3953-3973.
- Lamb, R. 1999. Calibration of a conceptual rainfall-runoff model for flood frequency estimation by continuous simulation. *Water Resources Research* 35(10): 3103-3114.
- Lamb, R., and A. L. Kay. 2004. Confidence intervals for a spatially generalized, continuous simulation flood frequency model for Great Britain. *Water Resources Research* 40(7).
- Leopold, L. B., M. G. Wolman, and J. P. Miller. 1964. *Fluvial processes in geomorphology*. A Series of books in geology. San Francisco, Ca.: W.H. Freeman.
- Lotspeich, R. R. 2009. Regional curves of bankfull channel geometry for non-urban streams in the Piedmont physiographic province, Virginia. U.S. Geological Survey 2009-5206. Reston, Va.: USGS.
- Maidment, D. R. 1993. *Handbook of Hydrology*. New York, N.Y.: McGraw-Hill.
- Maryland Hydrology Panel. 2010. Application of hydrologic methods in Maryland. 3rd ed. Maryland State Highway Administration and Maryland Department of the Environment.
- McCandless, T. L. and R. A. Everett. 2002. Maryland Stream Survey: Bankfull Discharge and Channel Characteristics of Streams in the Piedmont Hydrologic Region. Annapolis, Md.: U.S. Fish & Wildlife Service.
- McIntyre, N., H. Lee, H. Wheeler, A. Young, and T. Wagener. 2005. Ensemble predictions of runoff in ungauged catchments. *Water Resources Research* 41(12).
- Microsoft Corporation. 2011. Bing maps aerial layer. Available at: <http://www.arcgis.com/home/item.html?id=303116b7ebf44f4eb6dcf1648e346f46>. Accessed 23 July 2012.
- Mohamoud, Y. M., and R. S. Parmar. 2006. Estimating streamflow and associated hydraulic geometry, the Mid-Atlantic Region, USA. *Journal of the American Water Resources Association* 42(3): 755-768.
- Montgomery, D. C., E. A. Peck, and G. G. Vining. 2001. *Introduction to Linear Regression Analysis*. Wiley Series in Probability and Statistics. New York, N.Y.: John Wiley & Sons.

- Moore, R. J. 2007. The PDM rainfall-runoff model. *Hydrology and Earth System Sciences* 11(1): 483-499.
- Moore, R. J. 2012. PDM rainfall runoff model users' manual. Version 2.3. Wallingford, U.K.: Centre for Ecology & Hydrology
- Muncaster, S. H., P. E. Weinmann, and R. G. Mein. 1997. An application of continuous hydrologic modelling to design flood estimation. In *24th Hydrology and Water Resources Symposium Proceedings*. Auckland, NZ. Canberra, Australia: Institution of Engineers.
- Nash, J. E. and J. V. Sutcliffe. 1970. River flow forecasting through conceptual models part I — A discussion of principles. *Journal of Hydrology* 10(3): 282–290.
- NCDC. 2012. Global Historical Climatology Network-Daily. NOAA. Available at: <http://www.ncdc.noaa.gov>. Accessed 25 June 2012.
- NRCS. 2013. Soil Survey Geographic (SSURGO) Database for Fairfax, Fauquier, Louisa, Prince William, and Stafford Counties and Fairfax City, Va., Baltimore, Carroll, Cecil, Harford, Howard, and Montgomery Counties, Md. and Chester County, Pa.
- Neitsch, S. L., J. G. Arnold, J. R. Kiniry, R. Srinivasan, and J. R. Williams. 2002. Soil and Water Assessment Tool User's Manual. Agricultural Research Service. College Station, Texas: T. W. R. Institute.
- Oudin, L., V. Andreassian, C. Perrin, C. Michel, and N. Le Moine. 2008. Spatial proximity, physical similarity, regression and ungauged catchments: A comparison of regionalization approaches based on 913 French catchments. *Water Resources Research* 44(3).
- Parajka, J., R. Merz, and G. Blöschl. 2005. A comparison of regionalisation methods for catchment model parameters. *Hydrology and Earth System Sciences* 9(3): 157-171.
- Perrin, C., C. Michel, and V. Andreassian. 2003. Improvement of a parsimonious model for streamflow simulation. *Journal of Hydrology* 279(1-4): 275-289.
- Randrianasolo, A., M. H. Ramos, and V. Andréassian. 2011. Hydrological ensemble forecasting at ungauged basins: Using neighbour catchments for model setup and updating. *Advances in Geosciences* 29: 1-11.
- Soar, P. J., and C. R. Thorne. 2011. Design discharge for river restoration. *Geophysical Monograph Series* 194: 123-149.
- Stedinger, J. R., R. M. Vogel, and E. Foufoula-Georgiou. 1993. Frequency Analysis of Extreme Events. In *Handbook of Hydrology*, 66 pp. D. R. Maidment, ed: McGraw-Hill.
- Thomas, W. O., Jr., M. M. Grimm, and R. H. McCuen. 2001. An Approach for Evaluating Flood Frequency Estimates for Ungauged Watersheds. D. Phelps, and G. Shelke, eds. *Bridging the Gap: Meeting the World's Water and Environmental Resources Challenges*: ASCE.

Thomas, Jr., W. O. and G.E. Moglen. 2010. An Update of Regional Regression Equations for Maryland. Maryland Hydrology Panel, Maryland State Highway Administration, and Maryland Department of the Environment.

Thorntwaite, C. W. 1948. An approach toward a rational classification of climate. *Geographical Review* 38(1): 55–94.

USEPA. 2000. Estimating Hydrology and Hydraulic Parameters for HSPF. BASINS. USEPA Technical Note 6. USEPA.

USGS. 2012a. USGS surface-water data for the nation. National Water Information System: Web interface. Available at: <http://waterdata.usgs.gov/nwis/sw>. Accessed 27 April 2012.

USGS. 2012b. The StreamStats program for Maryland. Available at: <http://water.usgs.gov/osw/streamstats/maryland.html>. Accessed 15 August 2012.

USGS. 2012c. EarthExplorer. Available at: <http://earthexplorer.usgs.gov>. Accessed 24 August 2012.

USGS. 2012d. Historical Topographic Maps. In *The National Map*. Available at: <http://nationalmap.gov/historical>. Accessed 7 October 2012.

USGS. 2013. Chesapeake Bay Watershed Land Cover Data Series: 1984, 1992, 2001, and 2006. Available at: [ftp://ftp.chesapeakebay.net/Gis/CBLCD\\_Series](ftp://ftp.chesapeakebay.net/Gis/CBLCD_Series). Accessed 16 August 2012.

Venables, W. N., and B. D. Ripley. 2002. *Modern Applied Statistics with R*. New York, N.Y.: Springer.

Viviroli, D., H. Mittelbach, J. Gurtz, and R. Weingartner. 2009. Continuous simulation for flood estimation in ungauged mesoscale catchments of Switzerland - Part II: Parameter regionalisation and flood estimation results. *Journal of Hydrology* 377(1-2): 208-225.

Williams, G. P. 1978. Bank-full discharge of rivers. *Water Resources Research* 14(6): 1141-1154.

Wolman, M. G., and L. B. Leopold. 1957. *River flood plains: some observations on their formation*. Physiographic and hydraulic studies of rivers. Washington, D.C.: U.S. Government Printing Office.

Wolman, M. G., and W. P. Miller. 1960. Magnitude and frequency of forces in geomorphic processes. *Journal of Geology* 68: 54-74.

Young, A. R. 2006. Stream flow simulation within UK ungauged catchments using a daily rainfall-runoff model. *Journal of Hydrology* 320(1-2): 155-172.

Young, A. R., and N. S. Reynard. 2004. River flow simulation within ungauged catchments: The utility of regionalised models. C. Pahl-Wostl, S. Schmidt, and T. Jakeman, eds. In *iEMSs 2004*

*International Congress: "Complexity and Integrated Resources Management"*. Osnabrueck, Germany: International Environmental Modelling and Software Society.

Zambrano-Bigiarin, M. 2012. *Goodness-of-fit functions for comparison of simulated and observed hydrological time series (hydroGOF)*. Ver. 0.3-5. The Comprehensive R Archive Network.

## Appendix

Table A- 1. A list of aerial images used for historic land use analysis of Difficult Run (USGS gage no. 01646000) and Accotink Creek (USGS gage no. 01654000) watersheds. These images are from the Fairfax County GIS & Mapping Department, courtesy of Wetland Studies and Solutions, Inc. (WSSI, 2012).

Image Name	Date	Scale
FG113-138, FG113-140, FG113-142, FG113-144, FG113-146, FG113-58, FG113-59, FG113-61, FG113-63, FG113-80, FG113-81, FG113-83, FG113-85, FG113-87, FG118-26, FG118-28, FG118-30, FG118-28, FG118-31	Spring 1937	1:18000
1954_01, 1954_02, 1954_03, 1954_04, 1954_05, 1954_06, 1954_07, 1954_08, 1954_09, 1954_10, 1954_11, 1954_12, 1954_13, 1954_14, 1954_15, 1954_16, 1954_17, 1954_18, 1954_19, 1954_20, 1954_21, 1954_22, 1954_23, 1954_24, 1954_25, 1954_26, 1954_27	1954	1:20000

Table A- 2. Aerial images used for historic land use analysis. Image date, scale, and associated watershed are listed. Images are from the USGS EarthExplorer web application (2012c).

Station No.	Station Name	Image (*tiff files unless otherwise noted)	Date	Scale
01496000	Northeast River at Leslie, MD	ARB593500500359	19-Oct-1959	1:60000
		ARB593502702599	04-Dec-1959	1:60000
		AR1VDUW00010095	05-Nov-1975	1:78000
01496200	Principio Creek near Principio Furnace, MD	AR1VCLI00020054, AR1VCLI00020093, AR1VCLI00020095, AR1VCLI00020118	08-Mar-1970	1:24000
01581700	Winters Run near Benson, MD	AR1VDLJ00010030	01-Apr-1974	1:76000
01583000	Slade Run near Glyndon, MD	ARB593502202037	19-Nov-1959	1:60000
		AR1VBLA00020005	01-Feb-1966	1:24000
		AR1VDLJ00010016	01-Apr-1974	1:76000
01584050	Long Green Creek at Glen Arm, MD	AR1VDLJ00010029	01-Apr-1974	1:76000
01584500	Little Gunpowder Falls at Laurel Brook, MD	AR1VCY000010081, AR1VCY000010153	01-Apr-1955	1:24000
		ARB593500500392	19-Oct-1959	1:60000
		ARB593502202042	19-Nov-1959	1:60000
		AR1VDLJ00010008, AR1VDLJ00010030	01-Apr-1974	1:76000
01585500	Cranberry Branch near Westminster, MD	ARB593500500398	19-Oct-1959	1:72000
		AR1VCRJ00020317	16-Mar-1971	1:72000
01588000	Piney Run near Sykesville, MD	MD_Winfield_257022_1950_24000_geo.pdf*	1950	1:72000
		MD_Sykesville_256908_1953_24000_geo.pdf*	1953	1:72000
		ARB593502202089	19-Nov-1959	1:60000
01591000	Patuxent River near Unity, MD	1VCRJ0001X161	09-Mar-1971	1:72000
		1VCRJ00020524	21-Mar-1971	1:72000
01646000	Difficult Run near Great Falls, VA	ARB593503703789, ARB593503703790	26-Jan-1960	1:60000
		ARB593503803815	03-Feb-1960	1:60000
		AR1VAQW00020019	24-Mar-1963	1:36000
		AR1VCRJ00010230	09-Mar-1971	1:72000
		AR1VCRJ00020540	21-Mar-1971	1:72000

Table A- 2. (cont.) Aerial images used for historic land use analysis. Image date, scale, and associated watershed are listed. Images are from the USGS EarthExplorer web application (2012).

Station No.	Station Name	Image (*tiff files unless otherwise noted)	Date	Scale
01654000	Accotink Creek near Annandale, VA	ARB593501801739	09-Nov-1959	1:60000
		ARB593503703789, ARB593503703790	26-Jan-1960	1:60000
		AR1VCRJ00010012, AR1VCRJ00010230	09-Mar-1971	1:72000
01658500	SF Quantico Creek near Independent Hill, VA	AR1VCRJ00020368	18-Mar-1971	1:72000
01660400	Aquia Creek near Garrisonville, VA	1VCZM00010024	26-Mar-1972	1:76000
		1VCZM00040024	09-Apr-1972	1:76000
01671500	Bunch Creek near Boswells Tavern, VA	1VST000010039, 1VST000010210	08-Mar-1959	1:28000
		1VAOZ00010115, 1VAOZ00010116	21-Apr-1963	1:27000
		1VCGM00010014, 1VCGM00010024	07-Apr-1969	1:24000

\*Image from USGS topographic map database (USGS, 2012d).

Table A- 3. Land use as a percentage of watershed area for each of the study gages for dates ranging from 1937 to 2006. Land use is classified urban, agricultural, forest, and open water.

Stream Gage No.	Stream Gage Name	Year	Land Use Coverage (as percent off watershed area)			
			Urban	Agricultural	Forest	Water
01496000	Northeast River at Leslie, MD	1984	5.3	66.9	27.6	0.1
		1970	5.3	66.9	27.6	0.1
		1959	2.7	69.5	27.6	0.1
01496200	Principio Creek near Principio Furnace, MD	1992	0.9	76.4	22.7	0.0
		1984	0.8	76.5	22.6	0.0
		1970	0.8	76.5	22.6	0.0
01581700	Winters Run near Benson, MD	2006	18.7	40.2	41.0	0.1
		2001	18.6	40.1	41.2	0.1
		1992	17.2	41.5	41.2	0.1
		1984	15.3	42.3	42.3	0.1
		1970	15.1	41.4	43.8	0.1
01583000	Slade Run near Glyndon, MD	2006	4.4	40.6	54.9	0.0
		2001	4.3	40.5	55.2	0.0
		1992	4.3	40.5	55.2	0.0
		1984	4.3	40.4	55.2	0.0
		1970	4.3	40.4	55.2	0.0
		1959	4.3	37.5	58.1	0.0
01584050	Long Green Creek at Glen Arm, MD	2006	10.1	60.6	29.3	0.0
		2001	10.0	60.3	29.7	0.0
		1992	9.9	60.2	29.8	0.0
		1984	9.4	60.8	29.8	0.0
		1970	9.4	60.8	29.8	0.0
01584500	Little Gunpowder Falls at Laurel Brook, MD	2006	11.1	49.0	39.8	0.1
		2001	11.0	48.9	40.0	0.1
		1992	10.9	49.0	40.0	0.1
		1984	10.2	49.6	40.1	0.1
		1970	10.0	50.1	39.8	0.1
		1959	2.8	57.9	39.2	0.1
01585500	Cranberry Branch near Westminster, MD	2006	12.3	56.3	30.6	0.8
		2001	12.3	56.1	30.8	0.8
		1992	12.3	56.1	30.8	0.8
		1984	12.1	56.1	30.9	0.9
		1970	6.8	61.7	30.6	0.9
		1959	6.8	61.7	30.6	0.9
01588000	Piney Run near Sykesville, MD	1959	1.3	70.6	28.1	0.0
		1950	1.3	70.6	28.1	0.0

Table A- 3. (cont.) Land use as a percentage of watershed area for each of the study gages for dates ranging from 1937 to 2006. Land use is classified urban, agricultural, forest, and open water.

Stream Gage No.	Stream Gage Name	Year	Land Use Coverage (as percent off watershed area)			
			Urban	Agricultural	Forest	Water
01591000	Patuxent River near Unity, MD	2006	2.4	53.8	43.6	0.0
		2001	2.4	53.8	43.6	0.0
		1992	2.4	53.8	43.6	0.0
		1984	1.9	54.3	43.6	0.0
		1970	1.9	55.4	42.5	0.0
1591400	Cattail Creek near Glenwood, MD	2006	5.9	63.6	30.2	0.2
		2001	5.7	63.7	30.3	0.2
		1992	5.5	63.9	30.3	0.2
		1984	5.3	64.1	30.4	0.1
1591700	Hawlings River near Sandy Spring, MD	2006	16.9	46.2	36.8	0.2
		2001	15.5	47.3	36.9	0.2
		1992	13.7	48.3	37.8	0.2
		1984	11.5	49.8	38.5	0.2
01646000	Difficult Run near Great Falls, VA	2006	44.5	3.0	52.1	0.4
		2001	43.7	2.9	52.9	0.4
		1992	41.3	3.8	54.5	0.4
		1984	39.5	4.0	56.1	0.4
		1954	1.6	49.0	49.4	0.0
		1937	0.8	47.8	51.4	0.0
01654000	Accotink Creek near Annandale, VA	2006	66.5	0.4	33.1	0.0
		2001	66.3	0.2	33.4	0.0
		1992	65.3	0.3	34.2	0.0
		1984	64.1	1.1	34.7	0.0
01658500	SF Quantico Creek near Independent Hill, VA	2006	2.6	3.5	94.0	0.0
		2001	2.5	1.5	95.9	0.0
		1992	2.6	1.4	96.0	0.0
		1984	2.5	1.4	96.1	0.0
		1971	2.5	1.4	96.1	0.0
01660400	Aquia Creek near Garrisonville, VA	2006	11.0	10.2	77.2	0.2
		2001	10.6	9.7	78.6	0.2
		1992	9.8	9.8	78.9	0.2
		1984	8.3	10.3	80.3	0.2
		1972	8.3	10.3	80.3	0.2
01671500	Bunch Creek near Boswells Tavern, VA	1959	1.5	13.1	85.3	0.2
		1969	1.3	14.5	84.1	0.2

```

//average
PDM: Cattail Creek near Glenwood, MD
objtyp maxfun konvge objtol
 221 9999 4 8.
analys qmin qmax pkmin pkrge
 2 0. 30 8. -48
prtfnf prptot common file name of plot files (<= 64 chars)
 0 3
indx xs smpstp smptol xs name (<= 8 chars)
 0 1.00 0.01 0.01 'rainfac'
 0 0.00 0.10 0.10 'cmin'
 0 125.0 1.00 1.00 'cmax'
 0 0.50 0.01 0.01 'b'
 0 2.50 0.01 0.01 'be'
 1 23.86 0.10 0.10 'k1'
 0 0.00 0.10 0.10 'k2'
 1 200.00 0.10 0.10 'kb'
 0 12000.00 10.00 10.00 'kg'
 0 0.00 0.10 0.10 'st'
 0 1.50 0.01 0.01 'bg'
 0 0.00 0.01 0.01 'qconst'
 0 0.00 0.01 0.01 'tdly'
/
PROBABILITY DISTRIBUTED LOSS MODEL
Flow Rainfall Climate-station Daily Rain
'Cattail' 'Brighton79-88' 'ETCattail' 'Brighton79-88' /
loss runoff surface base tdly i_sdp nsdr sqmodel oap
 1 0 22 3 -13 /
Catchment area (km**2)
59.3
Event begin Event end noi End 15' Rain (<= 20 chars)
'09:00 1 JAN 1979' '09:00 1 JAN 1979' /
'09:00 31 DEC 1988' '09:00 31 DEC 1988' /
/
error parameters: 0(SIM) /, or 1(UPD) upd miter gaintyp, or 2(ARMA) p q
0 /
forecast mode: 0 = no forecast, 1 = fixed origin, 2 = fixed lead-time
0
forecast times ( 1 read-statement per event)
///
/
prtfng
-1

```

Figure A- 1. An example PDM input file.

Table A- 4. Additional rain gages used in this study to fill data gaps the records of primary rain gages. Also listed is the distance from the watershed centroid to each rain gage.

Stream Gage No.	Stream Gage Name	Modeled Time Periods	Rain Gage(s) Used to Fill Data Gaps	Dist. to Watershed Centroid (km)
01496000	Northeast River at Leslie, MD	1957-66, 1967-76	USC00076410 Newark U	20.8
01496200	Principio Creek near Principio Furnace, MD	1967-77, 1978-87	USC00076410 Newark U until 1984, then USW00013701 Alberdeen	24.6 23.3
01581700	Winters Run near Benson, MD	1975-84, 1985-94	USC00182060 Cowingo Dam* & USW00013701 Alberdeen Phillips*	24.7 25.5
01583000	Slade Run near Glyndon, MD	1953-62, 1963-72	USC00189750 Woodstock	18.6
01584050	Long Green Creek at Glen Arm, MD	1975-84, 1985-95	USC00182060 Cowingo Dam* & USW00013701 Alberdeen Phillips*	33.5 27.9
01584500	Little Gunpowder Falls at Laurel Brook, MD	2002-11	USC00182060 Cowingo Dam	31.6
01585500	Cranberry Branch near Westminster, MD	1962-71, 1986-95	USC00189750 Woodstock	32.0
01588000	Piney Run near Sykesville, MD	1948-57	USC00189750 Woodstock	15.5
01591000	Patuxent River near Unity, MD	1969-78, 1981-90	USC00189750 Woodstock	23.3
01591400	Cattail Creek near Glenwood, MD	1979-88 1989-98	USC00189750 Woodstock N/A	17.2
01591700	Hawlings River near Sandy Spring, MD	1981-90 2000-09	N/A USC00181125 Brighton Dam***, USC00187272 Potomac Filter Plant & USC00183353 Frederick 2 NNE	N/A 6.2 23.4 37.8
01646000	Difficult Run near Great Falls, VA	1943-52 1984-93	USW00013743 Washington Reagan USW00093738 Washington Dulles	25.3 13.4
01654000	Accotink Creek near Annandale, VA	1984-93 2000-09	USW00013743 Washington Reagan N/A	19.4 N/A
01658500	SF Quantico Creek near Independent Hill, VA	1989-98, 2001-10	USC00445204 Manassass* & USC00443204 Fredricksburg Sewage*	30.9 27.2
01660400	Aquia Creek near Garrisonville, VA	1987-97, 2001-10	USC00445204 Manassass* & USC00443204 Fredricksburg Sewage*, USC00443192 Fredericksburg Ntl Park**	26.0 24.8 21.6
01671500	Bunch Creek near Boswells Tavern, VA	1958-67	USC00445050 Louisa	18.7

\*Values were averaged; \*\*Used for 1987-88 gaps; \*\*\*When available Brighton Dam was used, otherwise filled with Potomac Filter Plant. If both were unavailable, Frederick 2 NNE was used.

Table A- 5. Record of edits made to precipitation and streamflow time series by gage. Observed and edited values are listed by stream gage and date of observation.

Stream Gage No.	Stream Gage Name	Date	Observed Precipitation (mm)	Modeled Precipitation (mm)	Observed Discharge (m <sup>3</sup> /s)	Modeled Discharge (m <sup>3</sup> /s)
01581700	Winters Run near Benson, MD	7/1/1984	52.1	0	31.71	1.93
01585500	Cranberry Branch near Westminster, MD	8/20/1991	134.9	0	0.037	0.037
01588000	Piney Run near Sykesville, MD	7/4/1956	100.6	0	0.283	0.283
		7/20/1956	63.2	0	11.327	0.147
		7/21/1956	38.6	0	16.99	0.147
01591000	Patuxent River near Unity, MD	8/4/1971	50	0	40.49	0.65
		9/11/1971	22.1	0	73.06	0.65
		9/12/1971	65.5	0	58.62	0.65
01591700	Hawlings River near Sandy Spring, MD	9/6/2008	173.2	0	4.5	0.07
		9/7/2008	87.5	0	1.61	0.07
01658500	SF Quantico Creek near Independent Hill, VA	9/6/2008	0	0	12.03	0.01
01660400	Aquia Creek near Garrisonville, VA	9/28/1997	147.3	0	0.119	0.119

## R Code

```
##### Regression Analysis #####
Variables <-read.csv("Watershed Variables-All.csv")
attach(Variables)
names(Variables)

##### Correlation Analysis #####
#cor(x, y, method = c("pearson", "kendall", "spearman"))
#cmx b k1 kb kg St
#Area BasinSlope ChannelSlope HSG LU_Urban LU_Ag LU_For LU_Water

#to test for significance
cor.test(x,y, method = c("pearson", "kendall", "spearman"))

##### normalized(ish) variable list #####
#qqnorm was used to visually normalize using transforms (i.e., log, powers); e.g.,
#qqnorm(log(Area))

log(Area)
log(BasinSlope)
log(ChannelSlope)
log(HSG)
log(LU_Urban)
LU_Ag
log(LU_For)
log(LU_Water+1)

b          #normal
cmx        #one high outlier
k1         #another high-ish outlier
kb         #normal
kg         #very normal

##### Stepwise Regression #####
library(MASS)

### b ###
fit <- lm(b ~ log(Area) + log(BasinSlope) + log(ChannelSlope) + log(HSG) + log(LU_Urban) +
          LU_Ag + log(LU_For) + log(LU_Water+1))
step <- stepAIC(fit, direction="both")
step$anova      # display results
#stepwise final model
#b ~ log(Area)
```

```

#### cmax ####
fit <- lm(cmax ~ log(Area) + log(BasinSlope) + log(ChannelSlope) + log(HSG) +
log(LU_Urban) + LU_Ag + log(LU_For) + log(LU_Water+1))
step <- stepAIC(fit, direction="both")
step$anova          # display results
#stepwise final model
#cmax ~ log(BasinSlope) + log(ChannelSlope) + LU_Ag + sqrt(log(LU_Water + 1))

#### k1 ####
fit <- lm(k1 ~ log(Area) + log(BasinSlope) + log(ChannelSlope) + log(HSG) + log(LU_Urban) +
LU_Ag + log(LU_For) + log(LU_Water+1))
step <- stepAIC(fit, direction="both")
step$anova          # display results
#stepwise final model
#k1 ~ log(Area) + log(HSG) + log(LU_Urban)

#### kb ####
fit <- lm(kb ~ log(Area) + log(BasinSlope) + log(ChannelSlope) + log(HSG) + log(LU_Urban) +
LU_Ag + log(LU_For) + log(LU_Water+1))
step <- stepAIC(fit, direction="both")
step$anova          # display results
#all models statistically insignificant

#### kg ####
fit <- lm(kg ~ log(Area) + log(BasinSlope) + log(ChannelSlope) + log(HSG) + log(LU_Urban) +
LU_Ag + log(LU_For) + log(LU_Water+1))
step <- stepAIC(fit, direction="both")
step$anova          # display results
#stepwise final model
#kg ~ log(HSG) + log(LU_Urban) + LU_Ag + sqrt(log(LU_For))

##### Comparing Possible Regression Models #####
library(MPV) #Package for PRESS statistic

#### b ####
b.lm<-lm(b ~ log(Area))
summary(b.lm)      #significant (p=0.013) but v poor R2 (0.185)
#Diagnostic plots
layout(matrix(c(1,2,3,4),2,2))
plot(b.lm)         # residuals not exactly normal

#### cmax ####
cmax.lm <-lm(cmax ~ log(BasinSlope) + log(ChannelSlope) + LU_Ag + log(LU_Water + 1))
summary(cmax.lm)
#all variables show significance; ChannelSlope, BasinSlope, and LU_Ag correlated

```

```

cmax.lm2 <-lm(cmax ~ log(ChannelSlope))
summary(cmax.lm2)
cmax.lm3 <-lm(cmax ~ log(ChannelSlope) + log(LU_Water + 1))
summary(cmax.lm3)
# Press statistic
PRESS(cmax.lm2)    #91607
PRESS(cmax.lm3)    #79379
#Diagnostic plots
layout(matrix(c(1,2,3,4),2,2))
plot(cmax.lm3)
#shows nearly normally-distributed residuals, but not homoscedastic

### k1###
k1.lm <-lm(k1 ~ log(Area) + log(HSG) + log(LU_Urban))
summary(k1.lm)    #LU_Urban not significant in regression
k1.lm2 <-lm(k1 ~ log(Area) + log(HSG))
summary(k1.lm2)
k1.lm3 <-lm(k1 ~ log(Area))
summary(k1.lm3)
# Press statistic
PRESS(k1.lm)#1308 indicates first model is better fit
PRESS(k1.lm2)    #1381
PRESS(k1.lm3)    #1791
#Diagnostic plots
layout(matrix(c(1,2,3,4),2,2))
plot(k1.lm)    #shows normally-distributed, homoscedastic residuals

### kg ###
kg.lm<-lm(kg ~ log(HSG) + log(LU_Urban) + LU_Ag + log(LU_For))
summary(kg.lm)    #forest not significant
kg.lm2<-lm(kg ~ log(HSG) + log(LU_Urban) + LU_Ag)
summary(kg.lm2)    #urban also becomes insignificant when forest is removed
kg.lm3<-lm(kg ~ log(HSG) + LU_Ag)
summary(kg.lm3)    #both variables significant
# Press statistics
PRESS(kg.lm)#6.11e+8
PRESS(kg.lm2)    #5.79e+8
PRESS(kg.lm3)    #5.69e+8 ...best model
#Diagnostic plots
layout(matrix(c(1,2,3,4),2,2))
plot(kg.lm3)    # pts. 10, 13, 21 deviate from normal

```

```

##### “Leave one out” Regression by Watershed #####
#b ~ log(Area)
#cmav ~ log(ChannelSlope) + log(LU_Water + 1))
#k1 ~ log(Area) + log(HSG) + log(LU_Urban)
#kb = mean(kb)
#kg ~ log(HSG) + LU_Ag

Variables.NoAccotink <-read.csv("Watershed Variables-NoAccotink.csv")
attach(Variables.NoAccotink)

summary(lm(b ~ log(Area)))
summary(lm(cmav ~ log(ChannelSlope) + log(LU_Water + 1)))
summary(lm(k1 ~ log(Area) + log(HSG) + log(LU_Urban)))
summary(lm(kg ~ log(HSG) + LU_Ag))

PRESS(lm(b ~ log(Area)))
PRESS(lm(cmav ~ log(ChannelSlope) + log(LU_Water + 1)))
PRESS(lm(k1 ~ log(Area) + log(HSG) + log(LU_Urban)))
PRESS(lm(kg ~ log(HSG) + LU_Ag))

#Repeated for all watersheds...

##### Plot analysis #####
#download&load hydroGOF

plots <-read.csv("calibration Q2xBF+.csv")
attach(plots)
names(plots)

#NSE(sim, obs, ...)

NSE(acc84_c, acc84_o)
# Repeated for each time series . . .

##### ks test #####
peaks <-read.csv("calibration 20 peaks.csv")
attach(peaks)

#ks.test(x, y, ..., alternative = c("two.sided", "less", "greater"),exact = NULL)

ks.test(acc84_c, acc84_o)
# Repeated for each time series . . .

```

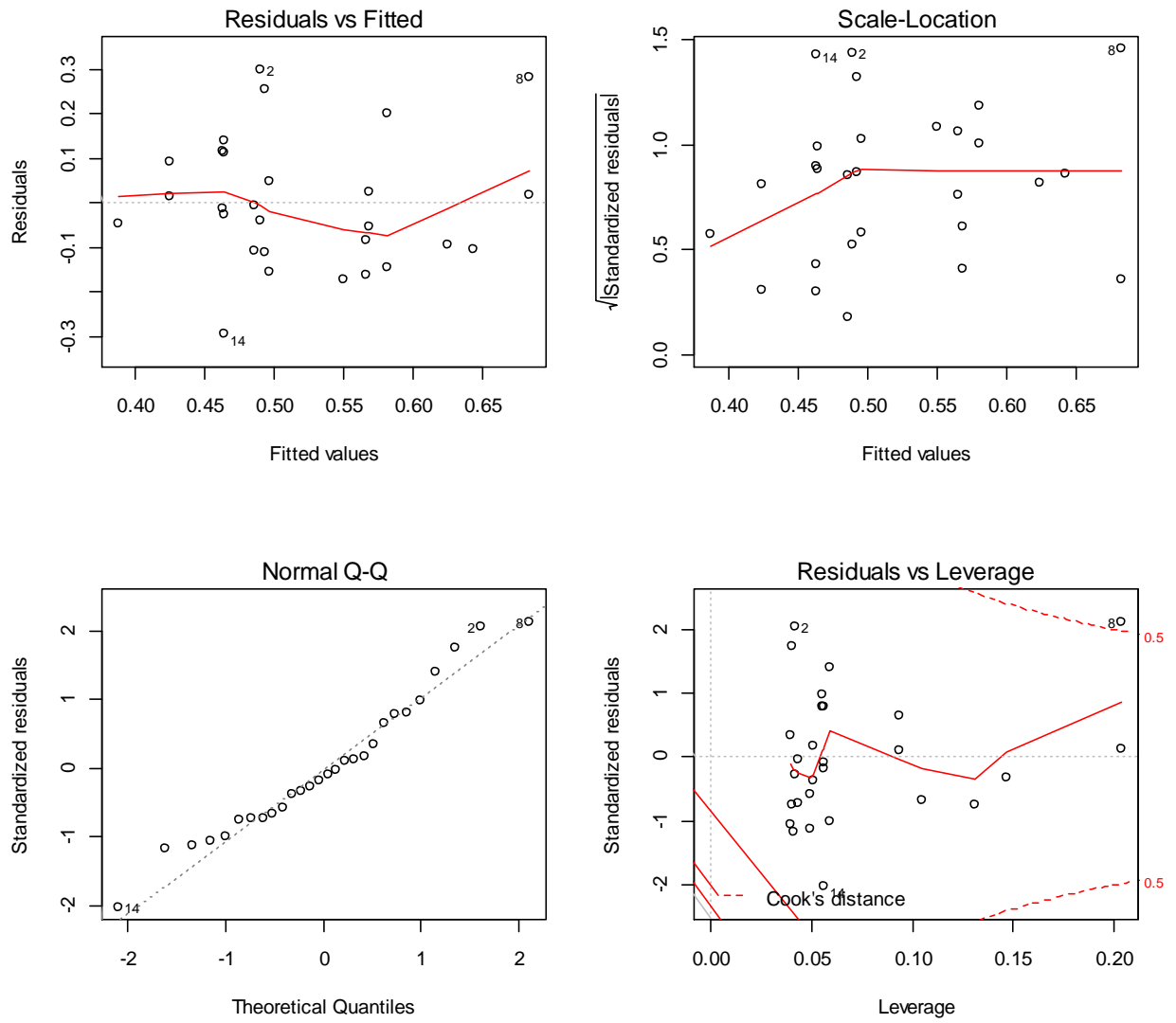


Figure A- 2. Diagnostic plots for the regression relationship  $b \sim \ln(\text{Area})$ . Plots clockwise from upper left: residuals vs. fitted values, scale-location plot, normal quantile-quantile plot of residuals, and residuals vs. leverage.

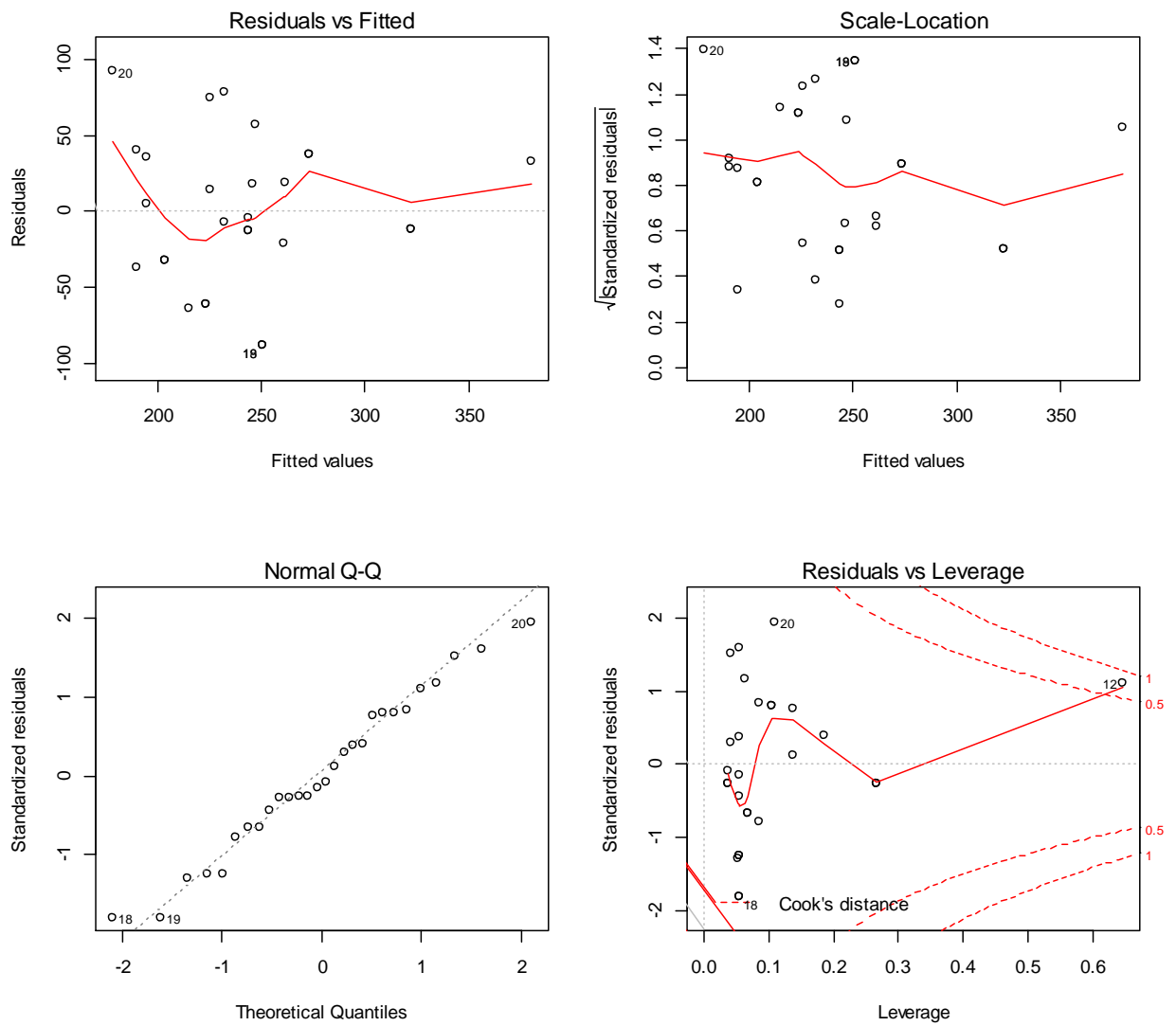


Figure A- 3. Diagnostic plots for the regression relationship  $c_{max} \sim \log(\text{ChannelSlope}) + \log(\text{LU\_Water} + 1)$ . Plots clockwise from upper left: residuals vs. fitted values, scale-location plot, normal quantile-quantile plot of residuals, and residuals vs. leverage.

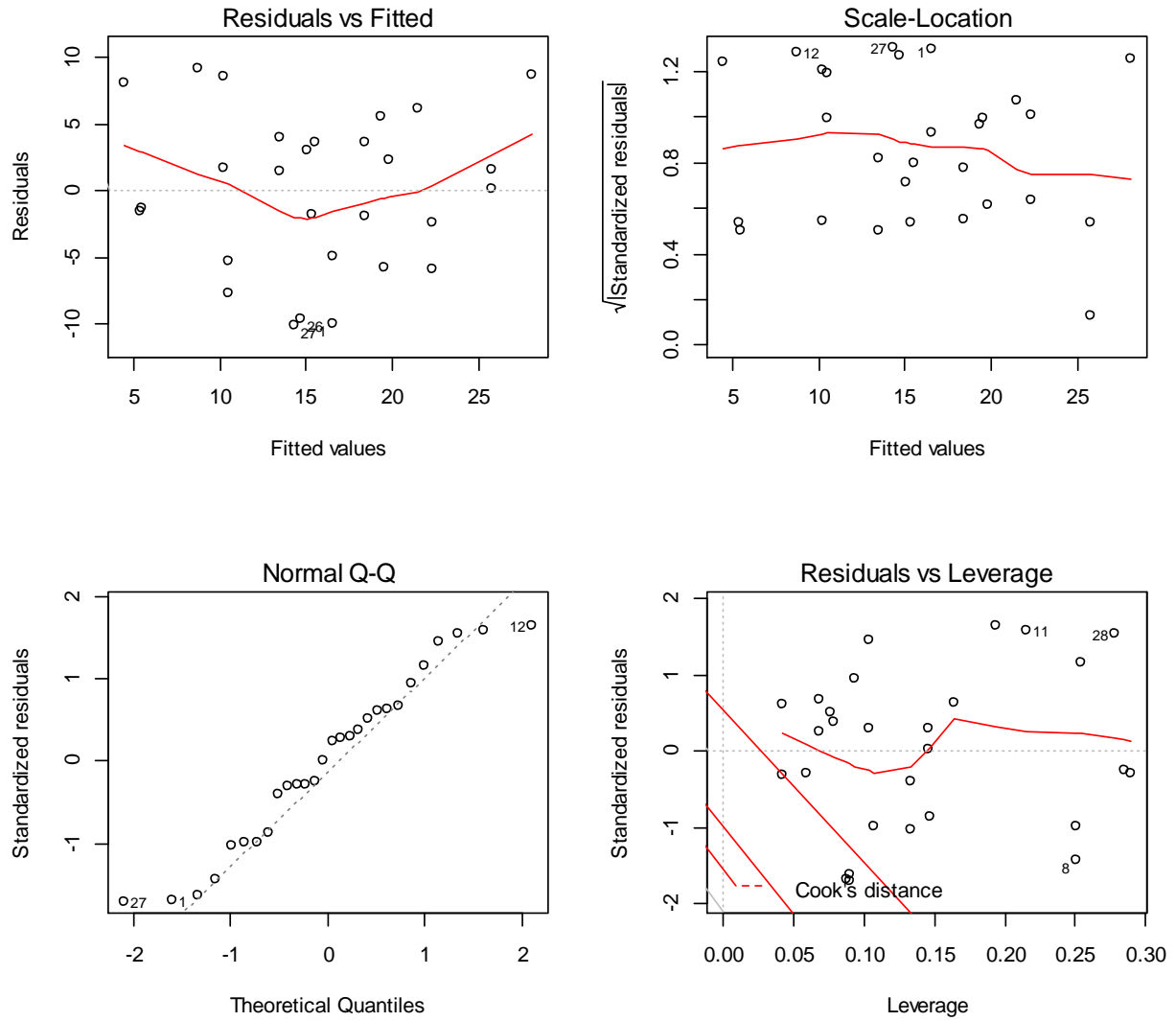


Figure A- 4. Diagnostic plots for the regression relationship  $k_I \sim \log(\text{Area}) + \log(\text{HSG}) + \log(\text{LU\_Urban})$ . Plots clockwise from upper left: residuals vs. fitted values, scale-location plot, normal quantile-quantile plot of residuals, and residuals vs. leverage.

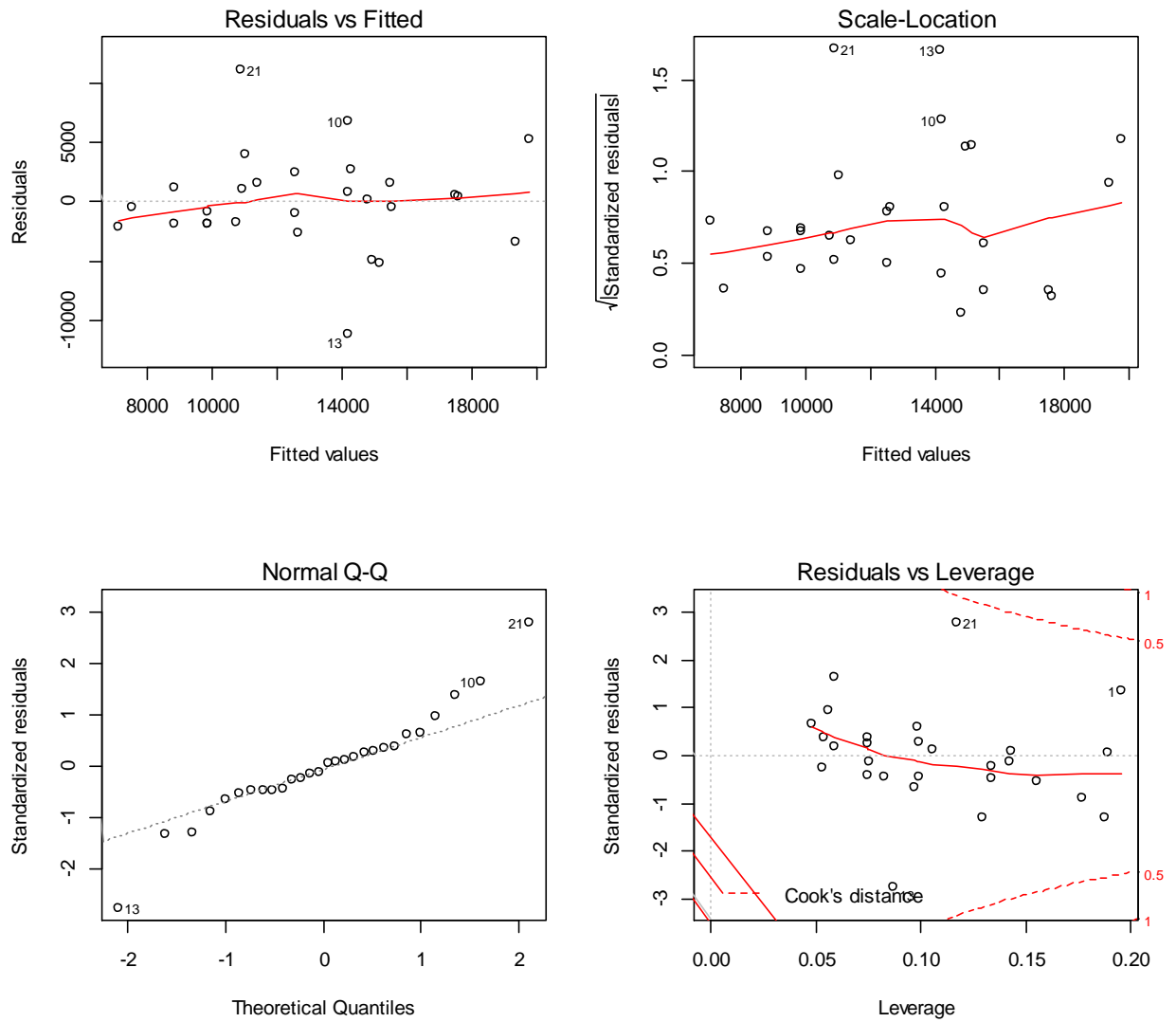


Figure A- 5. Diagnostic plots for the regression relationship  $k_g \sim \log(\text{HSG}) + \text{LU\_Ag}$ . Plots clockwise from upper left: residuals vs. fitted values, scale-location plot, normal quantile-quantile plot of residuals, and residuals vs. leverage.

Table A- 6. Regression equations relating model parameters  $b$ ,  $c_{max}$ ,  $k_1$ , and  $k_g$  to watershed characteristics for each of the study watersheds. Regression relationships are listed by the USGS stream gage watershed that was removed in the “leave one out” regression analysis. Also listed are the statistical significance (p-value), correlation coefficient ( $R^2$ ), and PRESS statistic for each regression relationship. [ $Area$  = basin area ( $km^2$ ),  $ChS$  = channel slope (fraction),  $Water$  = fraction of basin area covered by open water,  $HSG$  = hydrologic soil group index,  $Urban$  = fraction of basin area in urban land,  $Ag$  = fractional extent of watershed in agricultural land use].

Stream Station No.	Stream Station Name	Regression Equations	Regression P-Values	Regression Adjusted $R^2$	PRESS statistic
01496000	Northeast River at Leslie, MD	$\hat{b} = 0.740 - 0.0815 \ln (Area)$	0.0072	0.23	0.58
		$\hat{c}_{max} = 674 + 87.9 \ln (ChS) + 203 \ln (Water + 1)$	0.00033	0.46	74319
		$\hat{k}_1 = 38.3 + 5.57 \ln (Area) - 36.7 \ln (HSG) - 2.10 \ln (Urban)$	0.00028	0.51	1162
		$\hat{k}_g = -27334 + 37234 \ln (HSG) + 136 Ag$	0.014	0.25	$5.2 \times 10^8$
01496200	Principio Creek near Principio Furnace, MD	$\hat{b} = 0.741 - 0.0781 \ln (Area)$	0.017	0.18	0.69
		$\hat{c}_{max} = 653 + 84.0 \ln (ChS) + 217 \ln (Water + 1)$	0.00037	0.45	71209
		$\hat{k}_1 = 41.5 + 5.30 \ln (Area) - 40.1 \ln (HSG) - 1.94 \ln (Urban)$	0.00051	0.48	1287
		$\hat{k}_g = -29485 + 39227 \ln (HSG) + 143 Ag$	0.0041	0.33	$5.7 \times 10^8$
01581700	Winters Run near Benson, MD	$\hat{b} = 0.750 - 0.0852 \ln (Area)$	0.0087	0.22	0.64
		$\hat{c}_{max} = 663 + 84.9 \ln (ChS) + 202 \ln (Water + 1)$	0.00073	0.42	79026
		$\hat{k}_1 = 45.6 + 5.58 \ln (Area) - 46.0 \ln (HSG) - 1.39 \ln (Urban)$	0.00041	0.49	1292
		$\hat{k}_g = -29624 + 39363 \ln (HSG) + 147 Ag$	0.0046	0.32	$5.7 \times 10^8$
01583000	Slade Run near Glyndon, MD	$\hat{b} = 0.607 - 0.0371 \ln (Area)$	0.29	0.01	0.58
		$\hat{c}_{max} = 712 + 94.1 \ln (ChS) + 198 \ln (Water + 1)$	0.0020	0.37	80346
		$\hat{k}_1 = 56.9 + 3.22 \ln (Area) - 50.8 \ln (HSG) - 1.23 \ln (Urban)$	0.00044	0.49	1131
		$\hat{k}_g = -26853 + 36805 \ln (HSG) + 140 Ag$	0.011	0.26	$5.7 \times 10^8$
01584050	Long Green Creek at Glen Arm, MD	$\hat{b} = 0.765 - 0.0834 \ln (Area)$	0.0096	0.22	0.64
		$\hat{c}_{max} = 612 + 76.1 \ln (ChS) + 215 \ln (Water + 1)$	0.0011	0.40	75489
		$\hat{k}_1 = 40.0 + 5.47 \ln (Area) - 39.4 \ln (HSG) - 1.86 \ln (Urban)$	0.00055	0.48	1301
		$\hat{k}_g = -29606 + 39420 \ln (HSG) + 138 Ag$	0.0020	0.37	$5.2 \times 10^8$

Table A- 6. (cont.) Regression equations relating model parameters  $b$ ,  $c_{max}$ ,  $k_1$ , and  $k_g$  to watershed characteristics for each of the study watersheds. Regression relationships are listed by the USGS stream gage watershed that was removed in the “leave one out” regression analysis. Also Also listed are the statistical significance (p-value), correlation coefficient ( $R^2$ ), and PRESS statistic for each regression relationship. [Area = basin area (km<sup>2</sup>), ChS = channel slope (fraction), Water = fraction of basin area covered by open water, HSG = hydrologic soil group index, Urban = fraction of basin area in urban land, Ag = fractional extent of watershed in agricultural land use].

Stream Station No.	Stream Station Name	Regression Equations	Regression P-Values	Regression Adjusted $R^2$	PRESS statistic
01584500	Little	$\hat{b} = 0.730 - 0.0739 \ln(\text{Area})$	0.0267	0.15	0.69
	Gunpowder	$\hat{c}_{max} = 646 + 81.3 \ln(\text{ChS}) + 200 \ln(\text{Water} + 1)$	0.0026	0.38	74747
	Falls at Laurel	$\hat{k}_1 = 38.2 + 4.51 \ln(\text{Area}) - 34.8 \ln(\text{HSG}) - 1.82 \ln(\text{Urban})$	0.0026	0.38	1173
	Brook, MD	$\hat{k}_g = -29081 + 38843 \ln(\text{HSG}) + 147 \text{Ag}$	0.0026	0.34	$5.7 \times 10^8$
01585500	Cranberry	$\hat{b} = 0.762 - 0.084 \ln(\text{Area})$	0.011	0.20	0.67
	Branch near	$\hat{c}_{max} = 608 + 73.1 \ln(\text{ChS}) + 97.5 \ln(\text{Water} + 1)$	0.012	0.25	73501
	Westminster,	$\hat{k}_1 = 37.2 + 6.10 \ln(\text{Area}) - 37.9 \ln(\text{HSG}) - 2.19 \ln(\text{Urban})$	0.00013	0.53	1130
	MD	$\hat{k}_g = -29995 + 39696 \ln(\text{HSG}) + 149 \text{Ag}$	0.0019	0.36	$5.7 \times 10^8$
01588000	Piney Run near	$\hat{b} = 0.752 - 0.0799 \ln(\text{Area})$	0.010	0.20	0.65
	Sykesville,	$\hat{c}_{max} = 646 + 82.4 \ln(\text{ChS}) + 212 \ln(\text{Water} + 1)$	0.00043	0.43	74811
	MD	$\hat{k}_1 = 43.2 + 5.30 \ln(\text{Area}) - 41.7 \ln(\text{HSG}) - 1.96 \ln(\text{Urban})$	0.00031	0.49	1267
		$\hat{k}_g = -30376 + 39641 \ln(\text{HSG}) + 169 \text{Ag}$	0.00014	0.48	$4.1 \times 10^8$
01591000	Patuxent River	$\hat{b} = 0.723 - 0.0674 \ln(\text{Area})$	0.025	0.16	0.58
	near Unity,	$\hat{c}_{max} = 664 + 83.9 \ln(\text{ChS}) + 175 \ln(\text{Water} + 1)$	0.00059	0.43	76081
	MD	$\hat{k}_1 = 40.7 + 5.18 \ln(\text{Area}) - 39.6 \ln(\text{HSG}) - 1.63 \ln(\text{Urban})$	0.0029	0.39	1347
		$\hat{k}_g = -29829 + 39541 \ln(\text{HSG}) + 148 \text{Ag}$	0.0029	0.35	$5.7 \times 10^8$
01591400	Cattail Creek	$\hat{b} = 0.738 - 0.76 \ln(\text{Area})$	0.017	0.18	0.66
	near	$\hat{c}_{max} = 660 + 84.5 \ln(\text{ChS}) + 198 \ln(\text{Water} + 1)$	0.0008	0.41	82040
	Glenwood,	$\hat{k}_1 = 41.3 + 5.26 \ln(\text{Area}) - 40.3 \ln(\text{HSG}) - 1.70 \ln(\text{Urban})$	0.00071	0.47	1301
	MD	$\hat{k}_g = -29887 + 39614 \ln(\text{HSG}) + 146 \text{Ag}$	0.0033	0.39	$5.8 \times 10^8$

Table A- 6. (cont.) Regression equations relating model parameters  $b$ ,  $c_{max}$ ,  $k_1$ , and  $k_g$  to watershed characteristics for each of the study watersheds. Regression relationships are listed by the USGS stream gage watershed that was removed in the “leave one out” regression analysis. Also listed are the statistical significance (p-value), correlation coefficient ( $R^2$ ), and PRESS statistic for each regression relationship. [Area = basin area ( $km^2$ ), ChS = channel slope (fraction), Water = fraction of basin area covered by open water, HSG = hydrologic soil group index, Urban = fraction of basin area in urban land, Ag = fractional extent of watershed in agricultural land use].

Stream Station No.	Stream Station Name	Regression Equations	Regression P-Values	Regression Adjusted $R^2$	PRESS statistic
01591700	Hawlings River near Sandy Spring, MD	$\hat{b} = 0.737 - 0.0753 \ln (Area)$	0.020	0.17	0.672
		$\hat{c}_{max} = 657 + 83.1 \ln (ChS) + 238 \ln (Water + 1)$	0.000073	0.53	53136
		$\hat{k}_1 = 38.9 + 5.17 \ln (Area) - 37.3 \ln (HSG) - 1.97 \ln (Urban)$	0.00086	0.46	1276
		$\hat{k}_g = -32304 + 41820 \ln (HSG) + 151 Ag$	0.0016	0.38	$5.5 \times 10^8$
01646000	Difficult Run near Great Falls, VA	$\hat{b} = 0.751 - 0.0835 \ln (Area)$	0.015	0.19	0.68
		$\hat{c}_{max} = 716 + 96.4 \ln (ChS) + 216 \ln (Water + 1)$	0.00012	0.51	69586
		$\hat{k}_1 = 45.9 + 4.62 \ln (Area) - 44.4 \ln (HSG) - 1.34 \ln (Urban)$	0.00075	0.46	1289
		$\hat{k}_g = -31783 + 39880 \ln (HSG) + 176 Ag$	0.00023	0.48	$3.9 \times 10^8$
01654000	Accotink Creek near Annandale, VA	$\hat{b} = 0.738 - 0.0794 \ln (Area)$	0.010	0.22	0.60
		$\hat{c}_{max} = 663 + 85.0 \ln (ChS) + 203 \ln (Water + 1)$	0.0010	0.40	78572
		$\hat{k}_1 = 37.6 + 5.18 \ln (Area) - 36.5 \ln (HSG) - 1.33 \ln (Urban)$	0.0035	0.38	1356
		$\hat{k}_g = -33681 + 44246 \ln (HSG) + 1142 Ag$	0.0013	0.39	$5.6 \times 10^8$
01658500	SF Quantico Creek near Independent Hill, VA	$\hat{b} = 0.730 - 0.0754 \ln (Area)$	0.017	0.18	0.62
		$\hat{c}_{max} = 648 + 81.4 \ln (ChS) + 186 \ln (Water + 1)$	0.0014	0.39	82490
		$\hat{k}_1 = 43.7 + 5.65 \ln (Area) - 45.1 \ln (HSG) - 1.41 \ln (Urban)$	0.00026	0.51	1277
		$\hat{k}_g = -29024 + 39231 \ln (HSG) + 138 Ag$	0.0042	0.32	$5.9 \times 10^8$

Table A- 6. (cont.) Regression equations relating model parameters  $b$ ,  $c_{max}$ ,  $k_1$ , and  $k_g$  to watershed characteristics for each of the study watersheds. Regression relationships are listed by the USGS stream gage watershed that was removed in the “leave one out” regression analysis. Also listed are the statistical significance (p-value), correlation coefficient ( $R^2$ ), and PRESS statistic for each regression relationship. [Area = basin area ( $\text{km}^2$ ), ChS = channel slope (fraction), Water = fraction of basin area covered by open water, HSG = hydrologic soil group index, Urban = fraction of basin area in urban land, Ag = fractional extent of watershed in agricultural land use].

Stream Station No.	Stream Station Name	Regression Equations	Regression P-Values	Regression Adjusted $R^2$	PRESS statistic
01660400	Aquia Creek near Garrisonville, VA	$\hat{b} = 0.743 - 0.81 \ln(\text{Area})$	0.014	0.19	0.669
		$\hat{c}_{max} = 695 + 91.5 \ln(\text{ChS}) + 195 \ln(\text{Water} + 1)$	0.00069	0.42	80765
		$\hat{k}_1 = 33.0 + 5.81 \ln(\text{Area}) - 32.0 \ln(\text{HSG}) - 1.71 \ln(\text{Urban})$	0.00014	0.54	1014
		$\hat{k}_g = -30217 + 39932 \ln(\text{HSG}) + 148 \text{Ag}$	0.0022	0.36	$5.7 \times 10^8$
01671500	Bunch Creek near Boswells Tavern, VA	$\hat{b} = 0.757 - 0.0827 \ln(\text{Area})$	0.012	0.20	0.67
		$\hat{c}_{max} = 664 + 85.1 \ln(\text{ChS}) + 206 \ln(\text{Water} + 1)$	0.00051	0.42	78541
		$\hat{k}_1 = 46.5 + 5.85 \ln(\text{Area}) - 49.0 \ln(\text{HSG}) - 1.28 \ln(\text{Urban})$	0.00016	0.52	1178
		$\hat{k}_g = -32801 + 43012 \ln(\text{HSG}) + 147 \text{Ag}$	0.00095	0.39	$5.4 \times 10^8$

Table A- 7. Goodness-of-fit measures describing the model evaluation time series. Measures include RMSE of flows greater than two times baseflow ( $Q_{2XBF}$ ) and less than a storm with an average recurrence interval of 10 yrs ( $Q_{10}$ ), Nash-Sutcliffe model efficiency rating (NSE) of flows greater than  $Q_{2XBF}$  and of all flows, and a Kolmogorov–Smirnov test comparing the greatest 20 discharges of the observed and simulated time series.

Stream Station No.	Stream Station Name	Modeled Time Period	RMSE	NSE		Kolmogorov–Smirnov test
			(m <sup>3</sup> /s) $Q_{2XBF}$ - $Q_{10}$	$>Q_{2XBF}$	All Q	
01496000	Northeast River at Leslie, MD	1/1/1957 - 12/31/1966	3.8	-0.46	0.32	0.0047
01496000	Northeast River at Leslie, MD	1/1/1967 - 12/31/1976	7.4	0.31	0.53	0.035
01496200	Principio Creek near Principio Furnace, MD	6/1/1968 - 5/31/1977	12.5			
01496200	Principio Creek near Principio Furnace, MD	1/1/1978 - 12/31/1987	11.3			
01581700	Winters Run near Benson, MD	1/1/1975 - 12/31/1984	1.4			
01581700	Winters Run near Benson, MD	1/1/1985 - 12/31/1994	4.8			
01583000	Slade Run near Glyndon, MD	1/1/1953 - 12/31/1962	4.8			
01583000	Slade Run near Glyndon, MD	1/1/1963 - 12/31/1972	1.4			
01584050	Long Green Creek at Glen Arm, MD	10/1/1975 - 9/30/1985	8.8			
01584050	Long Green Creek at Glen Arm, MD	10/1/1985 - 9/30/1995	6.1			
01584500	Little Gunpowder Falls at Laurel Brook, MD	1/1/2002 - 12/31/2011	6.0			
01585500	Cranberry Branch near Westminster, MD	1/1/1986 - 12/31/1995	6.4			
01588000	Piney Run near Sykesville, MD	1/1/1948 - 12/31/1957	9.4			
01591000	Patuxent River near Unity, MD	1/1/1969 - 12/31/1978	3.7			
01591000	Patuxent River near Unity, MD	1/1/1981 - 12/31/1990	2.4			
01591400	Cattail Creek near Glenwood, MD	1/1/1979 - 12/31/1988	5.5			
01591400	Cattail Creek near Glenwood, MD	1/1/1989 - 12/31/1998	5.7			
01591700	Hawlings River near Sandy Spring, MD	1/1/1981 - 12/31/1990	10.4			
01591700	Hawlings River near Sandy Spring, MD	1/1/2000 - 12/31/2009	7.9			
01646000	Difficult Run near Great Falls, VA	1/1/1943 - 12/31/1952	2.7			
01646000	Difficult Run near Great Falls, VA	1/1/1984 - 12/31/1993	2.5			
01654000	Accotink Creek near Annandale, VA	1/1/1984 - 12/31/1993	3.4			

Table A- 7. (cont.) Goodness-of-fit measures describing the model evaluation time series. Measures include RMSE of flows greater than two times baseflow ( $Q_{2XBF}$ ) and less than a storm with an average recurrence interval of 10 yrs ( $Q_{10}$ ), Nash-Sutcliffe model efficiency rating (NSE) of flows greater than  $Q_{2XBF}$  and of all flows, and a Kolmogorov–Smirnov test comparing the greatest 20 discharges of the observed and simulated time series.

Stream Station No.	Stream Station Name	Modeled Time Period	RMSE (m <sup>3</sup> /s)		NSE		Kolmogorov–Smirnov test
			$Q_{2XBF}$ - $Q_{10}$	$>Q_{2xBF}$	All Q		
01654000	Accotink Creek near Annandale, VA	1/1/2000 - 12/31/2009	1.8				
01658500	SF Quantico Creek near Independent Hill, VA	1/1/1989 - 12/31/1998	1.6				
01658500	SF Quantico Creek near Independent Hill, VA	1/1/2001 - 12/31/2010	0.6				
01660400	Aquia Creek near Garrisonville, VA	10/17/1987 - 10/16/1997	0.8				
01660400	Aquia Creek near Garrisonville, VA	1/1/2001 - 12/31/2010	9.4				
01671500	Bunch Creek near Boswells Tavern, VA	1/1/1958 - 12/31/1967	9.1				

Table A- 8. Observed peak discharges for standard return periods. Discharges were calculated using a log-Pearson Type III flood frequency analysis of annual maxima of daily mean discharge time series.

Stream Station No.	Stream Station Name	Modeled Time Period	Peak flow (m <sup>3</sup> /s) for given return period in years					
			2	5	10	25	50	100
01496000	Northeast River at Leslie, MD	1/1/1957 - 12/31/1966	16	23	28	36	44	53
01496000	Northeast River at Leslie, MD	1/1/1967 - 12/31/1976	30	47	61	85	108	138
01496200	Principio Creek near Principio Furnace, MD	6/1/1968 - 5/31/1977	8	16	22	31	39	49
01496200	Principio Creek near Principio Furnace, MD	1/1/1978 - 12/31/1987	6	12	17	27	38	53
01581700	Winters Run near Benson, MD	1/1/1975 - 12/31/1984	24	39	48	58	64	70
01581700	Winters Run near Benson, MD	1/1/1985 - 12/31/1994	18	31	44	62	99	143
01583000	Slade Run near Glyndon, MD	1/1/1953 - 12/31/1962	1	1	2	2	3	4
01583000	Slade Run near Glyndon, MD	1/1/1963 - 12/31/1972	1	2	2	4	6	9
01584050	Long Green Creek at Glen Arm, MD	10/1/1975 - 9/30/1985	5	8	11	14	17	21
01584050	Long Green Creek at Glen Arm, MD	10/1/1985 - 9/30/1995	3	5	7	9	11	13
01584500	Little Gunpowder Falls at Laurel Brook, MD	1/1/2002 - 12/31/2011	21	36	45	55	61	66
01585500	Cranberry Branch near Westminster, MD	1/1/1986 - 12/31/1995	1	2	3	4	6	7
01588000	Piney Run near Sykesville, MD	1/1/1948 - 12/31/1957	4	7	11	21	34	57
01591000	Patuxent River near Unity, MD	1/1/1969 - 12/31/1978	25	54	85	153	238	376
01591000	Patuxent River near Unity, MD	1/1/1981 - 12/31/1990	16	27	35	49	61	75
01591400	Cattail Creek near Glenwood, MD	1/1/1979 - 12/31/1988	12	21	28	36	43	50
01591400	Cattail Creek near Glenwood, MD	1/1/1989 - 12/31/1998	9	14	18	23	28	33
01591700	Hawlings River near Sandy Spring, MD	1/1/1981 - 12/31/1990	17	29	38	50	59	69
01591700	Hawlings River near Sandy Spring, MD	1/1/2000 - 12/31/2009	15	26	36	52	68	89
01646000	Difficult Run near Great Falls, VA	1/1/1943 - 12/31/1952	21	25	27	29	29	30
01646000	Difficult Run near Great Falls, VA	1/1/1984 - 12/31/1993	33	50	64	85	105	129
01654000	Accotink Creek near Annandale, VA	1/1/1984 - 12/31/1993	21	35	49	73	100	139
01654000	Accotink Creek near Annandale, VA	1/1/2000 - 12/31/2009	17	29	40	57	75	97

Table A- 8. (cont.) Observed peak discharges for standard return periods. Discharges were calculated using a log-Pearson Type III flood frequency analysis of annual maxima of daily mean discharge time series.

Stream Station No.	Stream Station Name	Modeled Time Period	Peak flow (m <sup>3</sup> /s) for given return period in years					
			2	5	10	25	50	100
01658500	SF Quantico Creek near Independent Hill, VA	1/1/1989 - 12/31/1998	7	12	16	21	25	29
01658500	SF Quantico Creek near Independent Hill, VA	1/1/2001 - 12/31/2010	6	10	13	17	20	22
01660400	Aquia Creek near Garrisonville, VA	10/17/1987 - 10/16/1997	24	39	50	66	80	95
01660400	Aquia Creek near Garrisonville, VA	1/1/2001 - 12/31/2010	16	27	37	57	79	113
01671500	Bunch Creek near Boswells Tavern, VA	1/1/1958 - 12/31/1967	2	4	5	7	9	12

Table A- 9. Simulated peak discharges for standard return periods. Discharges were calculated using a log-Pearson Type III flood frequency analysis of annual maxima of daily mean discharge time series.

Stream Station No.	Stream Station Name	Modeled Time Period	Peak flow (m <sup>3</sup> /s) for given return period in years					
			2	5	10	25	50	100
01496000	Northeast River at Leslie, MD	1/1/1957 - 12/31/1966	12	20	30	50	77	124
01496000	Northeast River at Leslie, MD	1/1/1967 - 12/31/1976	18	24	28	33	37	42
01496200	Principio Creek near Principio Furnace, MD	6/1/1968 - 5/31/1977	6	8	9	12	15	19
01496200	Principio Creek near Principio Furnace, MD	1/1/1978 - 12/31/1987	6	9	11	14	16	18
01581700	Winters Run near Benson, MD	1/1/1975 - 12/31/1984	17	26	32	41	48	55
01581700	Winters Run near Benson, MD	1/1/1985 - 12/31/1994	12	16	18	22	25	29
01583000	Slade Run near Glyndon, MD	1/1/1953 - 12/31/1962	0	1	1	1	1	2
01583000	Slade Run near Glyndon, MD	1/1/1963 - 12/31/1972	0	1	2	4	8	19
01584050	Long Green Creek at Glen Arm, MD	10/1/1975 - 9/30/1985	7	10	12	17	21	27
01584050	Long Green Creek at Glen Arm, MD	10/1/1985 - 9/30/1995	6	8	10	11	12	14
01584500	Little Gunpowder Falls at Laurel Brook, MD	1/1/2002 - 12/31/2011	15	28	43	75	118	193
01585500	Cranberry Branch near Westminster, MD	1/1/1986 - 12/31/1995	2	4	6	11	17	28
01588000	Piney Run near Sykesville, MD	1/1/1948 - 12/31/1957	7	10	12	17	22	28
01591000	Patuxent River near Unity, MD	1/1/1969 - 12/31/1978	15	31	50	98	169	304
01591000	Patuxent River near Unity, MD	1/1/1981 - 12/31/1990	11	17	22	29	37	47
01591400	Cattail Creek near Glenwood, MD	1/1/1979 - 12/31/1988	10	16	21	28	35	44
01591400	Cattail Creek near Glenwood, MD	1/1/1989 - 12/31/1998	11	15	18	22	25	29
01591700	Hawlings River near Sandy Spring, MD	1/1/1981 - 12/31/1990	9	14	18	25	32	42
01591700	Hawlings River near Sandy Spring, MD	1/1/2000 - 12/31/2009	10	14	17	22	27	33
01646000	Difficult Run near Great Falls, VA	1/1/1943 - 12/31/1952	27	35	40	47	52	59
01646000	Difficult Run near Great Falls, VA	1/1/1984 - 12/31/1993	27	44	59	87	118	162
01654000	Accotink Creek near Annandale, VA	1/1/1984 - 12/31/1993	16	24	30	41	51	64
01654000	Accotink Creek near Annandale, VA	1/1/2000 - 12/31/2009	33	55	77	117	164	233
01658500	SF Quantico Creek near Independent Hill, VA	1/1/1989 - 12/31/1998	5	8	10	14	19	25

Table A- 9. (cont.) Simulated peak discharges for standard return periods. Discharges were calculated using a log-Pearson Type III flood frequency analysis of annual maxima of daily mean discharge time series.

Stream Station No.	Stream Station Name	Modeled Time Period	Peak flow (m <sup>3</sup> /s) for given return period in years					
			2	5	10	25	50	100
01658500	SF Quantico Creek near Independent Hill, VA	1/1/2001 - 12/31/2010	6	8	10	14	18	23
01660400	Aquia Creek near Garrisonville, VA	10/17/1987 - 10/16/1997	19	30	40	62	88	131
01660400	Aquia Creek near Garrisonville, VA	1/1/2001 - 12/31/2010	20	28	36	50	66	91
01671500	Bunch Creek near Boswells Tavern, VA	1/1/1958 - 12/31/1967	3	5	6	8	11	15

Table A- 10. Peak flow instantaneous discharges of standard return intervals calculated from USGS peak flow regression equations (Austin et al., 2011; Thomas and Moglen, 2010).

Stream Station No.	Stream Station Name	Modeled Time Period	Peak flow (m <sup>3</sup> /s) for given return period in years					
			2	5	10	25	50	100
01496000	Northeast River at Leslie, MD	1/1/1957 - 12/31/1966	40	73	103	154	202	260
01496000	Northeast River at Leslie, MD	1/1/1967 - 12/31/1976	40	73	103	154	202	260
01496200	Principio Creek near Principio Furnace, MD	6/1/1968 - 5/31/1977	20	37	53	81	107	140
01496200	Principio Creek near Principio Furnace, MD	1/1/1978 - 12/31/1987	16	32	48	75	102	136
01581700	Winters Run near Benson, MD	1/1/1975 - 12/31/1984	45	84	120	182	241	313
01581700	Winters Run near Benson, MD	1/1/1985 - 12/31/1994	45	84	120	182	241	313
01583000	Slade Run near Glyndon, MD	1/1/1953 - 12/31/1962	5	11	16	27	39	54
01583000	Slade Run near Glyndon, MD	1/1/1963 - 12/31/1972	5	11	17	28	39	54
01584050	Long Green Creek at Glen Arm, MD	10/1/1975 - 9/30/1985	19	36	52	80	107	141
01584050	Long Green Creek at Glen Arm, MD	10/1/1985 - 9/30/1995	19	36	52	80	107	141
01584500	Little Gunpowder Falls at Laurel Brook, MD	1/1/2002 - 12/31/2011	95	171	238	350	454	579
01585500	Cranberry Branch near Westminster, MD	1/1/1986 - 12/31/1995	9	18	26	41	57	76
01588000	Piney Run near Sykesville, MD	1/1/1948 - 12/31/1957	22	42	60	92	123	161
01591000	Patuxent River near Unity, MD	1/1/1969 - 12/31/1978	45	84	120	182	242	314
01591000	Patuxent River near Unity, MD	1/1/1981 - 12/31/1990	45	83	120	182	241	314
01591400	Cattail Creek near Glenwood, MD	1/1/1979 - 12/31/1988	37	67	96	144	190	246
01591400	Cattail Creek near Glenwood, MD	1/1/1989 - 12/31/1998	37	68	96	144	190	247
01591700	Hawlings River near Sandy Spring, MD	1/1/1981 - 12/31/1990	37	70	100	153	203	264
01591700	Hawlings River near Sandy Spring, MD	1/1/2000 - 12/31/2009	38	71	101	153	203	265
01646000	Difficult Run near Great Falls, VA	1/1/1943 - 12/31/1952	49	92	129	188	239	297
01646000	Difficult Run near Great Falls, VA	1/1/1984 - 12/31/1993	49	92	129	188	239	297
01654000	Accotink Creek near Annandale, VA	1/1/1984 - 12/31/1993	29	56	81	119	153	193
01654000	Accotink Creek near Annandale, VA	1/1/2000 - 12/31/2009	29	56	81	119	153	193

Table A- 10. (cont.) Peak flow instantaneous discharges of standard return intervals calculated from USGS peak flow regression equations (Austin et al., 2011; Thomas and Moglen, 2010).

Stream Station No.	Stream Station Name	Modeled Time Period	Peak flow (m <sup>3</sup> /s) for given return period in years					
			2	5	10	25	50	100
01658500	SF Quantico Creek near Independent Hill, VA	1/1/1989 - 12/31/1998	15	30	44	66	86	110
01658500	SF Quantico Creek near Independent Hill, VA	1/1/2001 - 12/31/2010	15	30	44	66	86	110
01660400	Aquia Creek near Garrisonville, VA	10/17/1987 - 10/16/1997	37	70	99	145	186	232
01660400	Aquia Creek near Garrisonville, VA	1/1/2001 - 12/31/2010	37	70	99	145	186	232
01671500	Bunch Creek near Boswells Tavern, VA	1/1/1958 - 12/31/1967	11	22	32	50	65	83

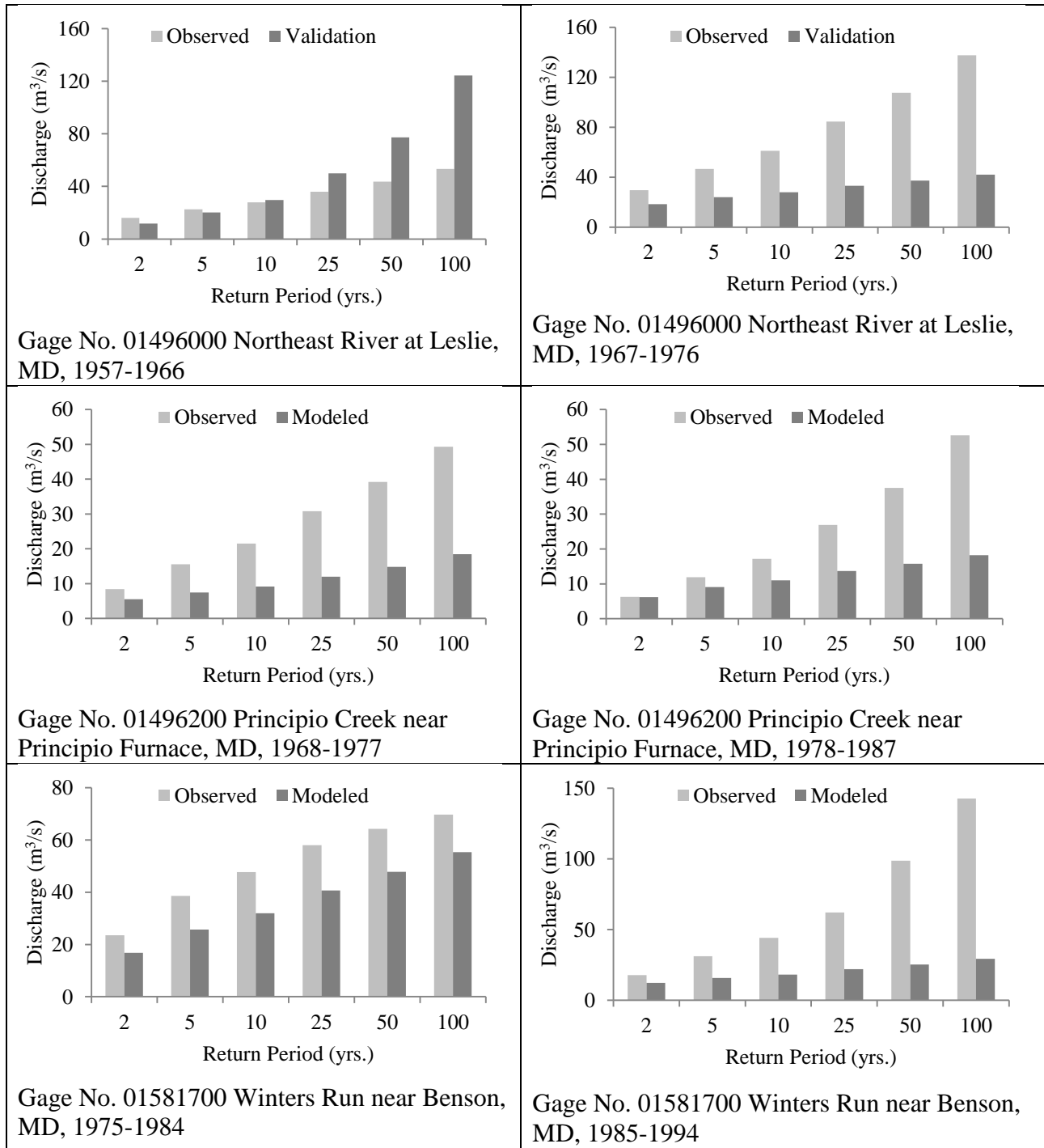


Figure A- 6. Bar charts comparing daily average discharges of standard return intervals for each of the 28 time series considered in this study. These discharges were calculated based on flood frequency analyses of observed and modeled daily average streamflow.

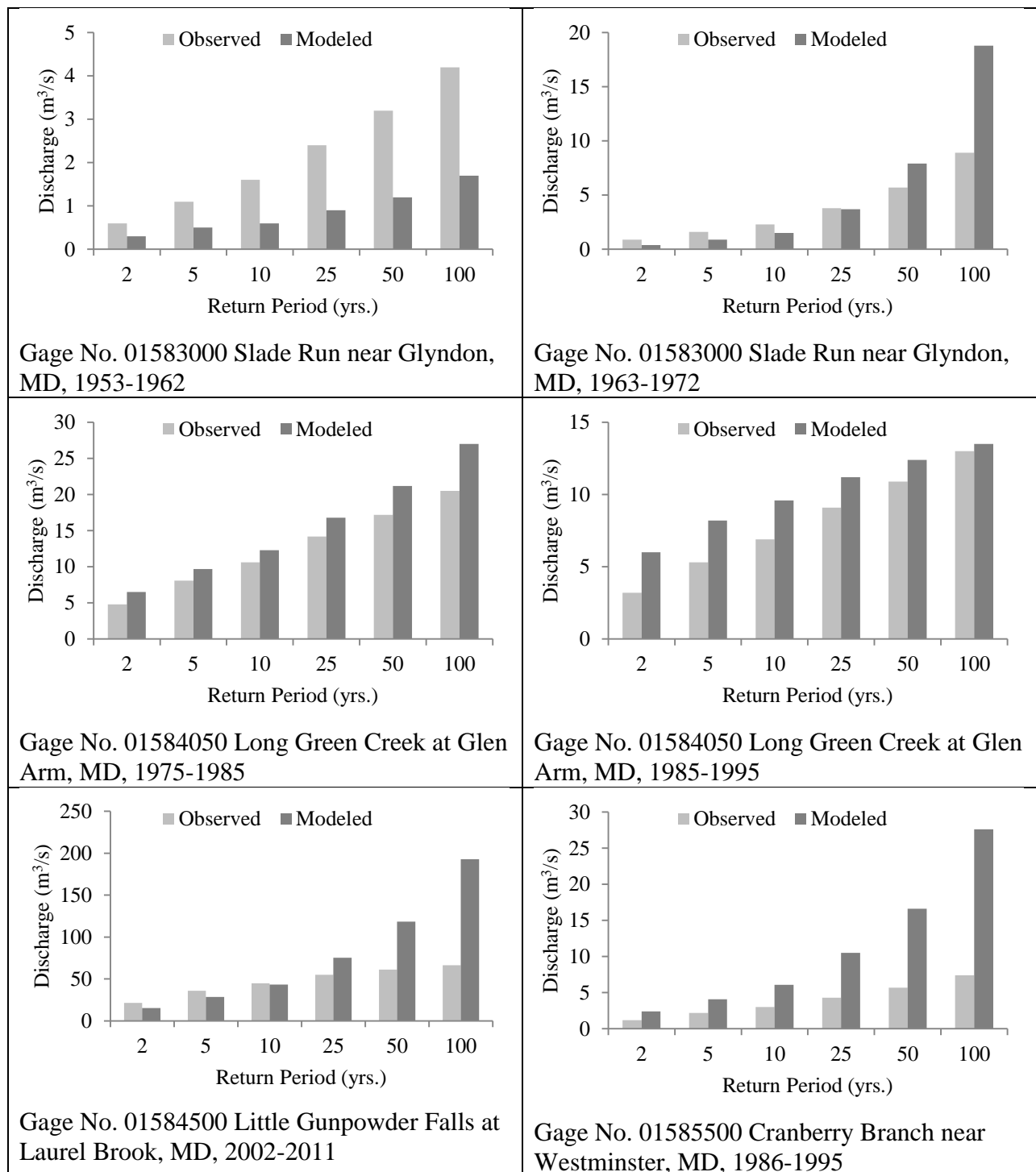


Figure A- 6. (cont.) Bar charts comparing daily average discharges of standard return intervals for each of the 28 time series considered in this study. These discharges were calculated based on flood frequency analyses of observed and modeled daily average streamflow.

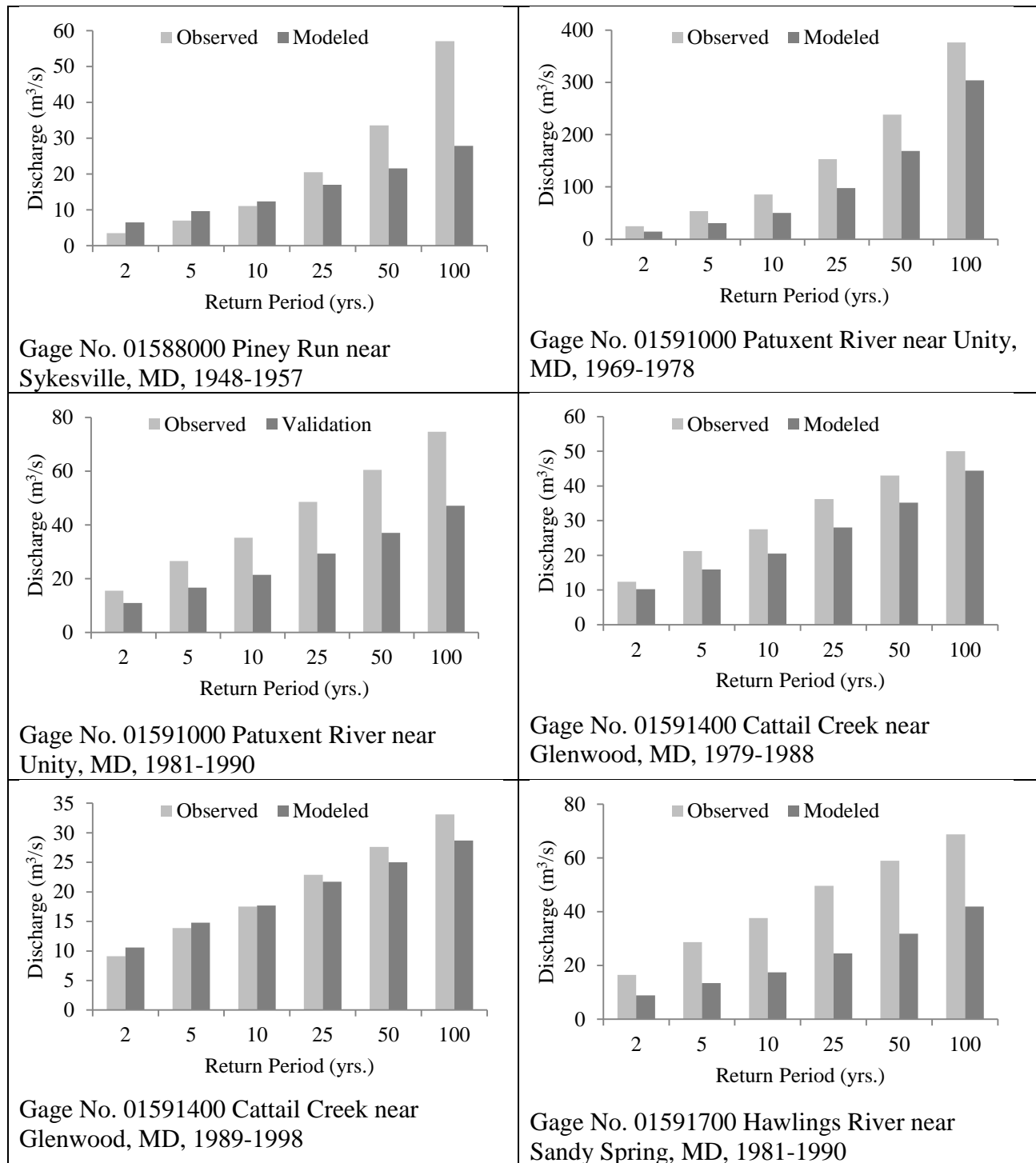


Figure A- 6. (cont.) Bar charts comparing daily average discharges of standard return intervals for each of the 28 time series considered in this study. These discharges were calculated based on flood frequency analyses of observed and modeled daily average streamflow.

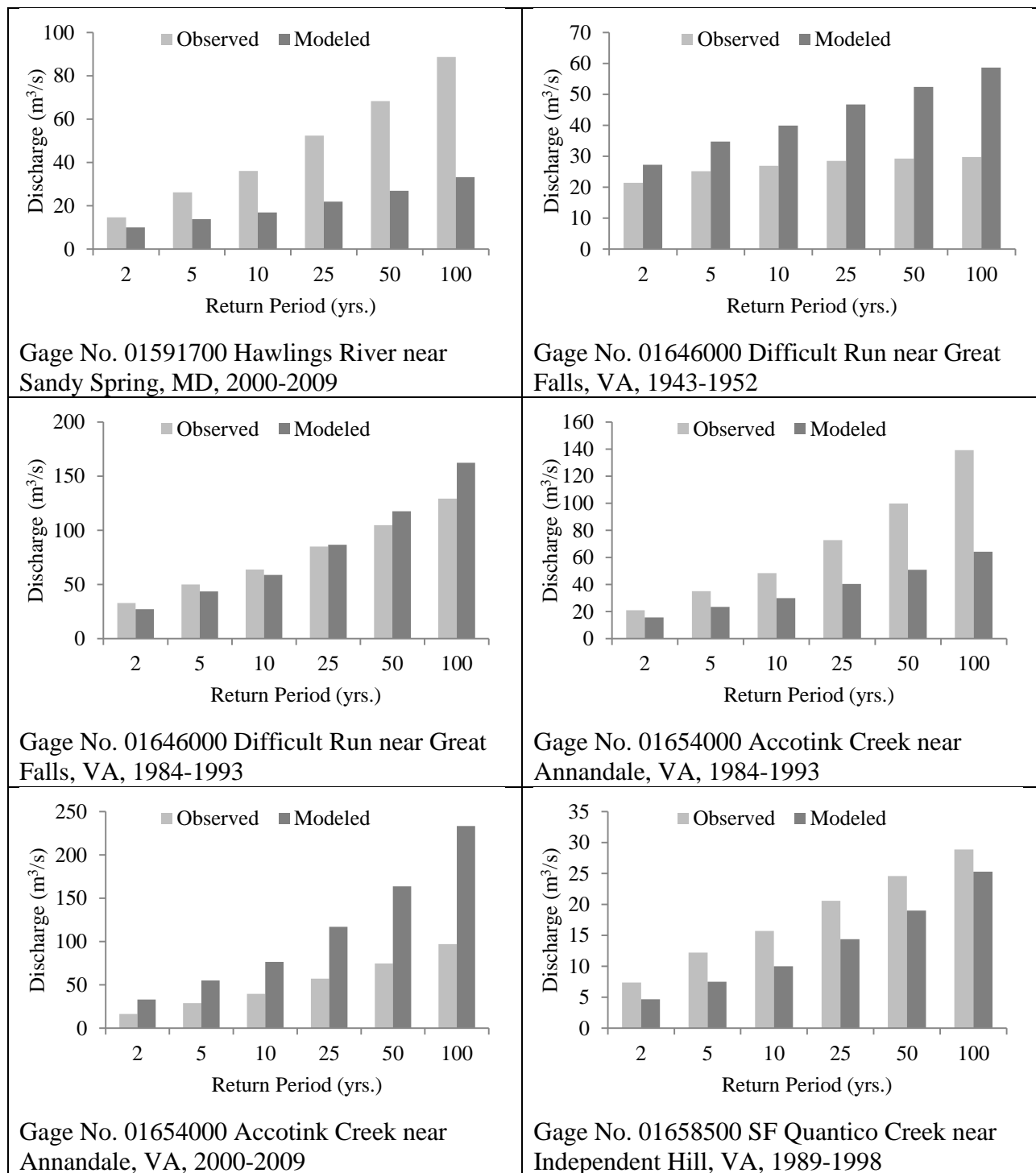


Figure A- 6. (cont.) Bar charts comparing daily average discharges of standard return intervals for each of the 28 time series considered in this study. These discharges were calculated based on flood frequency analyses of observed and modeled daily average streamflow.

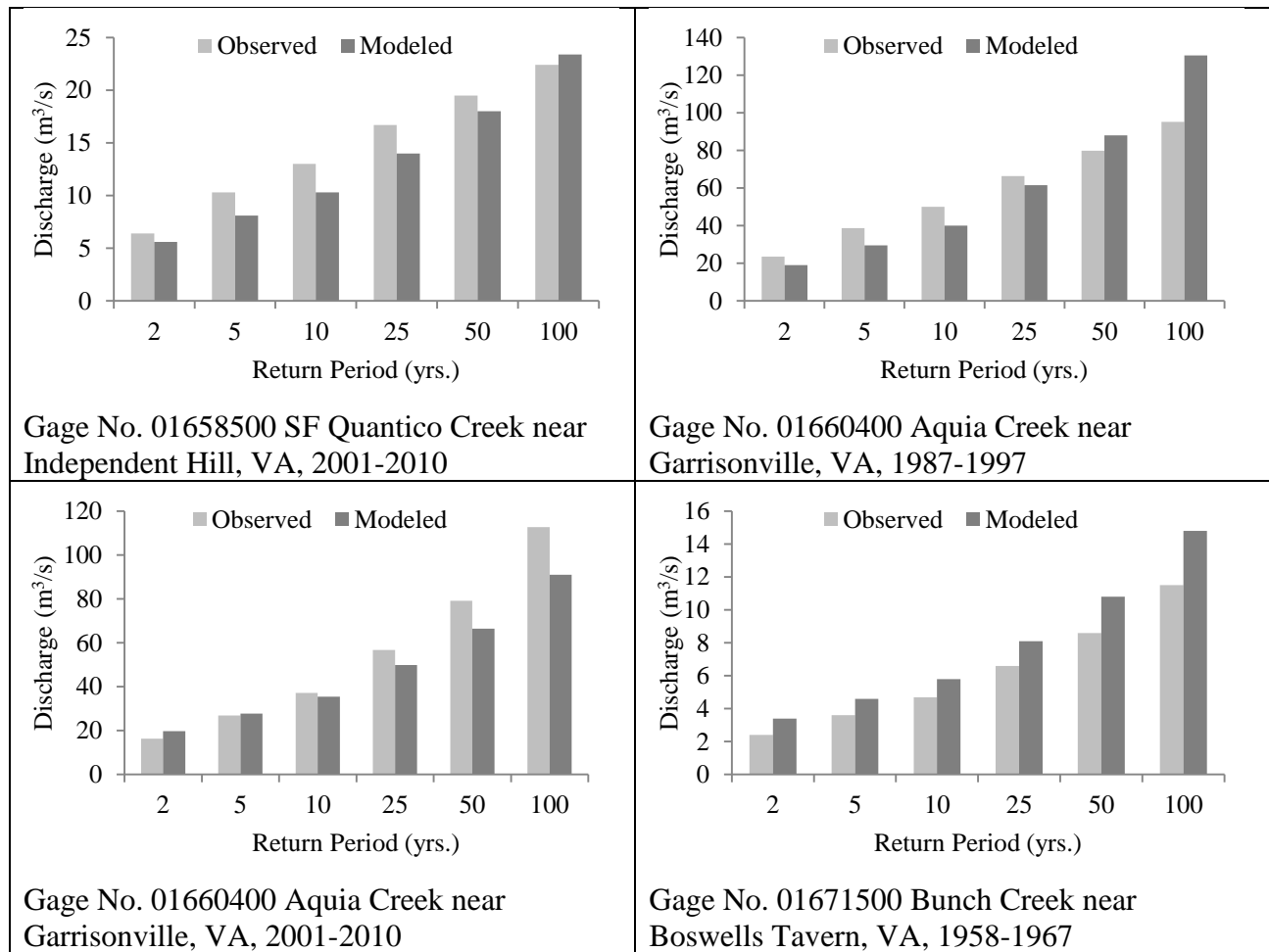


Figure A- 6. (cont.) Bar charts comparing daily average discharges of standard return intervals for each of the 28 time series considered in this study. These discharges were calculated based on flood frequency analyses of observed and modeled daily average streamflow.